UNIVERSITY OF NAPLES “FEDERICO II”

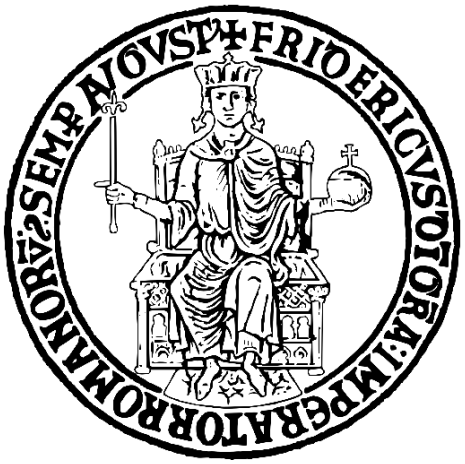

Ph.D. Course in Biology
(XXXVI Cycle)

Biological responses in Bryophytes exposed to environmentally relevant concentrations of heavy metals

TUTOR
PROF. ADRIANA BASILE

CO-TUTOR
DR. VIVIANA MARESCA

Ph.D. CANDIDATE
PIERGIORGIO CIANCIULLO

Ph.D. COORDINATOR
PROF SERGIO ESPOSITO

2020-2023

INDEX

SUMMARY AND AIMS

This PhD work is presented as a paper collection that comprises studies which explored how two widespread bryophytes, the thallose liverwort *Conocephalum conicum* and the aquatic moss *Leptodictyum riparium*, respond to environmental concentrations of heavy metals (ERC-HMs). *C. conicum* and *L. riparium* were chosen due to their widespread distribution and ease of recognition. The present work represents the first part of the scientific collaboration with the Italian Institute for Environmental Protection and Research (ISPRA) and the Regional Agency for Environmental Protection of Campania (ARPAC). The final purpose of the collaboration is to integrate the biomarkers data with physiochemical data into the ARPAC freshwaters monitoring network. I took into account heavy metal levels measured in different freshwater bodies from the Campania region (Italy): Regi Lagni Channels, Sarno river, and Savone river.

A wide range of responses were measured: chloroplast ultrastructure, enzymatic antioxidant activities, DNA damage, phytochelatins synthesis, glutathione synthesis, secondary metabolites to assess the impact on the selected bryophytes.

At the beginning (**Paper I**) I explored how *C. conicum* responded in an *in vitro* exposure experiment mimicking the heavy metal concentrations in the Sarno river at two sites with a different anthropic pressure(catalase, super oxide dismutase, glutathione-S-transferase), the reactive oxygen species (ROS) and thiolic compounds localization, cell ultrastructure and metabolite profiles were investigated. The levels of activity of the antioxidant enzymes were significantly higher in the samples exposed to the highest concentration of heavy metals. Comparably, confocal imaging evidenced higher accumulation of thiolic compounds and a marked ROS cytoplasmic outburnst. A difference in the quality of the metabolic profile was observed (glycolipids, betaine lipids and C-glycoside flavonoids) in the samples exposed at the highest HMs concentrations.

Subsequently, I aimed to compare the biomarkers responses in *C. conicum* both *in vitro* and field conditions (**Paper II**) in the Regi Lagni channels. I focalized on the activation of the enzymatic and non-enzymatic antioxidant responses (CAT, SOD, GST, phenolic content, thiol synthesis and localization), and ultrastructural alteration were investigated. The results showed that the samples from different sites and conditions (for *in vitro* tests) showed significant differences. In particular, the ultrastructural alterations show a trend correlated to the different exposure situations; ROS contents, glutathione, antioxidant enzyme activities, and phenolic contents were increased showing an enhancement of the antioxidant defense both by the enzymatic way and by using the synthesis of antioxidant phenolic compounds. This study confirms the ability of *C. conicum* to respond to heavy

metal pollution and the responses studied are, at least partially, correlated to the presence of heavy metals.

After measuring the photosynthetic efficiency under HMs stress in *C. conicum* with imaging PAM after the exposure to HMs mix, a strong decrease in Fv/Fm was observed localized in the central area of the thalli (i.e. nervature) (**Paper III**). Imaging PAM analysis allowed to measure the photosynthetic efficiency over the entire thalli surface, giving as results the mapping of photosynthetic parameters. Consequently, I investigated the differences in the activity of antioxidant enzymes (CAT, SOD, GST), HMs tissue localization and ultrastructural differences between the central nerve area and the lateral area of the thalli. As for spatial localization, HM preferentially accumulated in the nerve of gametophytes respect to the wings. With respect to tissue localization, HM were mainly found in the hyaline and in the photosynthetic parenchyma. Essential metals (Cu and Zn) were accumulated at higher concentrations with respect to non-essential metals (Pb and Cd). At the ultrastructural level, HM caused alterations of the fine structure of the cells, most evident along the nerve, inducing marked alterations of the chloroplast structure and therefore of the photosynthetic capacity. The results suggested that for short exposure times (7 days) a localized biomarkers measurement could be more informative rather than whole thalli analysis.

The fourth study had as object of study the aquatic moss *Leptodyctium riparium (***Paper IV***)* in which glutathione, phytochelatins and nitrogen metabolism was investigated in relation to heavy metal concentrations detected in one of most polluted river in Europe: the Sarno river. We simulated the concentrations of Cu, Zn, Cd, Pb detected in Regi Lagni, Italy, one of the most contaminated freshwater sites in Southern Europe, in the laboratory to test how the moss responds to heavy metal contamination. There was a steady decrease of photosynthetic efficiency correlated with the heavy metal concentrations and ultrastructural organization. All phytochelatins (PC2, PC3, PC4) levels increased significantly as the concentration of heavy metals increased, while the GSH levels did not appear to be particularly affected. Comparably confocal microscopy using the fluorescent probe monochlorobimane revealed the accumulation of thiolic compounds into the vacuole of phyllids cells. A significant increase of GDH and NADH-GOGAT activities increased with increasing heavy metal concentration. Immunoblotting analysis revealed an increase of the chl-GS2 while no significant increase was detected in the cyt-GS1. These results give insight into the molecular events underlying the metal-tolerance of the aquatic moss *L. riparium* exposed to environmental heavy metal concentrations.

1. INTRODUCTION

1.1 Heavy metals and metalloids: a persistent group of chemical pollutants

Heavy metals are a group of elements with metallic properties (e.g., transition metals, metalloids, lanthanides, actinides) having an atomic mass greater than 20 and a gravity greater than 5 g·cm−3 (Adnan et al., 2022; Duffus, 2002). Fifty-three elements fall into this category, and some examples are copper (Cu), tin (Sn), iron (Fe), cobalt (Co), zinc (Zn), cadmium (Cd), mercury (Hg), and lead (Pb). Among heavy metals, some are essential for living organisms (e.g., Zn, Cu, Fe, Co, etc.) whilst others are essentially toxic and cause harmful effects on the organisms (e.g., Hg, Cd, Pb, As, etc.) (Tchounwou et al., 2012). Naturally, heavy metals are present in the environment and are vital for the survival of all organisms, but they may become hazardous when they accumulate inside them reaching toxic internal concentrations (Mitra et al., 2022). Over the last decades, heavy metal pollution has become a threat to the environment and human health. The contamination has been observed in soil, water and air. The cause is mainly attributed to anthropogenic activities such as mining, industrial production, and the use of metal-containing compounds in domestic and agricultural settings (Tchounwou et al., 2012). Conversely, lithogenesis, weathering, erosion, and other geological processes are the natural sources (Stafilov et al., 2010). Unfortunately, heavy metal contamination is widely distributed, and persists long-term (Briffa et al., 2020). Data from several studies report that the annual worldwide release of heavy metals is about 22,000 ton for Cd, 939,000 ton for Cu, 783,000 ton for Pb and 1,350,000 ton for Zn (Cheng et al., 2014; Shrivastava et al., 2019). According to the Environmental Protection Agency (EPA), arsenic, cadmium, lead, and mercury, are among the most hazardous metals in the environment (Goyer, 2004). In plant and animal cells, heavy metals have been reported to damage cellular organelles and components such as cell membrane, mitochondrial, endoplasmic reticulum, and nuclei (Banfalvi, 2011). Metal ions have been found to interact with DNA and nuclear proteins, causing genotoxicity and negative conformational changes (Tchounwou et al., 2012).

1.2 Bryophytes responses to heavy metal exposure: a brief review

The bryophytes represent the most conservative group of land plants (Reski, 1998). They were the first plants colonizing the land, and as such had to develop mechanisms to cope with the much greater amounts of metals present in the environment (Degola et al., 2014). Tracheophytes have developed a series of histological-anatomical adaptations to limit the entry of heavy metals (i.e., a strong cutinization of the leaves, the limitation of exchanges at the stomatal level, protection of the stems with suberin, and endodermis compartmentalization at the root level, etc.), while bryophytes, not having these anatomic adaptations, have developed cellular responses that have allowed them to survive in polluted environments.

Heavy metals, especially those which do not have a role in bryophytes' physiology (e.g., Pb, Cd, Hg), cause harmful effects, starting from the cellular level, which may cause physiological impairments in the whole organism. This happens when the molecular machinery cannot manage the excess of heavy metal in the cytoplasm. Several studies have investigated the harmful effects of heavy metals in bryophytes. Some researchers have characterized the damage at the ultrastructural level. Basile et al., 2012 and Esposito et al., 2012 reported that metals such as Cd and Pb (Cd > Pb) cause severe alterations in the cell ultrastructure. The authors observed dose-dependent alterations: swollen chloroplasts, irregular thylakoids organization, increased plastoglobules, swollen mitochondria cristae; and cellular signs of senescence (i.e., multivesicular bodies). Similar alterations were observed by Choudhury & Panda, 2004, 2005, in the moss *Taxithelium nepalense* after Pb and As exposure. Other studies pointed out the fact that heavy metal uptake causes a decrease in chlorophyll content (Phaenark et al., 2023; Shakya et al., 2008; Stanković et al., 2021; Świsłowski et al., 2020; Tremper et al., 2004), and a decrease in photosynthetic activity (Brown & Wells, 1990; Chen et al., 2018; Díaz et al., 2013; Maresca et al., 2022). These changes at the cellular level cause toxicity at the organism level due to alteration of the normal metabolism. In fact, some other investigations reported growth inhibition of bryophytes exposed to toxic metals such as Pb and Cd (Gupta & Chopra, 1995; Sassmann et al., 2015; Sidhu & Brown, 1996; Stanković et al., 2021). The metal tolerance in bryophytes could have an explanation in precise cellular responses such as the activation of certain enzymes and the synthesis of defence proteins. As in other plant organisms, in bryophytes, the first barrier against heavy metal stress is mediated by the cell wall through chelation and immobilization via pectic compounds. Several studies have investigated the immobilization of heavy metals in the cell walls of bryophytes (Basile et al., 1994, 2001; Carginale et al., 2004; Krzesłowska, 2011; Krzesłowska et al., 2010). This passive mechanism reduces the amounts reaching young or reproductively affected parts and, at the cellular level, the amounts able to penetrate the cytoplasm

and exert toxic effects. Heavy metals bind to the negative charges of cell-wall polysaccharides rich in carboxyl groups (homogalacturonans) and other functional groups (–OH and –SH), as well as proteins, phenolics, and amino acids [54,55]. This process mainly affects tissues that exhibit cell-wall modifications, such as hydroids, placental "transfer cells", or hyaline parenchyma cells. This process seems to be increased by stress conditions. In fact, the break-up of cell membrane in dead or damaged cells may cause the freeing of more cation-binding sites, thus allowing a higher accumulation of metals in the cell wall of dead or damaged cells (Buck & Brown, 1979); there is proof that bryophytes under heavy metal stress can rearrange the cell wall by thickening it and increasing the amount of low-esterified and unesterified homogalacturonan (Itouga et al., 2017; Krzesłowska et al., 2009). In general, these mechanisms aim to provide more binding sites for the immobilization of heavy metals in the cell wall. The cell wall thus represents a passive barrier to prevent heavy metals from entering into and interacting with the cytoplasmic environment. However, heavy metals that enter the cytosol require a wide range of molecular responses to avoid harmful effects to cellular structures. Bryophytes have developed, like higher plants, a series of cellular responses to counteract heavy metal stresses that collectively take the name "fan response" (**Figure 1**). These cellular mechanisms include the chelation and compartmentalization of heavy metals, as well as the activation of non-enzymatic and enzymatic antioxidant defences to counteract the induced reactive-oxygen-species (ROS) production. Several studies have indicated that these mechanisms involve the synthesis of molecules capable of binding such ions (e.g., amino acids, citric acid, malic acid) (Kováčik et al., 2017, 2020), the modulation of the enzymatic antioxidant system (i.e., SOD, CAT, GPX, POX, etc.) (Choudhury & Panda, 2005; Dazy et al., 2009; Maresca et al., 2018; Maresca, Lettieri, et al., 2020; Maresca, Sorbo, et al., 2020), increased synthesis of phytochelatins, glutathione and "heat shock protein" (HPS) (Basile et al., 2013, 2015, 2017; Esposito et al., 2012, 2018), phenomena largely mediated by gene activation/repression (**Figure 1**).

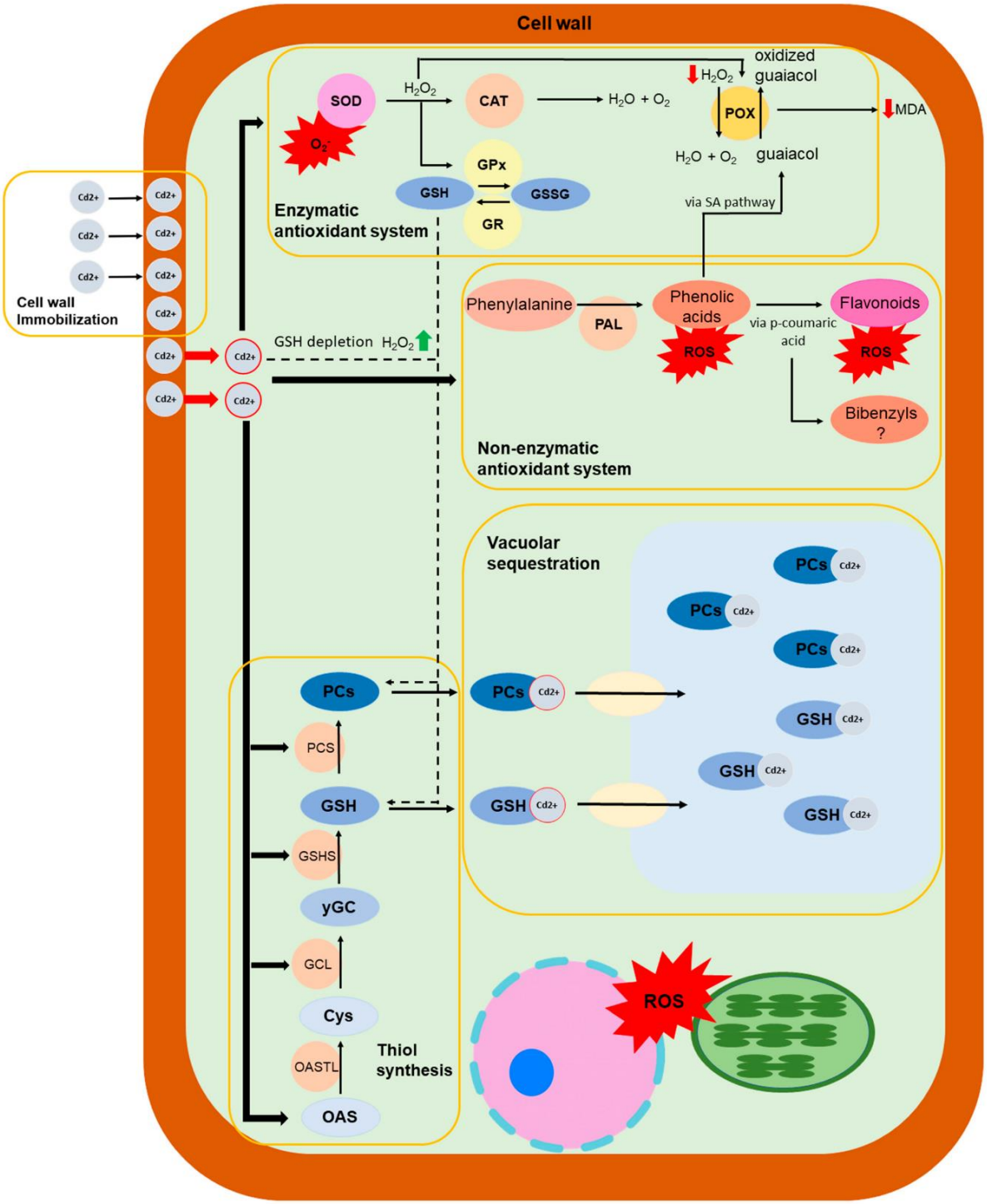

Figure1 . Schematic diagram of the mechanisms involved in metal tolerance in bryophytes. Cadmium is selected as an example specimen. List of abbreviations: SOD (superoxide dismutase), CAT (catalase), GPx (glutathione peroxidase), GR (glutathione reductase), POX (guaiacol peroxidase), PAL (phenylalanine ammonia lyase), OASTL (O-acetylserine (thiol) lyase), GCL (glutamate-cysteine ligase), GSHS (glutathione synthetase), PCS (phytochelatin synthetase), Cys (cysteine), OAS (O-acetylserine), yGC (y-glutamylcysteine), GSH, (reduced glutathione), GSSG (oxidized glutathione),

PCs (phytochelatins), MDA (malondialdehyde), ROS (Reactive Oxygen Species).

1.2.1. Enzymatic Antioxidant Systems in Bryophytes

Heavy metals can cause an overproduction of ROS, and for this reason bryophytes must possess an efficient antioxidant system to cope with ROS-induced oxidative stress (**Figure 1**). This antioxidant system is essential to maintain cellular redox homeostasis in plants. This system includes numerous enzymes and low-molecular-weight compounds (Zengin & Munzuroglu, 2005). The protection of cells against heavy-metal-induced oxidative stress can occur via nonenzymatic antioxidant systems (**Figure 1**). Non-enzymatic antioxidants include hydrophilic (ascorbate, glutathione), lipophilic (α-tocopherol and carotenoids), phenolic, and flavonoid small molecules. Glutathione and ascorbate are compounds implicated in redox signal transduction, acting as second messengers in hormone-mediated responses (C. Foyer & Noctor, 2005). α-tocopherol is a fat soluble antioxidant belonging to the vitamin E class, and is involved in the protection of cell membranes from the effects of ROS. Flavonoids, an important class of polyphenols that perform multiple functions in plants, appear to be cofactors of enzymatic action and antioxidant activity; their biosynthesis is stimulated in the presence of stress. Carotenoids are also important molecules in plant defence, as they act as negative regulators of oxidative stress; they are also able to interact synergistically with the other antioxidants, thus enhancing the protection of the plant. Other studies have demonstrated that, as in other plants (Zengin & Munzuroglu, 2005), ascorbic acid may play a role in the non-enzymatic antioxidant response against heavy metal stress in bryophytes, participating in both short- and long-term response. Accumulation of ascorbate was observed in *H. plumaeforme* with different concentrations of Pb and Ni (48 h) (Sun et al., 2009, 2010), in *Taxiphyllum nepalense* exposed to Pb and Cr (Choudhury & Panda, 2005), and in *Taxiphyllum barbieri* after a short exposure (24 h) to Cd (Kováčik et al., 2017). Similar results were obtained with the protonemata of the model moss *Physcomitrium patens* after a longterm exposure (40 days) to Cd (Kováčik et al., 2020). Furthermore, the authors observed an accumulation of citrate and malate, which could have acted as chelating agents against Cd. The enzymatic components of the antioxidant defence system include the superoxide dismutase (SOD) (Menezes-Benavente et al., 2004; Scandalios, 2005), catalase (CAT) (Scandalios, 2002, 2005), glutathione peroxidase (GPx), glutathione reductase (GR) (Margis et al., 2008), guaiacol peroxidase (POX) (Passardi et al., 2004), and peroxiredoxins (Prxs) (Foyer & Noctor, 2011; Wood et al., 2003). Several studies on bryophytes have demonstrated that enzymes involved in the antioxidant defence vary among the species and depend on the specific metal element. For example, Sun et al., 2009 and 2010 treated the moss *H. plumaeforme* with different concentrations of Pb and Ni, singly or combined. They found that peroxidase was the main enzyme active in

counteracting the resulting oxidative stress with a dose-dependent response. SOD enzyme activity increased only slightly, and CAT activity actually decreased. Aydogan et al., 2017 evaluated the impact of Pb, Ni, Cu and Cr oxidative stress in two bryophyte species, *Pleurochaete squarrosa* and *Timmiella barbuloides*. Cu treatment induced SOD activity in *P. squarrosa*, but not in *T. barbuloides*. Similarly, increased SOD activity was observed in *Fontinalis antipyretica* under Cu exposure (Dazy et al., 2009) and in *T. nepalense* under Cr exposure (Choudhury & Panda, 2005). The opposing results of SOD activity in response to Cu and Cr between the two species could be due to possible differences in the redox state of the cells. The same study by Aydogan et al., 2017 showed that exposure to Ni, Pb and Cr did not affect CAT activity in *P. squarrosa* and *T. barbuloides*. Conversely, Choudhury & Panda, 2005 demonstrated that treatment with Pb and Cr of *T. nepalense* caused a decrease in CAT in short-term exposure. Sun et al., 2009 also evaluated how Pb and Ni treatment of *Hypnum plumaeforme* caused a decrease in CAT activity. Therefore, this could suggest that CAT activity in response to Ni, Pb and Cr is strongly based on the specie's detoxification mechanisms and the retention capacity of these metals in the cell walls. However, Cu is a redox-active metal and a known catalase inhibitor, and thus is able to suppress CAT activity and cause oxidative stress in cells (Schützendübel & Polle, 2002). POX activity induced by toxic concentrations of Pb and Ni has been reported as a common response in various bryophyte species, such as *Hypnum plumaeforme*, *Thuidium cymbifolium* and *Brachhythecium piligerum* (Sun et al., 2011). However, the Cu induced POX activity in *P. squarrosa* but suppressed it in *T. barbuloides*. Cr-treated *T. barbuloides* samples accumulated excess H_2O_2 in correlation with suppressed POX activity (Choudhury & Panda, 2005)(Aydogan et al., 2017). The data agree with the results of decreased POX activity in the bryophyte *T. nepalense* (Choudhury & Panda, 2005) and *Taxiphyllum taxirameum* (Chen et al., 2015) exposed to Cr. The discrepancy in POX activity in moss species indicates that different enzymatic (CAT, APX) and non-enzymatic scavengers operate in the elimination of H_2O_2 from cells. The activity of antioxidant enzymes (CAT, SOD, GST and POX) was found to be increased in the aquatic moss *Leptodictyum riparium* by Maresca et al., 2018 after the exposure to a mixture of metals (Cd, Cu, Pb, Zn). This study showed that the enzymatic activities followed a metal-concentration-dependent increase. Similar results were observed in *Conocephalum conicum* under cadmium stress (Maresca et al., 2020). These results agree with those obtained by Bellini et al., 2020, who studied the effects of Cd on the enzymatic activity of *L. riparium*. Dazy et al., 2009 studied the activity of GR in *F. antipyretica* exposed to Cd, Cu, Pb, and Zn. In particular, after Cu exposure, a bell-shaped concentration-response trend in GR was observed, but only if the exposure was at 0.1 M. In contrast, regardless of whether the moss was exposed to Cd, or Zn, or Pb, no bell-shaped concentration-response trends were observed following exposure; indeed, GR activity remained unchanged. The

same authors (Dazy et al., 2009) found that chromium induced GR activity in the moss *F. antipyretica* (Dazy et al., 2009). The increase in GR activity upon Cr exposure was explained by a higher cellular consumption of reduced GSH resulting from at least two putative mechanisms: (i) an increase in the glutathione-ascorbate cycle rate in order to detoxify ROS; (ii) an incorporation of GSH into the unidentified thiol compounds. Furthermore, in the same work, the observed relationships between cell damage (malondialdehyde (MDA) level) and antioxidant enzymes suggested that the tolerance of *F. antipyretica* for heavy metals it depended at least in part on its ability to prevent oxidative action.

1.2.2. Heavy metal compartmentalization and chelation in Bryophytes

A significant role in heavy metal tolerance and detoxification is played by vacuolar compartmentalization, which prevents the circulation of free metal ions into the cytoplasm, where they might interfere with key metabolic processes. Generally, in higher plants, the process of intracellular heavy-metal chelation and sequestration within the vacuole is accomplished by thiol-compounds such as reduced glutathione (GSH) and phytochelatins (PCs).

GSH is a low-molecular-weight thiol tripeptide constituted of glutamate (Glu), cysteine (Cys), and glycine (Gly) (Banfalvi, 2011; Shrivastava et al., 2019). In plant cells, it was found in the different organelles, and it has been determined to have millimolar concentrations (0.08–15 mM) which differ markedly among plant species (Diaz-Vivancos et al., 2015; Gasperl et al., 2022; Gill et al., 2013; Jozefczak et al., 2012) . GSH plays an important role in the regulation of developmental processes such as cell division (Vernoux et al., 2000; Yadav, 2010), flowering (Ogawa et al., 2004; Yadav, 2010), and in protecting plants against abiotic stresses such as nutritional starvation, heavy metal exposure, drought, salinity, heat, cold, and certain exogenous and endogenous organic-chemical agents (Khalid et al., 2022; Salbitani et al., 2022; Yadav, 2010). GSH plays a crucial role in chelation and detoxification of heavy metals. In fact, GSH (i) may be directly involved, because its thiol group is susceptible to different metals, such as Hg and Cd; (ii) can mitigate the redox imbalance caused by toxic-metal accumulation through its antioxidant power; and (iii) may be indirectly involved as a precursor of phytochelatins (PCs), ligand peptides having a particularly high affinity for some heavy metals (Bruns et al., 2001; Salbitani et al., 2022; Stanković et al., 2018). In particular, the nucleophilic nature of the thiol group is involved in the formation of mercaptide bonds with metals and in reacting with selected electrophiles (Yadav, 2010). This reactivity makes GSH a suitable biochemical to protect plants against heavy metal exposure.

Phytochelatins (PCs) are a set of heavy-metal-binding peptides which consists mainly of the amino acids Glu, Cys, and Gly, where the latter two are linked and result in the formation of g-Glu-Cys

dipeptides (Sharma et al., 2022; Yadav, 2010). PCs were identified in all plant species, and investigated as well as in algae, fungi, and diatoms (Li et al., 2020; Rea et al., 2004). PCs are synthesized inductively by exposure not only to Cd, but also to other heavy metals such as Hg, Cu, Zn, Pb and Ni (Sharma et al., 2022; Yadav, 2010). Glutathione, hydroxymethyl-glutathione, and G-glutamylcysteine were reported as the major precursors for PC synthesis (Grill et al., 1989; Kaur, 2020; Sharma et al., 2022) through the enzyme PC synthase (PCS) (**Figure 1**). The main function of PCs is the ability to carry out metal complexation. PC-metal complexes are one of the ways to improve the resistance of plants to heavy metals, which proves that the roles of PCs are to protect plants against toxic metals (Cobbett, 2000). The formed complexes between the heavy metal ions and PCs can then be transported into the vacuole, decreasing the concentration of metals in the cytoplasm and protecting the plants from their deleterious effects.

The current data support the hypothesis that mosses and liverworts might respond in different ways when considering the chelation and compartimentalization of heavy metals. The results from several studies indicate that mosses rely on GSH, whilst liverworts on PCs.

Carginale et al., 2004 and Degola et al., 2014 demonstrated that Cd accumulated in the vacuoles of *Lunularia cruciata* and together with an increase in sulphur concentration in that organelle. In addition, it was also found in *L. cruciata* cells that most of the intracellular Cd was bound to the thiol-rich compounds of similar weight, such as phytochelatins. In a subsequent study by Maresca et al., 2020, the authors demonstrated the application of PCs as specific biomarkers in the biomonitoring of a heavy-metal-polluted site. L. cruciata samples were collected in three sites with different degrees of pollution. The researchers found a strong correlation between the accumulated heavy metals in the *L. cruciata* thalli and the synthesized amount of PC2.

Li et al., 2020 and observed that PCs play central roles in the liverworts *M. polymorpha*. The single-copy PC gene present in the genome of *M. polymorpha* has been isolated and functionally characterized by overexpression in heterologous systems, demonstrating that it is enzymatically active and able to complement the *Arabidopsis* knockout cad1–3 mutant.

In a study by Sutter et al. [143], the authors compared the GSH and PCs content in three species of foliose liverworts (*Calypogeia arguta, Trichocolea tomentella, Scapania nemorea*) and the moss *Sphagnum fallax* after 10 days of exposure to Cd. The results indicated a depletion of GSH and a synthesis of PC2, PC3 and PC4 in the foliose liverworts after Cd exposure. On the other hand, they observed the accumulation of GSH but the absence of PCs in the moss species. Bruns et al., 2001 studying glutathione pool in *Fontinalis antipyretica* noted that no PCs, or only a negligible amount, were synthesized in response to heavy metal exposure. In the same moss, there was an increase in GSH level and GSSG/GSH ratio in response to Cr exposure, but no dose-effect relationship could be

observed.

1.4 Aims of the PhD program

During the PhD program, I focused on how *Conocephalum conicum* and *Leptodyctium riparium* reacts to heavy metal pollution considering environmentally relevant heavy metal concentrations. The work has been carried out through both *in vitro* and in-field experiments, using several approaches: ultrastructural analysis, non-enzymatic/enzymatic antioxidant responses, DNA damage, thiol content, metabolomics etc. The present work put the basis for the use of this widespread thallose liverwort and aquatic mosses as a sentinel in heavy metal biomonitoring networks and possibly to investigate other environmental issues such as climate change.

References

Adnan, M., Xiao, B., Xiao, P., Zhao, P., Li, R., & Bibi, S. (2022). Research Progress on Heavy Metals Pollution in the Soil of Smelting Sites in China. *Toxics*, *10*(5), Article 5. https://doi.org/10.3390/toxics10050231

AYDOĞAN, S., ERDAĞ, B., & AKTAŞ, L. (2017). Bioaccumulation and oxidative stress impact of Pb, Ni, Cu, and Cr heavy metals in two bryophyte species, Pleurochaete squarrosa and Timmiella barbuloides. *Turkish Journal of Botany*, *41*(5), 464–475. https://doi.org/10.3906/bot-1608-33

Banfalvi, G. (n.d.). *Cellular Effects of Heavy Metals*. Springer Dordrecht. Retrieved January 20, 2023, from https://link.springer.com/book/10.1007/978-94-007-0428-2

Basile, A., Cogoni, A. E., Bassi, P., Fabrizi, E., Sorbo, S., Giordano, S., & Cobianchi, R. C. (2001). Accumulation of Pb and Zn in gametophytes and sporophytes of the moss Funaria hygrometrica (Funariales). *Annals of Botany*, *87*(4), 537–543. Scopus. https://doi.org/10.1006/anbo.2001.1368

Basile, A., Giordano, S., Cafiero, G., Spagnuolo, V., & Castaldo-Cobianchi, R. (1994). Tissue and cell localization of experimentally-supplied lead in Funaria hygrometrica Hedw. Using X-ray SEM and TEM microanalysis. *Journal of Bryology*, *18*(1), 69–81. https://doi.org/10.1179/jbr.1994.18.1.69

Basile, A., Sorbo, S., Cardi, M., Lentini, M., Castiglia, D., Cianciullo, P., Conte, B., Loppi, S., & Esposito, S. (2015). Effects of heavy metals on ultrastructure and Hsp70 induction in Lemna minor L. exposed to water along the Sarno River, Italy. *Ecotoxicology and Environmental Safety*, *114*, 93–101. https://doi.org/10.1016/j.ecoenv.2015.01.009

Basile, A., Sorbo, S., Conte, B., Cardi, M., & Esposito, S. (2013). Ultrastructural changes and Heat Shock Proteins 70 induced by atmospheric pollution are similar to the effects observed under in vitro heavy metals stress in Conocephalum conicum (Marchantiales – Bryophyta). *Environmental Pollution*, *182*, 209–216. https://doi.org/10.1016/j.envpol.2013.07.014

Basile, A., Sorbo, S., Conte, B., Cobianchi, R. C., Trinchella, F., Capasso, C., & Carginale, V. (2012). Toxicity, Accumulation, and Removal of Heavy Metals by Three Aquatic Macrophytes. *International Journal of Phytoremediation*, *14*(4), 374–387. https://doi.org/10.1080/15226514.2011.620653

Basile, A., Sorbo, S., Lentini, M., Conte, B., & Esposito, S. (2017). Water pollution causes ultrastructural and functional damages in Pellia neesiana (Gottsche) Limpr. *Journal of Trace Elements in Medicine and Biology*, *43*, 80–86. https://doi.org/10.1016/j.jtemb.2016.11.014

Bellini, E., Maresca, V., Betti, C., Castiglione, M. R., Fontanini, D., Capocchi, A., Sorce, C., Borsò, M., Bruno, L., Sorbo, S., Basile, A., & Sanità di Toppi, L. (2020). The Moss Leptodictyum riparium Counteracts Severe Cadmium Stress by Activation of Glutathione Transferase and Phytochelatin Synthase, but Slightly by Phytochelatins. *International Journal of Molecular Sciences*, *21*(5), Article 5. https://doi.org/10.3390/ijms21051583

Briffa, J., Sinagra, E., & Blundell, R. (2020). Heavy metal pollution in the environment and their toxicological effects on humans. *Heliyon*, *6*(9), e04691. https://doi.org/10.1016/j.heliyon.2020.e04691

BROWN, D. H., & WELLS, J. M. (1990). Physiological Effects of Heavy Metals on the Moss Rhytidiadelphus squarrosus. *Annals of Botany*, *66*(6), 641–647. https://doi.org/10.1093/oxfordjournals.aob.a088078

Bruns, I. n. a., Sutter, K., Menge, S., Neumann, D., & Krauss, G.-J. (2001). Cadmium lets increase the glutathione pool in bryophytes. *Journal of Plant Physiology*, *158*(1), 79–89. https://doi.org/10.1078/0176-1617-00071

BUCK, G. W., & BROWN, D. H. (1979). The Effect of Desiccation on Cation Location in Lichens. *Annals of Botany*, *44*(3), 265–277. https://doi.org/10.1093/oxfordjournals.aob.a085730

Carginale, V., Sorbo, S., Capasso, C., Trinchella, F., Cafiero, G., & Basile, A. (2004). Accumulation, localisation, and toxic effects of cadmium in the liverwort Lunularia cruciata. *Protoplasma*, *223*(1), 53–61. https://doi.org/10.1007/s00709-003-0028-0

Chen, Y., Yuan, M., Zhang, H., Zeng, X., Liu, H., & Du, X. (2015). Influences of cu and cr stress on antioxidant system and chlorophyll fluorescence in terrestrial moss taxiphyllum taxirameum. *Fresenius Environmental Bulletin*, *24*(6A), 2211–2219. Scopus.

Chen, Y.-E., Mao, H.-T., Ma, J., Wu, N., Zhang, C.-M., Su, Y.-Q., Zhang, Z.-W., Yuan, M., Zhang, H.-Y., Zeng, X.-Y., & Yuan, S. (2018). Biomonitoring chromium III or VI soluble pollution by moss chlorophyll fluorescence. *Chemosphere*, *194*, 220–228. https://doi.org/10.1016/j.chemosphere.2017.11.177

Cheng, K., Tian, H. Z., Dunhua, Z., Lu, L., Wang, Y., Chen, J., Liu, X., Jia, W., & Huang, Z. (2014). Atmospheric emission inventory of cadmium from anthropogenic sources. *International Journal of Environmental Science and Technology*, *11*. https://doi.org/10.1007/s13762-013-0206-3

Choudhury, S., & Panda, S. K. (2004). Induction of oxidative stress and ultrastructural changes in moss Taxithelium nepalense (Schwaegr.) Broth. Under lead and arsenic phytotoxicity. *Current Science*, *87*(3), 342–348.

Choudhury, S., & Panda, S. K. (2005). Toxic effects, oxidative stress and ultrastructural changes in moss Taxithelium nepalense (Schwaegr.) Broth. Under chromium and lead phytotoxicity. *Water, Air, and Soil Pollution*, *167*(1–4), 73–90. Scopus. https://doi.org/10.1007/s11270-005-8682-9

Cobbett, C. S. (2000). Phytochelatin biosynthesis and function in heavy-metal detoxification. *Current Opinion in Plant Biology*, *3*(3), Article 3. https://doi.org/10.1016/S1369-5266(00)80067-9

Dazy, M., Masfaraud, J.-F., & Férard, J.-F. (2009). Induction of oxidative stress biomarkers associated with heavy metal stress in Fontinalis antipyretica Hedw. *Chemosphere*, *75*(3), 297–302. https://doi.org/10.1016/j.chemosphere.2008.12.045

Degola, F., De Benedictis, M., Petraglia, A., Massimi, A., Fattorini, L., Sorbo, S., Basile, A., & Sanità di Toppi, L. (2014). A Cd/Fe/Zn-Responsive Phytochelatin Synthase is Constitutively Present in the Ancient Liverwort Lunularia cruciata (L.) Dumort. *Plant and Cell Physiology*, *55*(11), 1884–1891. https://doi.org/10.1093/pcp/pcu117

Díaz, S., Villares, R., Vázquez, M. D., & Carballeira, A. (2013). Physiological Effects of Exposure to Arsenic, Mercury, Antimony and Selenium in the Aquatic Moss Fontinalis antipyretica Hedw. *Water, Air, & Soil Pollution*, *224*(8), 1659. https://doi.org/10.1007/s11270-013-1659-1

Diaz-Vivancos, P., de Simone, A., Kiddle, G., & Foyer, C. H. (2015). Glutathione—Linking cell proliferation to oxidative stress. *Free Radical Biology & Medicine*, *89*, 1154–1164. https://doi.org/10.1016/j.freeradbiomed.2015.09.023

Duffus, J. H. (2002). Prepared for publication by. *Pure and Applied Chemistry*.

Esposito, S., Loppi, S., Monaci, F., Paoli, L., Vannini, A., Sorbo, S., Maresca, V., Fusaro, L., Karam, E. A., Lentini, M., Lillo, A. D., Conte, B., Cianciullo, P., & Basile, A. (2018). In-field and in-vitro study of the moss Leptodictyum riparium as bioindicator of toxic metal pollution in the aquatic environment: Ultrastructural damage, oxidative stress and HSP70 induction. *PLOS ONE*, *13*(4), e0195717. https://doi.org/10.1371/journal.pone.0195717

Esposito, S., Sorbo, S., Conte, B., & Basile, A. (2012). Effects of Heavy Metals on Ultrastructure and HSP70S Induction in the Aquatic Moss Leptodictyum Riparium Hedw. *International Journal of Phytoremediation*, *14*(4), 443–455. https://doi.org/10.1080/15226514.2011.620904

Foyer, C. H., & Noctor, G. (2011). Ascorbate and Glutathione: The Heart of the Redox Hub. *Plant Physiology*, *155*(1), Article 1. https://doi.org/10.1104/pp.110.167569

Foyer, C., & Noctor, G. (2005). Redox Homeostasis and Antioxidant Signaling: A Metabolic Interface Between Stress Perception and Physiological Responses. *The Plant Cell*, *17*, 1866–1875. https://doi.org/10.1105/tpc.105.033589

Gasperl, A., Zellnig, G., Kocsy, G., & Müller, M. (2022). Organelle-specific localization of glutathione in plants grown under different light intensities and spectra. *Histochemistry and Cell Biology*, *158*(3), Article 3. https://doi.org/10.1007/s00418-022-02103-2

Ghani, N. A., Ludwiczuk, A., Ismail, N. H., & Asakawa, Y. (2016). Volatile Components of the Stressed Liverwort Conocephalum Conicum. *Natural Product Communications*, *11*(1), 1934578X1601100130. https://doi.org/10.1177/1934578X1601100130

Gill, S. S., Anjum, N. A., Hasanuzzaman, M., Gill, R., Trivedi, D. K., Ahmad, I., Pereira, E., & Tuteja, N. (2013). Glutathione and glutathione reductase: A boon in disguise for plant abiotic stress defense operations. *Plant Physiology and Biochemistry: PPB*, *70*, 204–212. https://doi.org/10.1016/j.plaphy.2013.05.032

Goyer, R. (n.d.). *Issue Paper on the Human Health Effects of Metals*.

Grill, E., Löffler, S., Winnacker, E. L., & Zenk, M. H. (1989). Phytochelatins, the heavy-metal-binding peptides of plants, are synthesized from glutathione by a specific gamma-glutamylcysteine dipeptidyl transpeptidase (phytochelatin synthase). *Proceedings of the National Academy of Sciences of the United States of America*, *86*(18), Article 18. https://doi.org/10.1073/pnas.86.18.6838

Gupta, A., & Chopra, R. N. (1995). Effect of some heavy metals on growth and archegonial formation in the female clones of Riccia discolor (Hepaticae, Ricciaceae) grown in vitro. *Fragmenta Floristica et Geobotanica*, *40*(1), 533–544. Scopus.

Itouga, M., Hayatsu, M., Sato, M., Tsuboi, Y., Kato, Y., Toyooka, K., Suzuki, S., Nakatsuka, S., Kawakami, S., Kikuchi, J., & Sakakibara, H. (2017). Protonema of the moss Funaria hygrometrica can function as a lead (Pb) adsorbent. *PLOS ONE*, *12*(12), e0189726. https://doi.org/10.1371/journal.pone.0189726

Jozefczak, M., Remans, T., Vangronsveld, J., & Cuypers, A. (2012). Glutathione is a key player in metal-induced oxidative stress defenses. *International Journal of Molecular Sciences*, *13*(3), Article 3. https://doi.org/10.3390/ijms13033145

Kaur, L. (2020). *Role of Phytoremediation Strategies in Removal of Heavy Metals* (pp. 223–259). https://doi.org/10.1007/978-981-32-9771-5_13

Khalid, M., Rehman, H. M., Ahmed, N., Nawaz, S., Saleem, F., Ahmad, S., Uzair, M., Rana, I. A., Atif, R. M., Zaman, Q. U., & Lam, H.-M. (2022). Using Exogenous Melatonin, Glutathione, Proline, and Glycine Betaine Treatments to Combat Abiotic Stresses in Crops. *International Journal of Molecular Sciences*, *23*(21), Article 21. https://doi.org/10.3390/ijms232112913

Kováčik, J., Babula, P., & Hedbavny, J. (2017). Comparison of vascular and non-vascular aquatic plant as indicators of cadmium toxicity. *Chemosphere*, *180*, 86–92. https://doi.org/10.1016/j.chemosphere.2017.04.002

Kováčik, J., Dresler, S., & Babula, P. (2020). Long-term impact of cadmium in protonema cultures of Physcomitrella patens. *Ecotoxicology and Environmental Safety*, *193*. Scopus. https://doi.org/10.1016/j.ecoenv.2020.110333

Krzesłowska, M. (2011). The cell wall in plant cell response to trace metals: Polysaccharide remodeling and its role in defense strategy. *Acta Physiologiae Plantarum*, *33*(1), 35–51. https://doi.org/10.1007/s11738-010-0581-z

Krzesłowska, M., Lenartowska, M., Mellerowicz, E. J., Samardakiewicz, S., & Woźny, A. (2009). Pectinous cell wall thickenings formation-A response of moss protonemata cells to lead. *Environmental and Experimental Botany*, *65*(1), 119–131. Scopus. https://doi.org/10.1016/j.envexpbot.2008.05.006

Krzesłowska, M., Lenartowska, M., Samardakiewicz, S., Bilski, H., & Woźny, A. (2010). Lead deposited in the cell wall of Funaria hygrometrica protonemata is not stable – A remobilization can occur. *Environmental Pollution*, *158*(1), 325–338. https://doi.org/10.1016/j.envpol.2009.06.035

Li, M., Barbaro, E., Bellini, E., Saba, A., Sanità di Toppi, L., & Varotto, C. (2020). Ancestral function of the phytochelatin synthase C-terminal domain in inhibition of heavy metal-mediated enzyme overactivation. *Journal of Experimental Botany*, *71*(20), Article 20. https://doi.org/10.1093/jxb/eraa386

Ludwiczuk, A., Odrzykoski, I. J., & Asakawa, Y. (2013). Identification of cryptic species within liverwort Conocephalum conicum based on the volatile components. *Phytochemistry*, *95*, 234–241. https://doi.org/10.1016/j.phytochem.2013.06.011

Maresca, V., Bellini, E., Landi, S., Capasso, G., Cianciullo, P., Carraturo, F., Pirintsos, S., Sorbo, S., Sanità di Toppi, L., Esposito, S., & Basile, A. (2022). Biological responses to heavy metal stress in the moss Leptodictyum riparium (Hedw.) Warnst. *Ecotoxicology and Environmental Safety*, *229*, 113078. https://doi.org/10.1016/j.ecoenv.2021.113078

Maresca, V., Fusaro, L., Sorbo, S., Siciliano, A., Loppi, S., Paoli, L., Monaci, F., karam, E. A., Piscopo, M., Guida, M., Galdiero, E., Insolvibile, M., & Basile, A. (2018). Functional and structural biomarkers to monitor heavy metal pollution of one of the most contaminated freshwater sites in Southern Europe. *Ecotoxicology and Environmental Safety*, *163*, 665–673. https://doi.org/10.1016/j.ecoenv.2018.07.122

Maresca, V., Lettieri, G., Sorbo, S., Piscopo, M., & Basile, A. (2020). Biological Responses to Cadmium Stress in Liverwort Conocephalum conicum (Marchantiales). *International Journal of Molecular Sciences*, *21*(18), Article 18. https://doi.org/10.3390/ijms21186485

Maresca, V., Sorbo, S., Loppi, S., Funaro, F., Del Prete, D., & Basile, A. (2020). Biological effects from environmental pollution by toxic metals in the "land of fires" (Italy) assessed using the biomonitor species Lunularia cruciata L. (Dum). *Environmental Pollution*, *265*, 115000. https://doi.org/10.1016/j.envpol.2020.115000

Margis, R., Dunand, C., Teixeira, F. K., & Margis-Pinheiro, M. (2008). Glutathione peroxidase family – an evolutionary overview. *The FEBS Journal*, *275*(15), 3959–3970. https://doi.org/10.1111/j.1742-4658.2008.06542.x

Menezes-Benavente, L., Kernodle, S. P., Margis-Pinheiro, M., & Scandalios, J. G. (2004). Salt-induced antioxidant metabolism defenses in maize (Zea mays L.) seedlings. *Redox Report*, *9*(1), 29–36. https://doi.org/10.1179/135100004225003888

Mitra, S., Chakraborty, A. J., Tareq, A. M., Emran, T. B., Nainu, F., Khusro, A., Idris, A. M., Khandaker, M. U., Osman, H., Alhumaydhi, F. A., & Simal-Gandara, J. (2022). Impact of heavy metals on the environment and human health: Novel therapeutic insights to counter the toxicity. *Journal of King Saud University - Science*, *34*(3), 101865. https://doi.org/10.1016/j.jksus.2022.101865

Ogawa, K., Hatano-Iwasaki, A., Yanagida, M., & Iwabuchi, M. (2004). Level of Glutathione is Regulated by ATP-Dependent Ligation of Glutamate and Cysteine through Photosynthesis in Arabidopsis thaliana: Mechanism of Strong Interaction of Light Intensity with Flowering. *Plant and Cell Physiology*, *45*(1), Article 1. https://doi.org/10.1093/pcp/pch008

Passardi, F., Penel, C., & Dunand, C. (2004). Performing the paradoxical: How plant peroxidases modify the cell wall. *Trends in Plant Science*, *9*(11), 534–540. https://doi.org/10.1016/j.tplants.2004.09.002

Phaenark, C., Niamsuthi, A., Paejaroen, P., Chunchob, S., Cronberg, N., & Sawangproh, W. (2023). Comparative Toxicity of Heavy Metals Cd, Pb, and Zn to Three Acrocarpous Moss Species using Chlorophyll Contents. *Trends in Sciences*, *20*(2), Article 2. https://doi.org/10.48048/tis.2023.4287

Rea, P. A., Vatamaniuk, O. K., & Rigden, D. J. (2004). Weeds, Worms, and More. Papain's Long-Lost Cousin, Phytochelatin Synthase. *Plant Physiology*, *136*(1), Article 1. https://doi.org/10.1104/pp.104.048579

Reski, R. (1998). Development, Genetics and Molecular Biology of Mosses. *Botanica Acta*, *111*(1), 1–15. https://doi.org/10.1111/j.1438-8677.1998.tb00670.x

Salbitani, G., Perrone, A., Rosati, L., Laezza, C., & Carfagna, S. (2022). Sulfur Starvation in Extremophilic Microalga Galdieria sulphuraria: Can Glutathione Contribute to Stress Tolerance? *Plants*, *11*(4), Article 4. https://doi.org/10.3390/plants11040481

Sassmann, S., Weidinger, M., Adlassnig, W., Hofhansl, F., Bock, B., & Lang, I. (2015). Zinc and copper uptake in Physcomitrella patens: Limitations and effects on growth and morphology. *Environmental and Experimental Botany*, *118*, 12–20. https://doi.org/10.1016/j.envexpbot.2015.05.003

Scandalios, J. G. (2002). Oxidative stress responses—What have genome-scale studies taught us? *Genome Biology*, *3*(7), reviews1019.1. https://doi.org/10.1186/gb-2002-3-7-reviews1019

Scandalios, J. G. (2005). Oxidative stress: Molecular perception and transduction of signals triggering antioxidant gene defenses. *Brazilian Journal of Medical and Biological Research = Revista Brasileira De Pesquisas Medicas E Biologicas*, *38*(7), 995–1014. https://doi.org/10.1590/s0100-879x2005000700003

Schützendübel, A., & Polle, A. (2002). Plant responses to abiotic stresses: Heavy metal-induced oxidative stress and protection by mycorrhization. *Journal of Experimental Botany*, *53*(372), 1351–1365. https://doi.org/10.1093/jexbot/53.372.1351

Shakya, K., Chettri, M. K., & Sawidis, T. (2008). Impact of Heavy Metals (Copper, Zinc, and Lead) on the Chlorophyll Content of Some Mosses. *Archives of Environmental Contamination and Toxicology*, *54*(3), 412–421. https://doi.org/10.1007/s00244-007-9060-y

Sharma, I., Pandey, H., Thakur, K., & Pandey, D. (2022). Phytochelatins and Their Application in Bioremediation. In J. A. Malik (Ed.), *Microbial and Biotechnological Interventions in Bioremediation and Phytoremediation* (pp. 81–109). Springer International Publishing. https://doi.org/10.1007/978-3-031-08830-8_4

Shrivastava, M., Khandelwal, A., & Srivastava, S. (2019). Heavy Metal Hyperaccumulator Plants: The Resource to Understand the Extreme Adaptations of Plants Towards Heavy Metals. In S.

Srivastava, A. K. Srivastava, & P. Suprasanna (Eds.), *Plant-Metal Interactions* (pp. 79–97). Springer International Publishing. https://doi.org/10.1007/978-3-030-20732-8_5

SIDHU, M., & BROWN, D. H. (1996). A New Laboratory Technique for Studying the Effects of Heavy Metals on Bryophyte Growth. *Annals of Botany*, *78*(6), 711–717. https://doi.org/10.1006/anbo.1996.0181

Stafilov, T., Šajn, R., Boev, B., Cvetković, J., Mukaetov, D., Andreevski, M., & Lepitkova, S. (2010). Distribution of some elements in surface soil over the Kavadarci region, Republic of Macedonia. *Environmental Earth Sciences*, *61*(7), Article 7.

Stanković, J. D., Janković, S., Lang, I., Vujičić, M. M., Sabovljević, M. S., & Sabovljević, A. D. (2021). The toxic metal stress in two mosses of different growth forms under axenic and controlled conditions. *Botanica Serbica*, *45*(1), 31–47.

Stanković, J. D., Sabovljević, A. D., & Sabovljević, M. S. (2018). Bryophytes and heavy metals: A review. *Acta Botanica Croatica*, *77*(2), Article 2. https://doi.org/10.2478/botcro-2018-0014

Sun, S.-Q., He, M., Cao, T., Yusuyin, Y., Han, W., & Li, J.-L. (2010). Antioxidative responses related to H2O2 depletion in Hypnum plumaeforme under the combined stress induced by Pb and Ni. *Environmental Monitoring and Assessment*, *163*(1), 303–312. https://doi.org/10.1007/s10661-009-0835-7

Sun, S.-Q., He, M., Cao, T., Zhang, Y.-C., & Han, W. (2009). Response mechanisms of antioxidants in bryophyte (Hypnum plumaeforme) under the stress of single or combined Pb and/or Ni. *Environmental Monitoring and Assessment*, *149*(1), 291–302. https://doi.org/10.1007/s10661-008-0203-z

Sun, S.-Q., Wang, G.-X., He, M., & Cao, T. (2011). Effects of Pb and Ni stress on oxidative stress parameters in three moss species. *Ecotoxicology and Environmental Safety*, *74*(6), 1630–1635. https://doi.org/10.1016/j.ecoenv.2011.04.002

Świsłowski, P., Rajfur, M., & Wacławek, M. (2020). Influence of Heavy Metal Concentration on Chlorophyll Content in Mosses. *Ecological Chemistry and Engineering S*, *27*(4), 591–601. https://doi.org/10.2478/eces-2020-0037

Tchounwou, P. B., Yedjou, C. G., Patlolla, A. K., & Sutton, D. J. (2012). Heavy Metal Toxicity and the Environment. In A. Luch (Ed.), *Molecular, Clinical and Environmental Toxicology: Volume 3: Environmental Toxicology* (pp. 133–164). Springer. https://doi.org/10.1007/978-3-7643-8340-4_6

Tremper, A. H., Agneta, M., Burton, S., & Higgs, D. E. B. (2004). Field and laboratory exposures of two moss species to low level metal pollution. *Journal of Atmospheric Chemistry*, *49*(1–3), 111–120. Scopus. https://doi.org/10.1007/s10874-004-1218-7

Vernoux, T., Wilson, R. C., Seeley, K. A., Reichheld, J.-P., Muroy, S., Brown, S., Maughan, S. C., Cobbett, C. S., Van Montagu, M., Inzé, D., May, M. J., & Sung, Z. R. (2000). The ROOT MERISTEMLESS1/CADMIUM SENSITIVE2 Gene Defines a Glutathione-Dependent Pathway Involved in Initiation and Maintenance of Cell Division during Postembryonic Root Development. *The Plant Cell*, *12*(1), Article 1. https://doi.org/10.1105/tpc.12.1.97

Wood, Z. A., Schröder, E., Robin Harris, J., & Poole, L. B. (2003). Structure, mechanism and regulation of peroxiredoxins. *Trends in Biochemical Sciences*, *28*(1), 32–40. https://doi.org/10.1016/s0968-0004(02)00003-8

Yadav, S. K. (2010). Heavy metals toxicity in plants: An overview on the role of glutathione and phytochelatins in heavy metal stress tolerance of plants. *South African Journal of Botany*, *76*(2), 167–179. https://doi.org/10.1016/j.sajb.2009.10.007

Zengin, F. K., & Munzuroglu, O. (2005). Effects of some heavy metals on content of chlorophyll, proline and some antioxidant chemicals in bean [Phaseolus vulgaris L.] seedlings. *Acta Biologica Cracoviensia. Series Botanica*, *47*(2). http://agro.icm.edu.pl/agro/element/bwmeta1.element.agro-article-194d9de5-de29-488e-8a51-3ae04e829833

PAPER I

Environmental and Experimental Botany 209 (2023) 105292

Contents lists available at ScienceDirect

Environmental and Experimental Botany

journal homepage: www.elsevier.com/locate/envexpbot

Heavy metal stress induces adaptative responses in the liverwort *Conocephalum conicum* L. (Dum.): An integrated biologic and metabolomic study

Viviana Maresca [a], Roberta Teta [b], Claudia Finamore [b], **Piergiorgio Cianciullo**[a], Sergio Sorbo [c], Maria Valeria D'Auria [b*], Adriana Basile [a*]

a *Department of Biology, University of Naples Federico II, via Cinthia – Edificio 7, Naples 80126, Italy*
b *Department of Pharmacy, University of Naples, Via Domenico Montesano, 49, Naples 80131, Italy*
c *CeSMA, section of Microscopy, University of Naples Federico II, Naples, Italy*

DOI: https://doi.org/10.1016/j.envexpbot.2023.105292

Abstract

Bioaccumulation, ultrastructural and DNA damage, oxidative stress, and metabolomic analyses were carried out *in vitro* on the liverwort *Conocephalum conicum* L. in response to the heavy metal concentrations measured in two sites along the Sarno river (C1 and C2) representative of two different environmental conditions. Bioaccumulation and bioconcentration data confirm *C. conicum* is a good bioindicator. Our TEM observations showed typically preserved ultrastructure of the chloroplasts in C1 samples, nearly identical to the chloroplasts of the control sample (CTRL; freshly collected and not exposed), whereas in C2 samples they appeared misshaped, swollen and with poorly developed thylakoids in a rather clear stroma. DNA damage, antioxidant enzymatic activity, ROS production and localization showed no difference between CTRL and C1 samples, instead significant differences between C1 and C2 samples. In addition, in this study, we used for the first time the untargeted MS based molecular networking to examine the role of heavy metal stress in the differential production of the secondary metabolites (SM) in *C. conicum*. Metabolome analysis evidenced no changes between CTRL and C1 samples, instead a dramatic change in SM production under metal stress conditions, in particular a remodeling of the lipid metabolism through the production of members of betaine and oxidated lipid classes, as well as production of flavonoids was observed. All the occurred variations respond consistently with the heavy metal concentration trend so we can propose them as pollution biomarkers.

1. Introduction

Environmental pollution, that is, the deviation from an absolutely natural situation due to anthropogenic intervention, is something enormously complex and diverse in relation to a very large number of factors involved and, consequently, the response that living organisms enact is equally diverse and complex. Understanding the occurring events, however, is essential, not only to elucidate the complex biological response of the organisms studied, but also to be able to use the highlighted responses as potential biomarkers of pollution. The Sarno River (Campania, Italy) is known as one of the most impacted rivers in Europe. Due to the high environmental pressure of local activities, the entire river basin (500 km2, 700,000 inhabitants) has been declared by the Italian government as a "high risk area of environmental crisis" (Arienzo et al., 2019). Bryophytes are often used as model study plants for their ability to respond to pollution in general and heavy metal stress in particular. They could act both as bioindicators of elemental pollution and as bioremediation tools (Fasani et al., 2022). In a past study, we transplanted the aquatic moss *Leptodictyum riparium* into the Sarno River to evaluate the effects of heavy metals at three sites representative of three different environmental conditions by measuring ultrastructural changes, generation of reactive oxygen species (ROS), glutathione S-transferase (GST) activity, and induction of Heat Shock Proteins 70 (HSP70s) (Maresca et al., 2018). In this study we chose *Conocephalum conicum* (Dum.) (Marchantiales, Bryophyta), as the model organism for our analysis not only because it is one of the few bryophyte species able to grow in the Sarno River area, even in the presence of severe environmental degradation, but also because this species is able to respond consistently to heavy metal pollution both in the field and *in vitro*, inducing different biological responses such as antioxidant enzymatic responses, ROS production, and induction of HSP70s (Maresca, Lettieri, et al., 2020a). In addition, we have shown that, in response to increasing concentrations of heavy metals, the phenolic content *in C. conicum* increases, through the synthesis of antioxidant phenolic compounds, resulting in enhanced antioxidant defense (Maresca et al., 2022). As matter of fact, very recently interest has arisen in the ability of plants subjected to heavy metal stress, to modify their secondary metabolism (Berni et al., 2019) with metabolite production as a defense response. Specifically, under abiotic stress conditions, such as heavy metals, plants show increased synthesis of polyphenols, such as phenolic acids and flavonoids, which help the plant cope with environmental stresses (Sharma et al., 2019). Studies conducted on *Moringa oleifera* L. grown under conditions of cadmium and lead stress (Nouman et al., 2020), showed that the increase in polyphenols and enzymatic and nonenzymatic antioxidant activities is due to heavy metals. So far, the studies in this field were usually limited to the assessment of the total polyphenol content or to the determination of extent of the transcriptional levels of some

genes involved in the biosynthesis of phenolic compounds, with a few studies focused on the identification of the specific phenolic components whose biosynthesis was induced. The main purpose of this study is to analyze at molecular level the variation of the secondary metabolite production induced in *C. conicum* by heavy metal stress. Considering that the production of specific secondary metabolites is strongly influenced by multiple biotic and abiotic factors, (Ramakrishna & Ravishankar, 2011) in the present multidisciplinary study we evaluated the biological and chemical response of *C. conicum* to heavy metals (Cr, Zn, Cu, Cd, Pb), by reproducing *in vitro* heavy metal contamination, environmental conditions as measured in the field at the 2 sites of Sarno River. Specifically, *C. conicum* has been exposed to concentrations of heavy metals as those measured at upstream and downstream river: these two sites are characterized by very different environmental conditions being the first representative of the preserved environment, and the second a site affected by high anthropogenic pressure. Regarding biological effects, metal bioaccumulation and bioconcentration, ultrastructural damage, DNA damage, and oxidative stress (ROS content and localization, antioxidant enzyme activity) were analyzed, revealing variation in these parameters in relation to changes in heavy metal concentrations. As concerning the metabolomic analysis, in the present study, the small molecules, whose production is induced by metal exposure, have been comprehensively profiled using high resolution LC-MS/MS analysis and the chromatographic and spectrometric data used to elaborate a Feature-Based Molecular Network (FBMN) through the GNPS platform (Wang et al., 2016). With its intrinsic capability to group in clusters structurally related molecules, MS-based molecular networking enables the dereplication of complex extracts in a fast and high-throughput manner. To the best of our knowledge, this is one of the few reports in which the untargeted metabolomics technique that is molecular networking is applied in the study of the effects of the abiotic stress in a plant species.

2. Materials and methods

2.1. Plant material

Samples of *C. conicum* L. Dum were collected in March 2020 from upstream river Sarno, identified by prof. Adriana Basile and a sample were deposited in the herbarium of the Botanical Garden of the University Federico II Napoli. These samples were used for *in vitro* experiments.

2.2. Heavy metal analysis in water samples

Two sites were chosen: one upstream **(C1)** and the other downstream **(C2)** of the Sarno river and in each site three water samples were collected for the subsequent analysis of heavy metals (Section

3.4). The concentrations of heavy metals measured in the two selected sites were chosen as reference for the in vitro growth of the liverwort.

3.3. In vitro growth

C. conicum samples collected at the Sarno river, washed with deionized water, were cultured in Petri dishes (10 cm diameter), 20 specimens per dish, using sterile modified Mohr medium, pH 7.5, with the addition of the metal salts (Esposito et al., 2012). Liverwort, as it grew along the banks of the Sarno river, where the waters lapped the basal surface of the thallus, were placed in Petri dishes after careful but delicate removal of the layer of soil adhering to the lower surface held by the rhizoids, with a small brush, so that Mohr's solution with the metals wetted only the lower portion of the thallus. It was important not to "submerge" the samples to ensure that the plant was able to carry out gas exchange through the pores correctly. The cultures were maintained for 7 days in a climatic room and the environmental parameters were set according to the environmental conditions registered in the field. In particular: air temperature was maintained at 20 ± 1.5 ◦C, and 13 ± 1.3 ◦C, mean ± SD, during day and night, respectively; relative humidity was 70 ± 4% mean ± SD, 16 h light (Photosynthetic Active Radiation 400 μmolm2 s^{-1})/8 h dark photoperiod. These environmental parameters were chosen according to the period of the year in which the collection took place so as not to subject the samples to further stress. The *C. conicum* samples were treated with heavy metals adding to the medium the metals as soluble salts: CrCl3, CdCl2, CuSO4, Pb(CH3COO)2, and ZnCl2 with the relative anions as K salts in CTRL solutions. The concentration of heavy metals administered to the *in vitro* cultured samples are those that have been measured at the field sites, hereinafter referred to as: **C1**, using metals concentration upstream site (site C1 40◦49'56.269" N, 14◦35'27.103◦ E), **C2**, using metals concentration downstream site (site C2 40◦44'48.812" N, 14◦31'37.653" E). The *in vitro* cultures were performed in triplicate and repeated three times. At each time, the liverwort exposed to the same concentration of heavy metals were pulled and the analysis described hereafter were carried out on three subsamples.

2.4. Analytical determination of metals in water samples and in liverwort

The water samples collected in the field experimental sites were filtered through Whatman paper (no. 42) and analyzed by ICP-MS (Perkin-Elmer Sciex 6100) for the concentration of selected heavy metals: Cr, Cd, Cu, Pb, and Zn. Analytical quality was checked by analyzing the Standard Reference Material SRM 1463d "river water". The precision of analysis was estimated by the coefficient of variation of 3 replicates and was found to be < 10% for all elements. As regards the *C. conicum* samples, the protocol of Maresca et al. (2018) was followed. Concentrations of selected toxic metals (Cr, Cd, Cu, Pb, Zn), expressed on a dry weight basis, were determined by ICP-MS (Perkin- Elmer

Sciex 6100). Analytical quality was checked by analyzing the Certified Reference Material BCR 61 "aquatic moss" (*Platyhypnidium riparioides*, Hedw.) with a recovery percentage of 84%. The Precision of analysis was estimated by the coefficient of variation of 3 replicates and was found to be < 10% for all elements. For both experiments, Bioconcentration Factor (BF) was calculated as the ratio between of the metal in the plant (μg g^{-1}) to the metal in the water (μg L^{-1}) (Ahmad et al., 2014).

2.5. Ultrastructural observations

For our TEM observations subapical parts of the thalli, about 5 mm below the apex and above the central nerve, were cut out by a sharp blade. Specimens were fixed in 2.5% glutaraldehyde in phosphate buffer solution (pH 7.2–7.4) overnight at 4 ◦C and post-fixed with 1% OsO4 and 0,8% KFeCN, buffered as glutaraldehyde solution, for 1.5 h at room temperature, dehydrated with ethanol up to propylene oxide and embedded in Spurr's epoxy medium (Basile et al., 2001). Ultra-thin (70 nm thick) sections were put on 300-mesh copper grids, then stained with Uranyl Replacement Stain UAR (Electron Microscopy Science) and lead citrate and observed under a Philips EM 208 S TEM (Basile et al., 2001) (Basile et al., 2001). Ultrastructural observations focused on the photosynthetic parenchyma, a well-known target of pollution damage; 3 specimens from each site were observed.

2.6. Imaging of peroxides with 2',7'-dichlorofluorescein diacetate

To visualize intracellular ROS, we used fluorescent probe 2′ - 7′ dichlorofluorescein diacetate (DCF-DA) (Sigma-Aldrich Co., St Louis, MO, USA), which, solubilized in dimethyl sulfoxide DMSO, was diluted with 10 mM Tris-HCl (pH 7.4) up to a 50 μM stock solution. MilliQ water was employed to dilute the stock solution up to 25 μM. Thin cross sections from fresh sample thalli were treated with DCF-DA solution for 30 min and then washed for 10 min three times in the same buffer. C2 sample were also observed after treatment with the buffer solution without DFC-DA, to evaluate autofluorescence and the effect of the only buffer solution. Observations were performed under a laser-scanning confocal microscope (Leica TCS SP5, Wetzlar, Germany), with an excitation at 476 nm. Emissions were detected as bandwidths at 485/575 nm (green light) and 610/685 nm (red light) (beginning–end); gain and offset values were kept fixed under all the observations. Three samples were observed for each treatment.

2.7. Detection of ROS

A fluorescent technique using 2',7'-dichlorofluorescin diacetate (DCFH-DA) has been used for quantitative measurement of ROS production (Maresca et al., 2018). About 1 g of samples was

incubated with 5 µM DCFH-DA for 30 min at 37 ± 1 ◦C and analyzed using a with an automatic plate reader. ROS quantity was monitored by fluorescence (excitation wavelength of 350 nm and emission wavelength of 600 nm

2.8. Antioxidant enzymes' activity

Enzyme extraction and the determination of Superoxide Dismutase (SOD), Catalase (CAT) and Glutathione S-transferase (GST) activities was performed as in Maresca et al., (2018) with some modifications. One gram (fresh weight) of plant material was ground with 1 mL of chilled NaH2PO4/ Na2HPO4 buffer (PBS, 50 mM, pH 7.8) containing 0.1 mM ethylenediaminetetraacetic acid (EDTA) and 1% polyvinylpyrrolidone (PVP). The homogenate was centrifuged at 12,000g for 30 min, and the supernatant (enzyme extraction) was collected for protein assay and the determination of SOD, CAT, and GST. Protein concentration was quantified spectrophotometrically at 595 nm according to the Bradford method with bovine serum albumin (BSA) as the standard (Bradford, 1976). CAT activities were calculated and expressed as decrease in absorbance at 240 nm due to H2O2 consumption using a commercial kit (Sigma-Aldrich Co., St Louis, MO, USA) and according to the manufacturer's protocol. Superoxide dismutase (SOD, EC 1.15.1.1) activity was spectrophotometrically determined at 450 nm with a commercial kit (19160, Sigma). Glutathione S-transferase (GST, EC 2.5.1.18) activity was measured using a commercial kit (CS0410, Sigma).

2.9. DNA damage

The typical Comet assay for animal and human cells is not able to lyse plant cell wall, so plant nuclei have to isolated mechanically (Gichner & Plewa, 1998). The protocol was performed as reported in Maresca et al., (2018) with some modifications. The material plant was gently sliced using a fresh razor blade. The plate was kept tilted on ice so that the isolated nuclei would collect in the buffer 1.5 mL of cold 400 mM Tris buffer, pH 7.5. A nuclear suspension and 1% low melting point (LMP) agarose prepared with PBS were added. The nuclei and the LMP agarose were gently mixed and aliquots placed on microscope slides which were pre-coated with 1% normal melting point (NMP) agarose. The slides were placed in a horizontal gel electrophoresis tank containing freshly prepared cold electrophoresis buffer (1 mM Na2EDTA and 300 mM NaOH, pH > 13). The nuclei were incubated for 15 min prior to electrophoresis at 0.72 V/cm (26 V, 300 mA) for 5 min at 4 ◦C Finally, the slides were gently washed twice in a neutralization buffer to remove alkali and detergent and stained with DAPI. A fluorescence microscope (Nikon Eclipse 50i, Nikon, Japan) was used to examine the slides, analyzing a minimum of 50 randomly selected nuclei from each slide and avoiding overlapping figures. A computerized image-analysis system (CometScore) was employed. Twenty-

five nuclei were scored per slide, three slides were evaluated per treatment and each treatment was repeated at least twice. From the repeated experiments, DNA damages, Tail moment and Olive moment from each slide were calculated.

2.10. Preparation of crude extracts

C. conicum samples, C1 (150 mg, wet weight) and C2 (150 mg, wet weight) and CTRL (150 mg, wet weight), were frozen overnight and freeze-dried for 24 hours. The lyophilized material was dissolved in 10 mL of 80% MeOH/H2O solution, sonicated for 15 minutes and centrifuged at 1300 rpm for five minutes. Then, the supernatant was dried under vacuum to furnish about 9.8 mg of C1 and 5.6 mg of C2 and 7.2 mg of CTRL as crude extracts. The three extracts were dissolved in 200 µL of methanol and filtered on 0.20 µM Millipore filters and centrifuged for 5 minutes at 13,000 rpm. The supernatants were analyzed by LC-HRMS/MS analysis in triplicates.

2.11. LC-HRMS/MS analysis and data pre-processing

C1, C2 and CTRL polar extracts were subjected to LC-HRMS and LC-HRMS/MS analyses using a Thermo LTQ Orbitrap XL high-resolution ESI mass spectrometer coupled to an Agilent model 1100 LC system. A 2.6- µm Kinetex Polar C18 column (100 ×3 mm), maintained at room temperature, was eluted at 300 µL min-1 with H2O (supplemented with 0.1% HCOOH) and ACN, using gradient elution. The gradient program was as follows: 10% ACN for 10 min, 10%→95% ACN for 35 min, 95% ACN for 10 min. Mass spectra were acquired in positive ion detection mode. MS parameters were a spray voltage of 4.8 kV, a capillary temperature of 350 ◦C, a sheath gas rate of 35 units N2 (ca. 150 mL/min), and an auxiliary gas rate of 13 units N2 (ca. 50 mL/min). Data were collected in the data-dependent acquisition (DDA) mode, in which the first, the second, until the fifth most intense ions of a full-scan mass spectrum were subjected to high-resolution tandem mass spectrometry (HRMS/ MS) analysis. The m/z range for data dependent acquisition was set between 150 and 1500 amu. HRMS/MS scans were obtained for selected ions with CID fragmentation, isolation width of 2.0, normalized collision energy of 35, Activation Q of 0.250, and activation time of 30 ms. Data were analyzed using Thermo Xcalibur software. Raw files were imported into MZmine 2.53 (Pluskal et al., 2010; Teta et al., 2019) and processed as reported (Pluskal et al., 2010; Esposito et al., 2019; Teta et al., 2019) with the following specific parameters: noise level was set at 10000; chromatograms were built using an ADAP module with a minimum height of 10000, and m/z tolerance of 0.001 (or 5 ppm); peak alignment was performed using the Join aligner algorithm (m/z tolerance at 0.005 (or 10 ppm), absolute RT tolerance at 0.3 min). [M+Na–H] +, [M+K–H] +, [M+Mg–2 H]+, [M+NH3] +, [M-Na+NH4] +, [M+ 1, 13C] + , [M-35Cl+37Cl]+, [M+56Fe-3 H]+ adducts were filtered out by setting the maximum relative height at 100%. Peaks without associated MS/MS spectrum were finally

filtered out from the peak list. Clustered data were then exported to.mgf file, while chromatographic data including retention times, peak areas, and peak heights were exported to a.csv file. The.mgf and.csv files were then submitted to the GNPS website (https://gnps.ucsd.edu).

2.12. Molecular networking and dereplication

A molecular network was generated on GNPS' online platform using the Feature Based Molecular Networking (FBMN) workflow (Nothias et al., 2020) with the following parameters: the precursor ion and the MS/MS fragment ion mass tolerance were both set to 0.02Da, the cosine score at above 0.6 and matched peaks at above 6. The analogue search mode was used by searching against MS/MS spectra with a maximum difference of 100.0 in the precursor ion value. Search against GNPS spectral libraries was performed using a cosine score above 0.6 and at least 6 matched peaks. MolNetEnhancher (Nothias et al., 2020; Pluskal et al., 2010) and Dereplicator+ (Mohimani et al., 2018) workflows were used to annotate MS/MS spectra. The FBMN was visualized with Cytoscape v. 3.7.1 (Shannon et al., 2003) and nodes were color-coded according to the chemical class of compounds.

2.13. Nomenclature

The LIPID MAPS (http://www.lipidmaps.org) classification System and shorthand annotation for lipid mass spectra were used for lipid data presentation (Liebisch et al., 2020).

2.14. Statistical analysis

One-way ANOVA was applied for analyzing the differences among sites and CTRL in terms of heavy metals concentration in the water and liverwort, ROS production, antioxidant activity and DNA damage and data were appropriately log-transformed to meet statistical assumptions. The assumptions of normality (the Kolmogorov–Smirnov test) and homogeneity of variances (Levene test) were tested and when necessary, the data were log transformed. The significance of differences was estimated using the post-hoc Student–Newman–Keuls test at $p < 0.05$. Data were analyzed using the software Statistica, version 7.0 (StatSoft, Tulsa OK, USA).

3. Results and discussion

3.1. Heavy metal concentrations in water

The concentrations of all metals measured upstream Sarno river (C1 site) were within the limits permitted by law. In particular, the most toxic metals such as cadmium are below the detection value of the instrumentation and lead, although present, is in very low concentrations. The situation changes dramatically downstream the river (C2 site) where a strong increase of all metals is evident with

Chromium, Zinc, and Copper increasing to the greatest extent. The increment of Chromium is probably related to the industrial use of the territory, due to the presence of tanneries and dyes along the river, even copper can be related to the use of the territory, this time from an agricultural point of view, as it is still used as a sulphate in the treatment of crops. Zinc is released into the environment both naturally (e.g., volcanoes, wind-blown dust, and forest fires) and via anthropogenic activities such as electroplating industry, smelting and refining, mining, biosolids, but the majority of reported contaminations directly affecting people's health was caused by the latter (Tabelin et al., 2018). The most toxic ions, Cd and Pb, increase significantly but to a lesser extent (**Table 1**). Sarno River is the most polluted river in Europe (Ahuja, 2021), due to a number of unfavorable factors, from geological reasons, e.g. the chemical composition of the soil (Albanese et al., 2013) and the very low slope of the river flow, to the wide river basin (over 500 km2) despite of the reduced length of the river, only 25 km, and to the number of different industries established along the course (De Pippo et al., 2006). The high density of population represents a further and worrying factor: about 700,000 people live in the Sarno Basin. The presence of tanneries, different industries, agricultural activities along the river course and a high density of population combined with lacking in the observance of the environment preserving laws made the river Sarno a dumping place. Thus, monitoring of pollution is a priority for the whole area, given the evidence of an increased incidence of cancer pathologies in the population living within the basin. Finally, although the Sarno River is considered one of the most polluted waterways in Europe, significantly higher values of heavy metal concentration were measured in the Ganga River (Paul, 2017), Hindon River (Jain et al., 2005), and in the Regi Lagni (Maresca et al., 2018).

Table 1. Concentrations of heavy metals measured in the waters of the Sarno river expressed as µg L^{-1} at the sites C1 and C2. Three water samples were analyzed for each site. Statistical significance was calculated with one-way ANOVA followed by Tukey's test. * ($p < 0.05$) and * * ($p < 0.01$) indicate significant differences.

	Cr	Zn	Cu	Cd	Pb
Site C1	0.75 ± 0.01	< 0.01	0.83 ± 0.02	< 0.01	0.08 ± 0.001
Site C2	8.24 ± 0.27 * *	18.41 ± 1.34 * *	2.87 ± 0.32 *	0.32 ± 0.01 *	0.78 ± 0.02 *

3.2. Metal bioaccumulation and bioconcentration in the liverwort

After 7 days exposure to the solutions mimicking C1 and C2 heavy metal concentrations, an increase in their concentrations was observed (**Table 2**). The observed increases in C1 samples were lower

with respect to C2. In C1 exposed thalli, the ECs (exposed to control ratios) ranged from 1.1 to 1.6, whilst in C2 samples they ranged from 2.4 to 5.4. Data indicated that the concentrations of heavy metals in the thalli of *C. conicum* reflect those from the exposure solution. Only cadmium was < LOD (Limit of Detection) in the thalli of *C. conicum* both cultured *in vitro* at C1 concentrations and in CTRL samples, which demonstrate the preservation of the upstream river site respect to the downstream. The presence of Pb was observed in traceable quantities in controls thalli (Maresca et al., 2020). These data are in line with the presence of Pb observed in the water sampled in the upstream site. The reported data however are not representative of an environmental scenario since the bioavailability of metals in the in vitro experiments is approximately total. On the contrary, in the environment several factors concur to the bioavailability of the heavy metal (i.e. pH, organic matter content, redox condition) (Magalhães et al., 2015). Overall, *C. conicum* exposed in vitro to environmental relevant concentrations was able to accumulate all the analyzed heavy metals, which have no biological function in plants (Yan et al., 2020). Previous studies reported the ability of foliose liverworts to bioconcentrate relevant amounts of Ni, Fe, and Mn (Parzych et al., 2018) and Cu, Ni, Mn and Fe (Sut-Lohmann et al., 2020). Accordingly, the present study indicates that *C. conicum* might be a promising organism in the biomonitoring of water pollution and phytoremediation projects. The freshly collected samples have a lower concentration of Cr, Cu and Pb, respect sample exposed to C1 concentration, while for Zn and Cd, they are not measurable, like C1 samples. It is surprising that samples exposed for a long time, perhaps for their entire life, to the concentrations of metals measured in water, have lower values than those exposed for only 7 days, but a possible explanation could be the different bioavailability of the metal. In river waters the metal can be linked to chelating organic and inorganic compounds, clay in suspension and so on, while in *in vitro* samples the bioavailability of the metals, administered as inorganic soluble salts, is total.

Table 2. Concentration of the metals (μg g^{-1}) in *C. conicum* gametophytes cultured *in vitro* with C1 and C2 concentrations for 7 days. Data are expressed as mean ± SD. ECs (exposed to control ratios) are calculated following the formula [mean C]exposed / [mean C]control. Bars not accompanied by the same letter are significantly different at $p < 0.05$, using the post-hoc Student–Newman–Keuls test.

	Cr	**Zn**	**Cu**	**Cd**	**Pb**
CTRL	6.7 ± 1.3^{a}	24.7 ± 2.5^{a}	18.4 ± 2.6^{a}	< 0.01	1.7 ± 0.9^{a}
C1	8.2 ± 1.5^{b}	26.5 ± 3.1^{b}	21.1 ± 1.7^{b}	< 0.01	2.7 ± 0.4^{b}
EC	1.2	1.1	1.1	n.d.	1.6
C2	36.2 ± 2.4^{c}	58.4 ± 11.2^{c}	46.5 ± 3.6^{c}	3.3 ± 0.7^{c}	7.3 ± 1.5^{c}

	Cr	Zn	Cu	Cd	Pb
EC	5.4	2.4	2.5	330	4.3
C2/C1 ratio	4.41	2.2	2.2	n.d.	2.7

3.3. Ultrastructural alterations

TEM observations of the photosynthetic parenchyma above the nerve zone of the thallus clearly show that the chloroplasts from CTRL and C1-treated samples appeared typically oblong, with abundant grana and intergrana thylakoids in a rather dense stroma, starch grains and a few small plastoglobules. That is the typical appearance for chloroplasts. (**Fig. 1a and b**). Differently, in the C2-treated specimens' chloroplasts (**Fig. 1c**) are are swollen and misshaped with bulges and invaginations and show shortage of thylakoids in a clearer stroma, which are signs of damage to the ultrastructure. Chloroplasts are a well-known target of pollution stress, as already shown in other pollutant-treated liverworts such as *Lunularia cruciata* (Basile et al., 2017a)(Basile et al., 2017a) and *Pellia neesiana* (Basile et al., 2017b), and in *C. conicum* too (Basile et al., 2013). The last paper reports that on the same species heavy metal treatments induced an ultrastructure appearance of the chloroplasts comparable to that found in the present work with swelling of the organelle, shortage of thylakoids and clearness of stroma. The swelling of the organelle suggests an income of water inside the chloroplast, which can be a consequence of impairment to selective permeability of the limiting double membrane or depletion of energy due to damage to metabolism (Schwartzman & Cidlowski, 1993). In both cases the imbalance of ion concentrations across the membranes can account for movement of water due to osmotic pressure. Swelling of cell compartments by water income may also explain the found clearness appearance of the stroma, which can take a "more diluted" texture. The structural changes are also consistent with the occurrence of ROS: in fact, oxidants are known to induce lipid peroxidation in cell membranes, (Farmer & Mueller, 2013), and consequently injury to thylakoids (Blokhina et al., 2003)

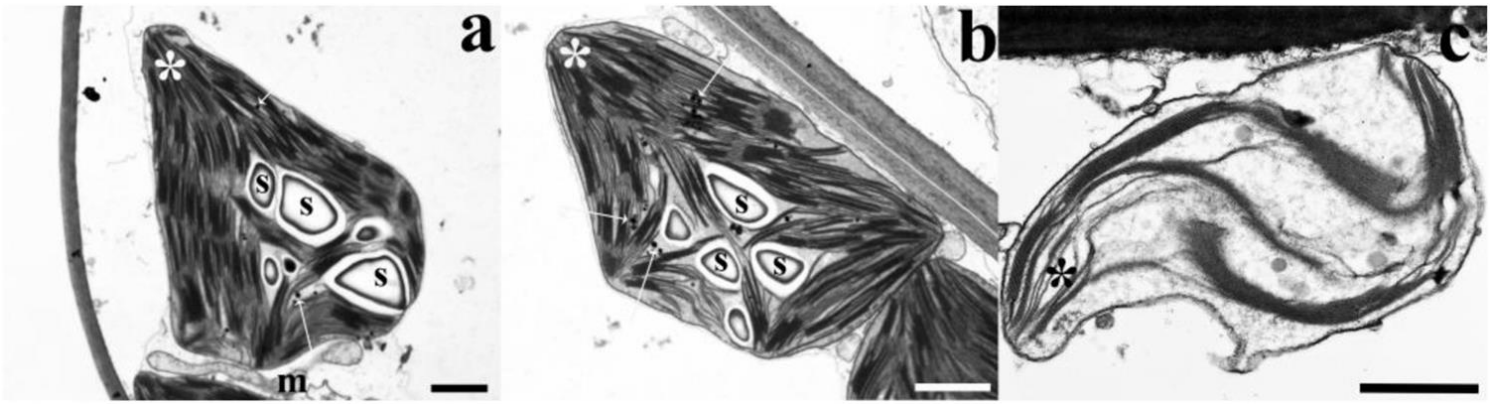

Figure 1. TEM micrographs from the photosynthetic parenchyma of *C. conicum* thallus above the central nerve. CTRL sample (a). The chloroplast shows a typical appearance, with well-developed grana and intergrana thylakoids (asterisk) in a rather dense stroma, a few small plastoglobules (arrows) and starch grains (s). A mitochondrion (m) is visible under the chloroplast. C1-treated sample (b). The long-shaped chloroplast is well-equipped with both grana and intergrana thylakoids (asterisk), contained in a rather electron-dense stroma. A few small plastoglobules (arrows) and starch grains (s) are shown. C2-treated sample (c). The swollen and misshaped chloroplast still presents a few grana and intergrana thylakoids (asterisk) dispersed in a rather clear stroma. Scale bars: 1 μ (a, b, c).

3.4. Imaging of peroxides with 2',7'-dichlorofluorescein diacetate (DFC)

Confocal observations showed DFC green signals from both C1 and C2 samples, the latter emitting stronger than the former. No DFC emission was detected in both the non-treated stained CTRL and treated non-stained C2 (C2ns) samples. Red autofluorescence from chlorophyll was detected as a strong signal from all the samples (**Fig. 2**). Under the fixed imaging settings of our confocal microscopy, confocal observations show green signals from DFC-treated C1 and C2 samples, visualizing intracellular ROS increasing from C1 to C2 specimens. Processing of C2 samples with only buffer and no DFC gives no green emission, but only red autofluorescence from chloroplasts, which demonstrates that green signals arise only from ROS-DFC conjugated. Our observation results are consistent with our chemical data, with ROS amount higher in the C2 samples. The small amount of ROS in the non-treated CTRL samples are also consistent with the absence of any detectable DFC signal from those samples. ROS are visible in the cytoplasm beneath the cell wall, the most metabolically active compartment of the cell, and are almost absent in the central vacuole, as it was shown in the same species exposed to Regi Lagni pollution (Maresca et al., 2022), and to Cd-treatments (Maresca et al., 2020b).

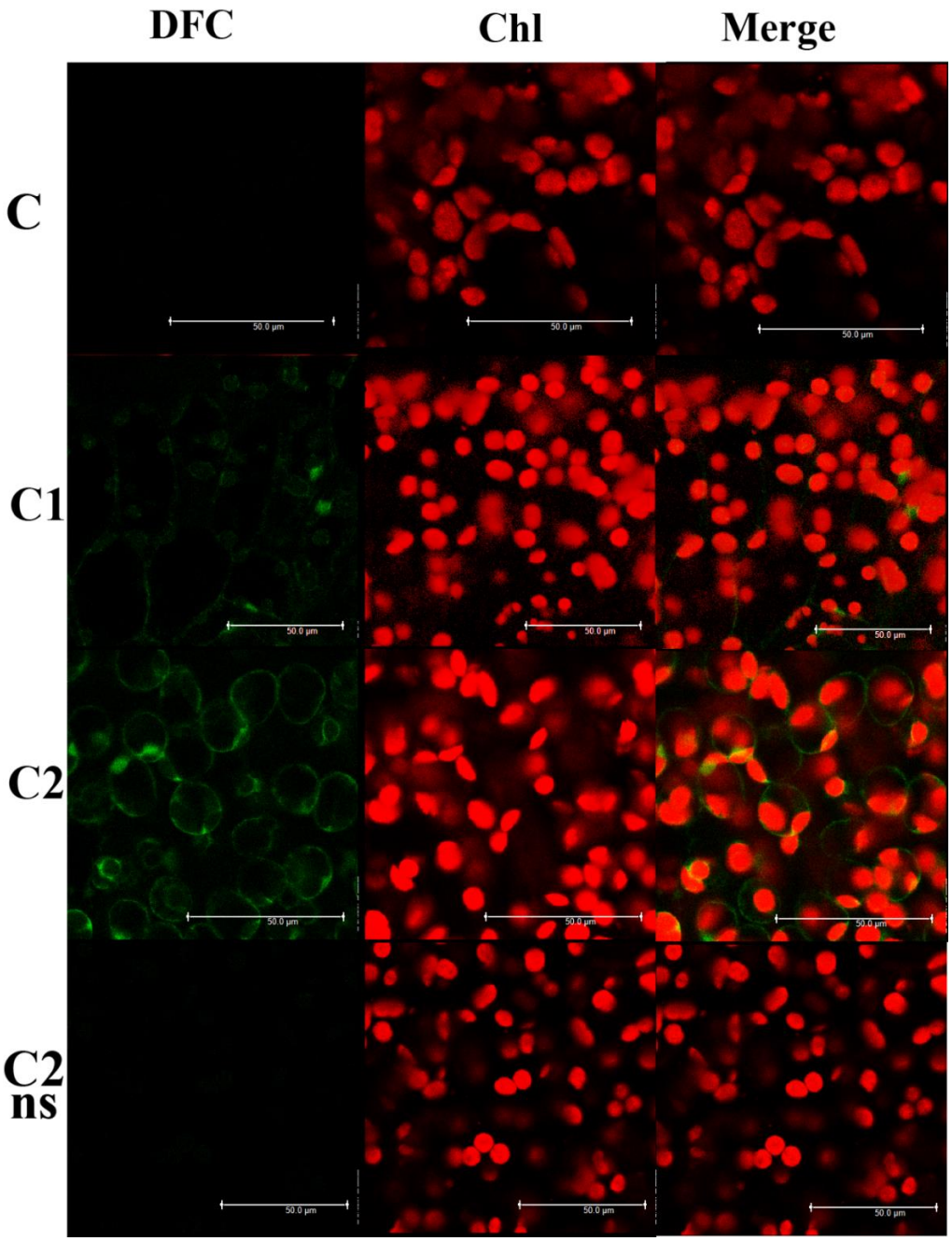

Figure 2. Confocal laser scanning microscopy (CLSM) micrographs of the photosynthetic layer from the in vitro-cultured, DCF-DA-stained *C. conicum* non-treated C (control), treated C1 and C2 samples and non-stained treated C2 (C2ns) one. In the I column DCF signal is displayed in green, in the II one red chloroplast autofluorescence is shown and the III column is the merge. Scale bars: 50 µ.

3.5. Detection of ROS and antioxidant activity enzyme

ROS levels measured both in CTRL and C1 samples showed completely overlapping values. The absence of differences between the CTRL samples (i.e. subjected to tests just taken from the site upstream of the Sarno river and not subjected to any treatment) and the C1 samples should not surprise us, since the in vitro culture conditions reproduce those found in the field at time of collection. Moreover, the sampling method (Section 3.3) ensures that there is no cause for stress. Compared with CTRL and C1 samples, ROS levels in C2 samples are statistically higher. The assessment of antioxidant enzyme catalase (CAT), superoxide dismutase (SOD) and Glutathione S-transferase (GST) activity gave comparable results (**Fig. 3**).

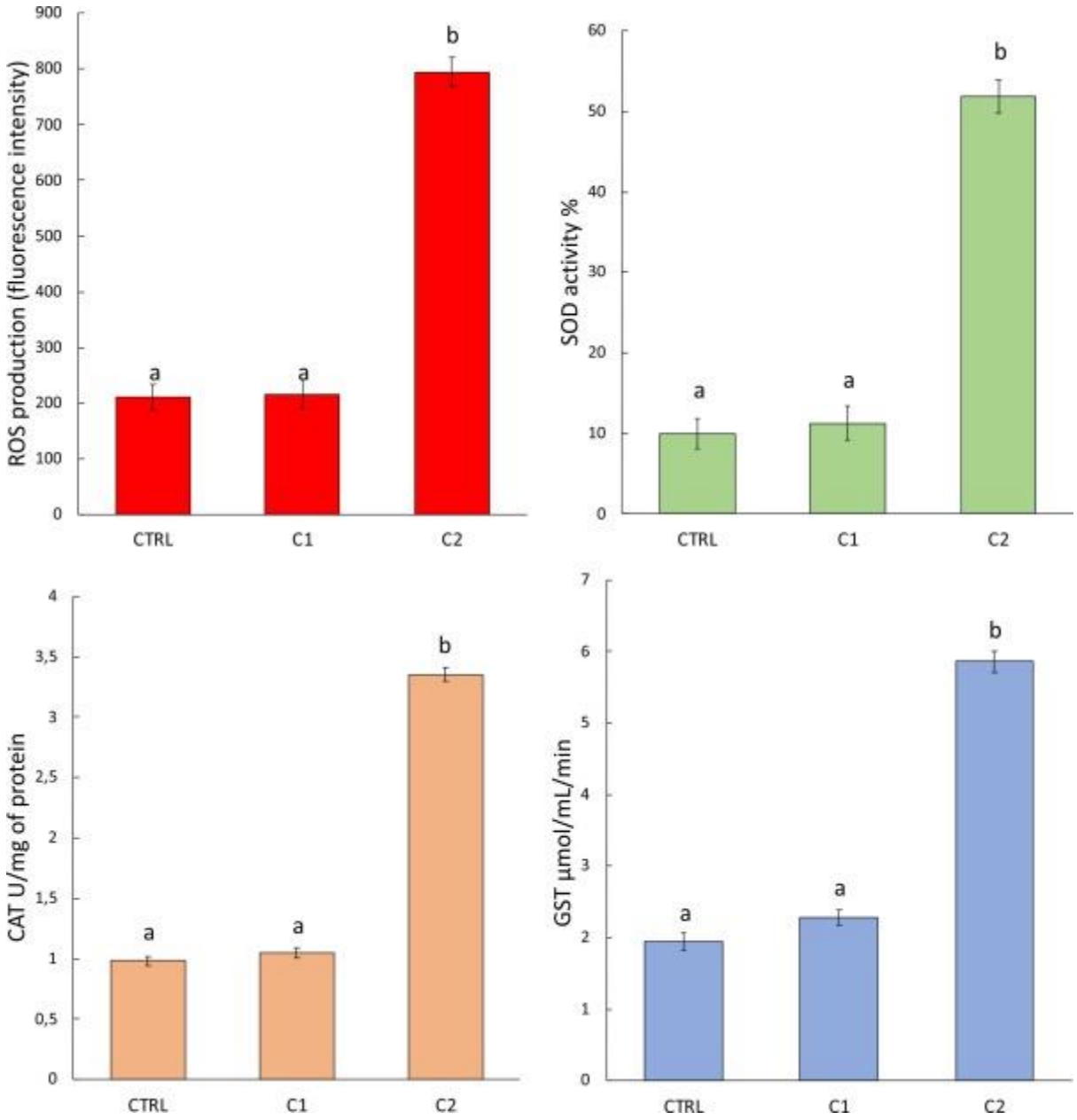

Figure 3. ROS production (fluorescence intensity) and antioxidant responses (SOD, SOD activity inhibition %, CAT, U/mg of protein, GST, mmol/mL/min) in the CTRL, C1 and C2 samples. Values are presented as mean ± st. dev. Means not accompanied by the same letter are significantly different at $p < 0.05$.

These results are in line with those obtained from our previous work. In fact, *C. conicum* was exposed *in vivo* in the Regi Lagni channel (Campania, Italy) (Maresca et al., 2022) and *in vitro* at the same concentrations measured in the field, and the levels of ROS and some antioxidant enzymes were measured. The variation of these parameters was consistent with environmental perturbations, that is, as the levels of heavy metals increase, the levels of ROS and the activity of antioxidant enzymes increase. The same result was also obtained using *L. riparium* exposed along the Sarno river as a model organism (Esposito et al., 2018). Also in this case, the biological responses and their variations have been studied in experiments both in the field and in vitro by reproducing the concentrations measured in the field. Many abiotic stresses, including exposure to heavy metals, can cause plant cell damage directly or indirectly through the blast of ROS. Plant cells are able to respond to high ROS levels by activating their antioxidant defense systems. The main enzymes involved in these defense mechanisms are ROS-quenching enzymes such as catalase, superoxide dismutase and peroxidase. There is increasing evidence suggesting that mechanisms of stress caused by non-Fenton metals (e.g. Pb, Ni, Cd, Cr, etc.) in plant cells can indirectly lead to the production of superoxide radicals, induce lipid peroxidation, elevate the level of some of the key enzymes of antioxidant metabolism and causes severe damage to different cell organelles and biomolecules in plants (Radotić et al., 2000), we can speculate that *C. conicum* owns an enzymatic arsenal that is collectively able to quench ROS even after 7 days of severe heavy metals exposure.

3.6. DNA damage

Using three of the many parameters available to evaluate DNA damage through a comet assay, in particular the Olive Moment, Tail Moment and percentage of DNA in tail, we evaluated that DNA damage level increases statistically significantly from C1 to C2 (Fig. 3) following the trend of concentrations of heavy metals (Table 1). The Comet Assay is a sensitive technique in estimating DNA damage on the single and the double strand (Gedik et al., 1992). The determination of DNA damage using the Comet assay in indicator organisms provides us with early information on the genotoxic potential of the environment in which they live, making it possible to improve environmental intervention strategies. Studies have shown that DNA damage, measured in plants, using comet assay, is an excellent biomarker, extremely sensitive for estimating the genotoxic potential of environmental contaminants, both in environmental monitoring studies and for environmental screening. Maresca et al., for the first time, confirmed the use of Comet assay also in liverworts, as reliable biomarker of environmental pollution (Maresca et al., 2020b). A similar result was also obtained in Maresca et al. (2018), which used the comet assay to evaluate the genotoxic damage in *L. riparium* exposed in the field and in vitro along the Regi Lagni channel. Both studies

show a correlation between the increase in ROS levels and DNA damage in relation to the increase in heavy metals and therefore in environmental pollution. This should not be surprising as an excess of ROS can, among other effects, also cause damage to DNA including its breakdown, which however can also depend on a direct effect of heavy metals on the nucleotide (Roldán-Arjona & Ariza, 2009).

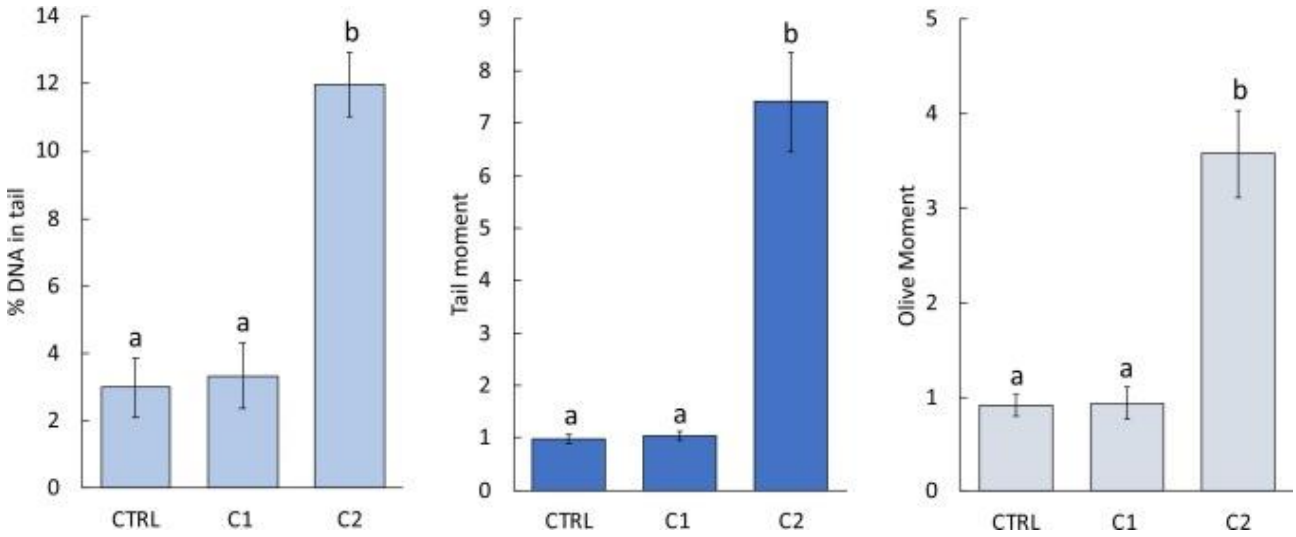

Figure 4. Comet assay results (DNA damages, Tail moment and Olive moment) in the sample C1 and C2 and CTRL. Values are presented as mean ± st. dev. Means not accompanied by the same letter are significantly different at $p < 0.05$.

3.7. Untargeted MS-based molecular networking analysis of the effect of metal stress on the metabolome of *C. conicum*

Due to the tiny morphology of *C. conicum* and in general of liverworts, there are very few previous reports on the phytochemistry of this species (Asakawa & Ludwiczuk, 2018; Radulović et al., 2020). The difficulty to collect adequate amounts of biomass for secondary metabolite isolation requires a microscale fast and reliable chemical analysis method for exploring the variation of secondary metabolite production induced in the liverwort by heavy metal exposition. High resolution liquid chromatography coupled with tandem mass spectrometry (LC-HRMS/MS) represents a well-suited untargeted methodology to analyze the complete metabolome within a heterogeneous mixture, thus enabling a deep and sensitive dereplication. Molecular networking, developed on the web-based open-access platform Global Natural Products Society Molecular Networking (GNPS) (Wang et al., 2016) is an excellent tool for a rapid annotation of natural products (Jouaneh et al., 2022). By clustering structurally related metabolites, according to similarity of the fragmentation pattern, this tool strongly eases the chemical dereplication work, allowing the rapid identification of known

compounds and providing useful hints for structural identification of unknown compounds. Further, by direct visualization and comparison of the results from the analysis of the extracts from the same or close related species, molecular networking is particularly suitable to asset the influence of environmental, geographic (Tong et al., 2021), stress factors, cultivation (Vitale et al., 2020) on the production of the secondary metabolites within a single species. Therefore, samples (in triplicate) of *C. conicum* arising from C1 and C2 and non-treated CTRL subgroups were analyzed by LC-HRMS/MS. Mass spectra were acquired in the positive ion detection mode (mass accuracy ≤ 3 ppm) where the five most intense ions detected in the full MS scan were fragmented in subsequent MS2 scans. The raw LC-HRMS and HRMS/MS data were pre-processed using the MZmine program 2.53 and then the global.mgf file and quantitation table (.csv) were used tognps.ucsd.edu/ProteoSAFe/status.jsp? task=27425adbe8cb4ffea7c677ecac22ff84). The comparative molecular network contains 303 features, 57 of which grouped in 12 clusters (Fig. S2). Clustered features belong solely to C2 (downstream, in blue) extracts, revealing a complete differential metabolism in the three samples. Indeed, the comparative analysis of the molecular fingerprint from the two C1 (upstream, in green) and C2 (downstream, in blue) and CTRL (untreated, in yellow) extracts revealed a complete differential metabolism in the three samples. As concerning the secondary metabolites from C1 and CTRL samples, we observed several self-loop nodes, that didn't cluster each other, indicating that likely they belong to different structural classes. The structural identification of these nodes is beyond the scope of the present study. On the other hand, in C2 samples in addition to isolated nodes, we observed three populated clusters of related molecules, not observed in C1 and CTRL samples, indicating that the production of these molecules is triggered by the heavy metal exposure. Thus, our following analysis was focused on the above three clusters to shed light on the metabolic responses induced by the heavy metal exposure in *C. conicum*.

2.8. Cluster 1 - Glycolipids

Among the three clusters disclosed in the present study, this cluster (**Fig. 5**) is the larger one, in terms of metabolites. None of the molecular formula entered for each node of this subset was automatically annotated by the program. However manual inspection in the LIPID MAPS data bank (http:// www.lipidmaps.org) allowed to tentatively assign the node at *m/z* 509.2721 to a monogalactosyl monoacylglycerol (MGMG), with an acyl 16:3 moiety (16:3 MGMG) (Kwon et al., 1998). The fragmentation pattern features an ion at *m/z* 347.2173 (C19H32O4Na) arising from neutral loss a hexose residue (162 amu). Two further members of this lipid subclass in the cluster (Compounds 2 and 3, Table 3) were tentatively identified by manual inspection of molecular formulas and by diagnostic fragmentation fingerprints, such as the characteristic [(M+ Na) - 162]+ fragment

ion. In particular, the mono-oxidated 16:3 and 18:3 fatty acid chains were assigned to the MGMGs at *m/z* 525 and 553, respectively. The intense MS2 fragmentation ion at [(M+ Na) - 70]+ in both compounds was interpreted as result of β-cleavage around the terminal double bond with γ-H shift (Tatituri et al., 2012), indicative that the terminal double bond is localized at ω7. The nature, the position of the remaining two unsaturation as well as of the oxygen function remain undetermined. With these information elements, we were able to propagate the annotations of the cluster by characterizing all nodes. Indeed, additional 9 nodes (4-12) within the cluster were assigned as members of mono-galactosyldiacylglycerols (MGDG) from the analysis of the positive pseudomolecular ion [M+Na]+ and consequent determination of the molecular formulas and from inspection of the MS2 spectra. The fragmentation pattern of MGDG and of the related di-galactosyldiacylglycerols DGDG has been extensively studied (Tatituri et al., 2012). The analysis of relative intensity of the diagnostic product ions originated by the neutral loss of the variable fatty acid chains gives not only the length, the unsaturation and oxidative degree of each fatty acid chain, but also allows to discriminate the regiochemistry of the acyl chains on the glycerol backbone. In particular, the loss of the acyl group on *sn*-1 position is assisted by the vicinal acyl group on *sn*-2 resulting in the relative fragmentation peak of major intensity (Guella et al., 2003). As exemplified in **Fig. 4**, MGDG at *m/z* 801.4733 (**5**, *R*t 40.1 min) showed a molecular formula C43H70O12 compatible with a (34:6; 2 O) MGDG structure. The MS2 spectrum showed a weak fragment ion at *m/z* [(M+ Na) - 162]+ corresponding to the loss of an hexose residue, and preferential cleavage of a double oxidated 18:3 fatty acid from the *sn*-1 position of glycerol, resulting in the prominent *m/z* 491 fragment ion that contained galactose, glycerol, and the 16:3 fatty acid attached to the *sn*-2 position of glycerol. The less prominent *m/z* 551 fragment ion indicated that 16:3 fatty acid chain was less preferentially cleaved from the *sn-2* position to leave galactose, glycerol, and the 18:3;2 O fatty acid in the *sn*-1 position. To further confirm the assignment, we also acquired the mass spectra in the negative ion mode (Fig. S8). In addition to fragment ions that parallel those observed in the positive ion mode, it is also possible to observe the [R1CO2] and the [R2CO2] at *m/z* 309.3 and 249.2 corresponding to fatty carboxylate anions. The analysis of the fragmentation pattern of the isomeric node (6) at Rt 37.2 min suggested that the compound 6 differs from 5 only for the oxidation status of the two 18:3 and 16:3 acyl chains at *sn*-1 and *sn*-2, respectively. Analogously, remaining MGDG species (Table 3), showing mainly various degrees of oxidation and unsaturation of the fatty acid unit esterified at *sn*-1 positions of the glycerol unit, were tentatively assigned. The mass spectrum profiles of digalactosyldiacylglycerols DGDG (compounds 13-20 in **Table 3**) are very similar to those observed for the corresponding monogalactosyl derivatives. As exemplified for compound **14** (*m/z* 963, Rt 36.5 min), two low intensity fragmentation peaks due to the sequential losses of one galactose

moieties were observed at *m/z* 801 and 639 (**Fig. S18**). Remaining peaks were assigned to the loss of the acyl chains from glycerol backbone. Monogalactosyldiacylglycerols (MGDG) and digalactosyldiacylglycerols (DGDG) represent the main non-phosphorous lipid class, accounting for 80% of the membrane lipids found in green plant tissues (Kelly & Dörmann, 2004), where they are located in the thylakoids of the chloroplasts. There are two distinct biosynthetic pathways for the synthesis of this lipid classes: the eukaryotic pathway via the endoplasmic reticulum, and the prokaryotic pathway that occurs exclusively in plastids. The plastid pathway gives rise to thylakoid lipids with 16-carbon fatty acids in the carbon-2 (C-2) position of the glycerol backbone, whereas lipids derived from the ER pathway contain 18-carbon fatty acids in this position (Kalisch et al., 2016). The presence, almost invariably, of a 16:3 polyunsaturated fatty acid chain at C-2 position of the members of oxidated mono- and digalactosyldiacylglycerols MGDG and DGDG, disclosed in the present study, suggest that these compounds could arose from the chloroplast thylakoid lipids, released in the cytosol as consequence of the observed chloroplast injury caused by heavy metal stress (Fig. 1). Non-enzymatic oxidation reactions of the released lipids by means of the ROS elicited by heavy metal exposure might cause various extent of lipid peroxidation as already observed in plants subjected to heavy metal exposure (Giannakoula et al., 2021; Prado et al., 2015). However, since non enzymatic lipid oxidation usually involved free fatty acids released by the chloroplast membranes, and since in the oxidated lipids identified in the present study, the oxidation occurs regiospecifically at the acyl chain at *sn*-1 position, is also possible to assume the role of specific enzymes in the oxidation, as observed for related oxylipins (Stelmach et al., 2001).

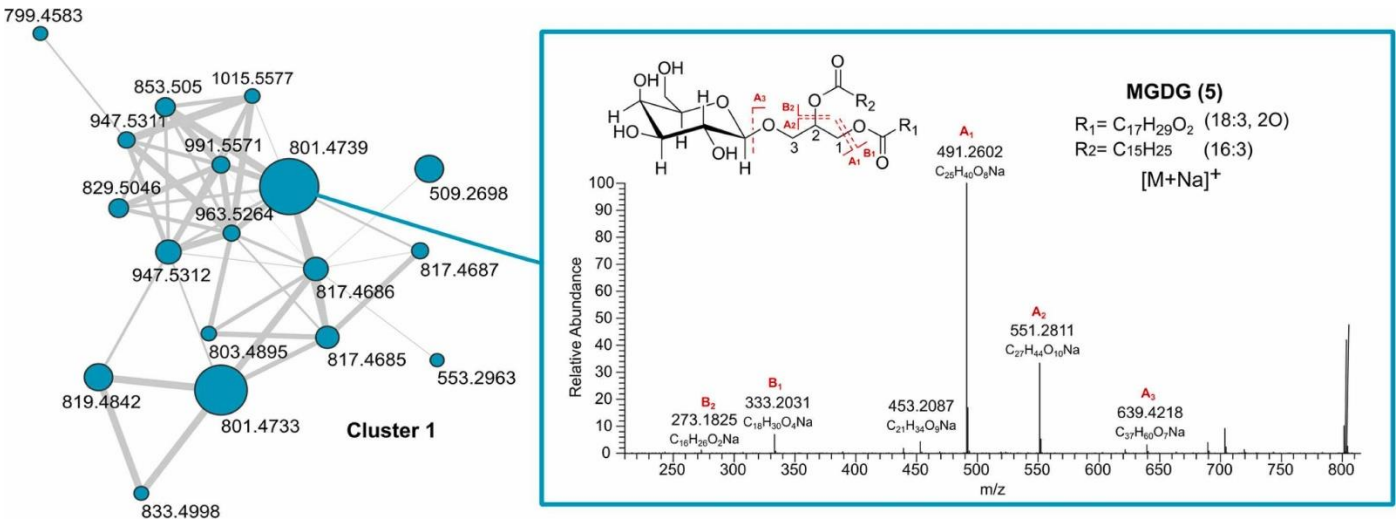

Figure 4. Left: glycolipid [M+Na]+ adduct cluster, the size of the nodes is directly proportional to the precursor ion intensity; right: representative example of the fragmentation pattern.

2.9. Cluster 2 - Monoacyl Betaine Lipids

This cluster contains 1 unrelated node at 496.338 and 4 nodes (17- 19) which were easily identified as monoacylglyceryl-N,N,N-trimethylhomoserines (MGTSs) by manual database search in freely accessible databases of LIPID MAPS. The presence in the MS2 spectrum of the characteristic fragmentation peak at 236.1489 (C10H22O5N), corresponding to the loss of the acyl chain allowed to confirm the positive charged head group and to assign the length and unsaturation degree of the acyl chain, as exemplified in **Fig. 6** and S21. The acyl chains in this cluster range from palmitic acid (16:0) to usual oleic/ linoleic/linolenic acids (18:1, 18:2. 18:3, respectively). Betain lipids (diacylglyceryl-N,N,N-trimethylhomoserines, DGTS or monoacylglyceryl-N,N,N-trimethylhomoserines, MGTS) are a class of polar glycerolipids with a positive quaternary amine alcohol head linked to the glycerol moiety. Betain lipids with two acyl chains (DGTS) were common lipid components in algae (Maciel et al., 2016); in some plants (Rozentsvet et al., 2000), including liverworts (Dembitsky & Rezanka, 1995); whereas the monoacyl MGTS derivatives were so far reported only in the green alga *Chlamydomonas reinhardtii* P. A. Dang. (Abreu et al., 2020). Interestingly, enhanced production of MGTS and DGTS was observed in this green alga as main metabolic response to the oxidative stress caused by transient CO2 shortage. The observed production of MGTS in *C. conicum* as metal stress response could confirm the previous finding and evidenced for the first time the role of this betaine lipids in the tolerance responses activated in plants to heavy metal stress.

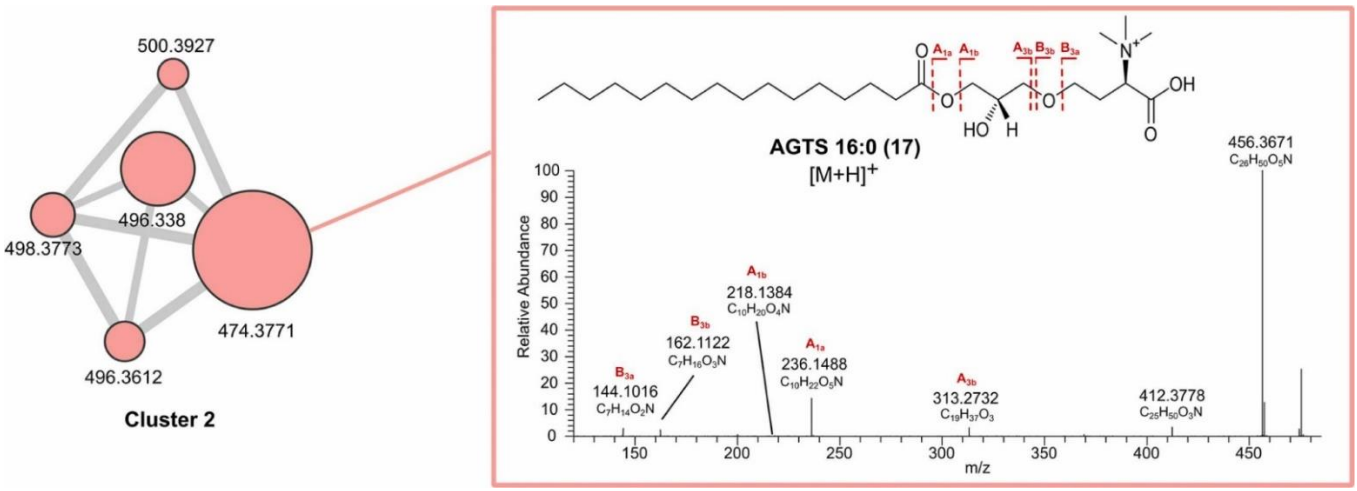

Figure 6. Left: monoacyl betaine lipid [M+H]+ adduct cluster, the size of the nodes is directly proportional to the precursor ion intensity and right: representative example of the fragmentation pattern.

2.10. Cluster 3 - C-glycoside flavones

GNPS library automatically annotated three members of this cluster as flavone C-glycoside derivatives as schaftoside (Li et al., 2018), isoshaftoside (Li et al., 2018) and vicenin-2 (Marrassini et al., 2011). This putative annotation was confirmed by accurate comparison of the mass data in the literature. The fragmentation of C-glycoside flavones in both positive (de Moraes et al., 2007) and negative mode (Ferreres et al., 2008) was extensively studied and rationalized. Usually, due to the acidic nature of the phenol group in flavonoids, more diagnostic fragmentations were observed in the negative mode. For instance the discrimination between isomeric shaftoside (6-C-glucosyl-8-C-arabinosyl apigenin) and isoshaftoside (6-C-arabinosyl-8-C-glucosyl apigenin), only differing for the position of hexose and pentose sugar moieties on the aglycone portion, arose from the analysis of the relative intensities of the fragmentation pattern relative to the pentose unit (losses of 18, 60, 120). These fragmentations were more abundant when the pentose was in position 6 with comparison to position 8. To confirm the identity of schaftoside, isoshaftoside and vicenin-2 we also acquired the MSn spectra of contaminated crude extract in the negative ion mode. The fragmentation pattern perfectly matches those reported in the literature (McCullagh et al., 2021; Silva et al., 2014). The analysis allowed to discriminate between the isomeric nodes at *R*t 17.4 and 17.1 min, assigned to shaftoside/isoshaftoside, respectively. The molecular formula of the node at 607.1657 [M+H]+ was 42 Da (C2H2O) more than shaftoside/isoshaftoside, suggesting that the compound is an acetyl derivative of shaftoside/isoshaftoside. The MSn analysis (Cao et al., 2014) allowed to assign the relative position of the two sugar units on the flavone aglycone as well as the position of the acetyl group. On the basis of the fragment ion peaks observed in the positive ion mode, an apigenin-6-C-hexosyl-8-C- (2''-acetyl pentoside) structure was tentatively assigned. By analogy with shaftoside, apigenin 6-C-glucosyl-8-C-(2''-acetyl arabinoside) structure was tentatively annotated. Two acetyl shaftosides were already described as product of metabolism in bio-samples from rats administered with shaftoside (Liu et al., 2020). The node at *R*t 18.7 min (**28**, [M+H]+ 579.1689), has a molecular formula corresponding to a deoxy-vicenin-2. Likely, it corresponds to a vicenin-2 derivative, with a deoxy-hexose replacing the one of two glucose units in vicenin-2. The careful analysis of the fragmentation pattern evidenced fragment ions relative to the loss of 44, 74 and 104, confirming the presence of a 6-deoxy-hexosyl residue, whereas fragmentation ions corresponding to the loss of 90 and 120 (base peak) were characteristic of a hexose residue (see Fig. S34). Based on the relative intensity of the fragment ions, the hexosyl substitution at C-6 and the 6- deoxy-hexosyl substitution at C8 was tentatively assigned. Isomeric apigenin 6-C-β-chinovopyranosyl-8-C-β-galactopyranoside (Rayyan et al., 2010) was isolated from seeds of *Trigonellafoenum-graecum* L. The node **22** at *R*t min and [M+H]+ at 579.1689 was tentatively annotated as a member of pinnatifinoside family.

Pinnatifinosides C and D were so far reported only from the *Crataegus pinnatifida* Bge. var. major N.E.Br (Zhang & Xu, 2001). Both these unusual C-glycosides, contain an unusual 6''- acetyl-ketohexosefuranoside moiety with a double C7 -O8 connection to the apigenin aglycone moiety resulting in an unprecedented 5,5 spiroketal moiety and were stereoisomeric at spiroketal junction. The observed fragmentation ions match well with the proposed structure (Fig. S26), whereas mass spectrometry didn't allow to discriminate between the stereoisomeric structures. The analysis of the fragmentation pattern of the node **22**, at *m/z* 487.1217, clearly indicated that the compound is a further, undescribed member of pinnatifinoside family with an additional CH2O group. The data in our hands didn't allow a complete chemical characterization of this compound. Analogously, the structure of some nodes within the cluster were left unassigned, since the fragmentation pattern didn't lead to an unambiguous definition of their planar structure. The enhanced production of phenolics in plants under metal stress was observed in many vegetable species (Sharma et al., 2019). Flavonoids are known to exert metal chelation which reduce the effective concentration of metal in cells and their impact on the level of harmful hydroxyl radicals. In addition, flavonoids are considered as H_2O_2 scavengers and have indispensable role in phenolic/ascorbate-peroxidase cycle, the main constituent of ROS homeostasis mechanism (Sharma et al., 2019). Our study disclosed for the first time the production of C-glycosyl flavonoid derivatives with an apigenin aglycone as adaptative response to heavy metal stress in *C. conicum*. Interestingly, vicenin-2 was already described as component of gametophyte tissues of two samples of *C. conicum* from different geographical areas (Markham et al., 1976). C-Glycosylflavones are important bioactive constituents of some medicinal plants, and they demonstrate a range of biological effects including antioxidant, antifungal, and antimicrobial activities. Due to their better chemical stability, as compared to their corresponding O-glycosides, in most studies C-glycosides were found to possess even higher antioxidant potential than O-glycosides or aglycones (Materska, 2015; Xiao et al., 2016). Therefore, *C. conicum* can acquire heavy metal tolerance and to decrease the oxidative damage and overall phytotoxicity induced by metals, by producing a unique mixture of C-glycoside flavonoids with potentially improved antioxidant potential. Further studies, aimed to a better chemical and biological characterization of this fraction will be performed. (**Fig. 7**).

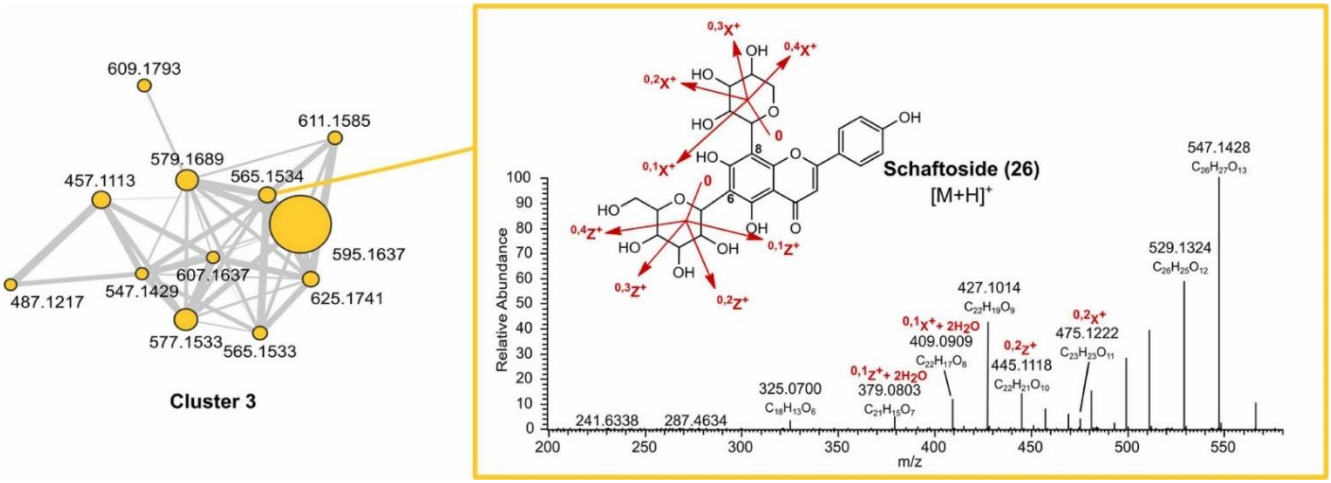

Figure 7. Left: C-glycoside flavone [M+H]+ adduct cluster, the size of the nodes is directly proportional to the precursor ion intensity and right: representative example of the fragmentation pattern.

4. Conclusions

Heavy metal environmental pollution exerts its effects by causing damage at different levels and a range of responses that are addressed to counteract the varied effects of the pollutants. The main purpose of this study is to analyze at molecular level the adaptative response induced by heavy metal stress in *C. conicum* by analyzing the differentiated production of secondary metabolites. For a fast and reliable dereplication of the secondary metabolites in *C. conicum* we used advanced mass spectrometry-based metabolomics and molecular networking tools. This approach allowed to unravel of the metabolome induced by metal stress in *C. conicum* permitting a fast-tentative annotation of several known and unknown metabolites. The enhanced production of oxidated lipids, of members of betain lipid class and of C-glycosides matches all well with previous findings on the role of these metabolites as both stress chemical markers and protective agents and damage markers. The results of the chemical investigation match well with those on ultrastructural damage and antioxidant response. arising from the analysis of ultrastructural organization and damage to DNA. Therefore, the multidisciplinary roadmap proposed in the present study paved the way to future investigations aimed to further mining the secondary metabolome of plants, including those of medicinal and alimentary interest, when exposed to abiotic stress.

References

Abreu, I. N., Aksmann, A., Bajhaiya, A. K., Benlloch, R., Giordano, M., Pokora, W., Selstam, E., & Moritz, T. (2020). Changes in lipid and carotenoid metabolism in Chlamydomonas reinhardtii during induction of CO2-concentrating mechanism: Cellular response to low CO2 stress. *Algal Research*, *52*, 102099. https://doi.org/10.1016/j.algal.2020.102099

Ahmad, S. S., Reshi, Z. A., Shah, M. A., Rashid, I., Ara, R., & Andrabi, S. M. A. (2014). Phytoremediation Potential of Phragmites australis in Hokersar Wetland—A Ramsar Site of Kashmir Himalaya. *International Journal of Phytoremediation*, *16*(12), 1183–1191. https://doi.org/10.1080/15226514.2013.821449

Ahuja, S. (Ed.). (2021). Title page. In *Handbook of Water Purity and Quality (Second Edition)* (pp. i–iii). Academic Press. https://doi.org/10.1016/B978-0-12-821057-4.00022-7

Albanese, S., Iavazzo, P., Adamo, P., Lima, A., & De Vivo, B. (2013). Assessment of the environmental conditions of the Sarno river basin (south Italy): A stream sediment approach. *Environmental Geochemistry and Health*, *35*(3), 283–297. https://doi.org/10.1007/s10653-012-9483-x

Arienzo, M., Toscanesi, M., Trifuoggi, M., Ferrara, L., Stanislao, C., Donadio, C., Grazia, V., Gionata, D. V., & Carella, F. (2019). Contaminants bioaccumulation and pathological assessment in Mytilus galloprovincialis in coastal waters facing the brownfield site of Bagnoli, Italy. *Marine Pollution Bulletin*, *140*, 341–352. https://doi.org/10.1016/j.marpolbul.2019.01.064

Asakawa, Y., & Ludwiczuk, A. (2018). Chemical Constituents of Bryophytes: Structures and Biological Activity. *Journal of Natural Products*, *81*(3), 641–660. https://doi.org/10.1021/acs.jnatprod.6b01046

Basile, A., Cogoni, A. E., Bassi, P., Fabrizi, E., Sorbo, S., Giordano, S., & Cobianchi, R. C. (2001). Accumulation of Pb and Zn in gametophytes and sporophytes of the moss Funaria hygrometrica (Funariales). *Annals of Botany*, *87*(4), 537–543. Scopus. https://doi.org/10.1006/anbo.2001.1368

Basile, A., Loppi, S., Piscopo, M., Paoli, L., Vannini, A., Monaci, F., Sorbo, S., Lentini, M., & Esposito, S. (2017). The biological response chain to pollution: A case study from the "Italian Triangle of Death" assessed with the liverwort Lunularia cruciata. *Environmental Science and Pollution Research*, *24*(34), 26185–26193. https://doi.org/10.1007/s11356-017-9304-y

Basile, A., Sorbo, S., Conte, B., Cardi, M., & Esposito, S. (2013). Ultrastructural changes and Heat Shock Proteins 70 induced by atmospheric pollution are similar to the effects observed under in vitro heavy metals stress in Conocephalum conicum (Marchantiales – Bryophyta). *Environmental Pollution*, *182*, 209–216. https://doi.org/10.1016/j.envpol.2013.07.014

Basile, A., Sorbo, S., Lentini, M., Conte, B., & Esposito, S. (2017). Water pollution causes ultrastructural and functional damages in Pellia neesiana (Gottsche) Limpr. *Journal of Trace Elements in Medicine and Biology*, *43*, 80–86. https://doi.org/10.1016/j.jtemb.2016.11.014

Berni, R., Luyckx, M., Xu, X., Legay, S., Sergeant, K., Hausman, J.-F., Lutts, S., Cai, G., & Guerriero, G. (2019). Reactive oxygen species and heavy metal stress in plants: Impact on the cell wall and secondary metabolism. *Environmental and Experimental Botany*, *161*, 98–106. https://doi.org/10.1016/j.envexpbot.2018.10.017

Blokhina, O., Virolainen, E., & Fagerstedt, K. V. (2003). Antioxidants, oxidative damage and oxygen deprivation stress: A review. *Annals of Botany*, *91 Spec No*, 179–194. https://doi.org/10.1093/aob/mcf118

Cao, J., Yin, C., Qin, Y., Cheng, Z., & Chen, D. (2014). Approach to the study of flavone di-C-glycosides by high performance liquid chromatography-tandem ion trap mass spectrometry and its application to characterization of flavonoid composition in Viola yedoensis. *Journal of Mass Spectrometry*, *49*(10), 1010–1024. https://doi.org/10.1002/jms.3413

de Moraes, S. L., Tomaz, J. C., & Lopes, N. P. (2007). Liquid chromatography-tandem mass spectrometric method for determination of the anti-inflammatory compound vicenin-2 in the leaves

of L. ericoides Mart. *Biomedical Chromatography: BMC*, *21*(9), 925–930. https://doi.org/10.1002/bmc.828

de Paiva Magalhães, D., da Costa Marques, M. R., Baptista, D. F., & Buss, D. F. (2015). Metal bioavailability and toxicity in freshwaters. *Environmental Chemistry Letters*, *13*(1), 69–87. https://doi.org/10.1007/s10311-015-0491-9

De Pippo, T., Donadio, C., Guida, M., & Petrosino, C. (2006). The case of Sarno River (Southern Italy): Effects of geomorphology on the environmental impacts. *Environmental Science and Pollution Research International*, *13*(3), 184–191. https://doi.org/10.1065/espr2005.08.287

Dembitsky, V. M., & Rezanka, T. (1995). Distribution of diacylglycerylhomoserines, phospholipids and fatty acids in thirteen moss species from Southwestern Siberia. *Biochemical Systematics and Ecology*, *23*(1), 71–78. https://doi.org/10.1016/0305-1978(95)93660-U

Esposito, S., Loppi, S., Monaci, F., Paoli, L., Vannini, A., Sorbo, S., Maresca, V., Fusaro, L., Karam, E. A., Lentini, M., Lillo, A. D., Conte, B., Cianciullo, P., & Basile, A. (2018). In-field and in-vitro study of the moss Leptodictyum riparium as bioindicator of toxic metal pollution in the aquatic environment: Ultrastructural damage, oxidative stress and HSP70 induction. *PLOS ONE*, *13*(4), e0195717. https://doi.org/10.1371/journal.pone.0195717

Esposito, S., Sorbo, S., Conte, B., & Basile, A. (2012). Effects of Heavy Metals on Ultrastructure and HSP70S Induction in the Aquatic Moss Leptodictyum Riparium Hedw. *International Journal of Phytoremediation*, *14*(4), 443–455. https://doi.org/10.1080/15226514.2011.620904

Farmer, E. E., & Mueller, M. J. (2013). ROS-mediated lipid peroxidation and RES-activated signaling. *Annual Review of Plant Biology*, *64*, 429–450. https://doi.org/10.1146/annurev-arplant-050312-120132

Fasani, E., Li, M., Varotto, C., Furini, A., & DalCorso, G. (2022). Metal Detoxification in Land Plants: From Bryophytes to Vascular Plants. STATE of the Art and Opportunities. *Plants*, *11*(3), Article 3. https://doi.org/10.3390/plants11030237

Ferreres, F., Andrade, P. B., Valentão, P., & Gil-Izquierdo, A. (2008). Further knowledge on barley (Hordeum vulgare L.) leaves O-glycosyl-C-glycosyl flavones by liquid chromatography-UV diode-array detection-electrospray ionisation mass spectrometry. *Journal of Chromatography. A*, *1182*(1), 56–64. https://doi.org/10.1016/j.chroma.2007.12.070

Giannakoula, A., Therios, I., & Chatzissavvidis, C. (2021). Effect of Lead and Copper on Photosynthetic Apparatus in Citrus (Citrus aurantium L.) Plants. The Role of Antioxidants in Oxidative Damage as a Response to Heavy Metal Stress. *Plants*, *10*(1), Article 1. https://doi.org/10.3390/plants10010155

Gichner, T., & Plewa, M. J. (1998). Induction of somatic DNA damage as measured by single cell gel electrophoresis and point mutation in leaves of tobacco plants. *Mutation Research/Fundamental and*

Molecular Mechanisms of Mutagenesis, *401*(1), 143–152. https://doi.org/10.1016/S0027-5107(98)00003-7

Guella, G., Frassanito, R., & Mancini, I. (2003). A new solution for an old problem: The regiochemical distribution of the acyl chains in galactolipids can be established by electrospray ionization tandem mass spectrometry. *Rapid Communications in Mass Spectrometry: RCM*, *17*(17), 1982–1994. https://doi.org/10.1002/rcm.1142

Jain, C. K., Singhal, D. C., & Sharma, M. K. (2005). Metal Pollution Assessment of Sediment and Water in the River Hindon, India. *Environmental Monitoring and Assessment*, *105*(1), 193–207. https://doi.org/10.1007/s10661-005-3498-z

Jouaneh, T. M. M., Motta, N., Wu, C., Coffey, C., Via, C. W., Kirk, R. D., & Bertin, M. J. (2022). Analysis of botanicals and botanical supplements by LC-MS/MS-based molecular networking: Approaches for annotating plant metabolites and authentication. *Fitoterapia*, *159*, 105200. https://doi.org/10.1016/j.fitote.2022.105200

Kalisch, B., Dörmann, P., & Hölzl, G. (2016). DGDG and Glycolipids in Plants and Algae. *Sub-Cellular Biochemistry*, *86*, 51–83. https://doi.org/10.1007/978-3-319-25979-6_3

Kelly, A. A., & Dörmann, P. (2004). Green light for galactolipid trafficking. *Current Opinion in Plant Biology*, *7*(3), 262–269. https://doi.org/10.1016/j.pbi.2004.03.009

Kwon, H. C., Zee, O. P., & Lee, K. R. (1998). Two New Monogalactosylacylglycerols from Hydrocotyle ramiflora. *Planta Medica*, *64*(05), 477–479. https://doi.org/10.1055/s-2006-957491

Li, K., He, Z., Wang, X., Pineda, M., Chen, R., Liu, H., Ma, K., Shen, H., Wu, C., Huang, N., Pan, T., Liu, Y., & Guo, J. (2018). Apigenin C-glycosides of Microcos paniculata protects lipopolysaccharide induced apoptosis and inflammation in acute lung injury through TLR4 signaling pathway. *Free Radical Biology and Medicine*, *124*, 163–175. https://doi.org/10.1016/j.freeradbiomed.2018.06.009

Liebisch, G., Fahy, E., Aoki, J., Dennis, E. A., Durand, T., Ejsing, C. S., Fedorova, M., Feussner, I., Griffiths, W. J., Köfeler, H., Merrill, A. H., Murphy, R. C., O'Donnell, V. B., Oskolkova, O., Subramaniam, S., Wakelam, M. J. O., & Spener, F. (2020). Update on LIPID MAPS classification, nomenclature, and shorthand notation for MS-derived lipid structures. *Journal of Lipid Research*, *61*(12), 1539–1555. https://doi.org/10.1194/jlr.S120001025

Liu, R., Meng, C., Zhang, Z., Ma, H., Lv, T., Xie, S., Liu, Y., & Wang, C. (2020). Comparative metabolism of schaftoside in healthy and calcium oxalate kidney stone rats by UHPLC-Q-TOF-MS/MS method. *Analytical Biochemistry*, *597*, 113673. https://doi.org/10.1016/j.ab.2020.113673

Maciel, E., Leal, M. C., Lillebø, A. I., Domingues, P., Domingues, M. R., & Calado, R. (2016). Bioprospecting of Marine Macrophytes Using MS-Based Lipidomics as a New Approach. *Marine Drugs*, *14*(3), 49. https://doi.org/10.3390/md14030049

Maresca, V., Fusaro, L., Sorbo, S., Siciliano, A., Loppi, S., Paoli, L., Monaci, F., karam, E. A., Piscopo, M., Guida, M., Galdiero, E., Insolvibile, M., & Basile, A. (2018). Functional and structural biomarkers to monitor heavy metal pollution of one of the most contaminated freshwater sites in Southern Europe. *Ecotoxicology and Environmental Safety*, *163*, 665–673. https://doi.org/10.1016/j.ecoenv.2018.07.122

Maresca, V., Lettieri, G., Sorbo, S., Piscopo, M., & Basile, A. (2020a). Biological Responses to Cadmium Stress in Liverwort Conocephalum conicum (Marchantiales). *International Journal of Molecular Sciences*, *21*(18), Article 18. https://doi.org/10.3390/ijms21186485

Maresca, V., Lettieri, G., Sorbo, S., Piscopo, M., & Basile, A. (2020b). Biological Responses to Cadmium Stress in Liverwort Conocephalum conicum (Marchantiales). *International Journal of Molecular Sciences*, *21*(18), Article 18. https://doi.org/10.3390/ijms21186485

Maresca, V., Salbitani, G., Moccia, F., Cianciullo, P., Carraturo, F., Sorbo, S., Insolvibile, M., Carfagna, S., Panzella, L., & Basile, A. (2022). Antioxidant response to heavy metal pollution of Regi Lagni freshwater in Conocephalum conicum L. (Dum.). *Ecotoxicology and Environmental Safety*, *234*, 113365. https://doi.org/10.1016/j.ecoenv.2022.113365

Maresca, V., Sorbo, S., Loppi, S., Funaro, F., Del Prete, D., & Basile, A. (2020). Biological effects from environmental pollution by toxic metals in the “land of fires” (Italy) assessed using the biomonitor species Lunularia cruciata L. (Dum). *Environmental Pollution*, *265*, 115000. https://doi.org/10.1016/j.envpol.2020.115000

Markham, K. R., Porter, L. J., Mues, R., Zinsmeister, H. D., & Brehm, B. G. (1976). Flavonoid variation in the liverwort Conocephalum conicum: Evidence for geographic races. *Phytochemistry*, *15*(1), 147–150. https://doi.org/10.1016/S0031-9422(00)89072-X

Marrassini, C., Davicino, R., Acevedo, C., Anesini, C., Gorzalczany, S., & Ferraro, G. (2011). Vicenin-2, a Potential Anti-inflammatory Constituent of Urtica circularis. *Journal of Natural Products*, *74*(6), 1503–1507. https://doi.org/10.1021/np100937e

Materska, M. (2015). Flavone C-glycosides from Capsicum annuum L.: Relationships between antioxidant activity and lipophilicity. *European Food Research and Technology*, *240*(3), 549–557. https://doi.org/10.1007/s00217-014-2353-2

McCullagh, M., Goshawk, J., Eatough, D., Mortishire-Smith, R. J., Pereira, C. A., Yariwake, J. H., & Vissers, J. P. (2021). Profiling of the known-unknown Passiflora variant complement by liquid chromatography—Ion mobility—Mass spectrometry. *Talanta*, *221*, 121311. https://doi.org/10.1016/j.talanta.2020.121311

Nothias, L.-F., Petras, D., Schmid, R., Dührkop, K., Rainer, J., Sarvepalli, A., Protsyuk, I., Ernst, M., Tsugawa, H., Fleischauer, M., Aicheler, F., Aksenov, A. A., Alka, O., Allard, P.-M., Barsch, A., Cachet, X., Caraballo-Rodriguez, A. M., Da Silva, R. R., Dang, T., … Dorrestein, P. C. (2020).

Feature-based molecular networking in the GNPS analysis environment. *Nature Methods*, *17*(9), Article 9. https://doi.org/10.1038/s41592-020-0933-6

Nouman, W., Bashir, T., Gul, R., Gull, T., Olson, M. E., Shaheen, M., Rosa, E., Domínguez-Perles, R., & Soliman, W. S. (2020). Metalliferous conditions induce regulation in antioxidant activities, polyphenolics and nutritional quality of Moringa oleifera L. *International Journal of Phytoremediation*, *22*(13), 1348–1361. https://doi.org/10.1080/15226514.2020.1775547

Parzych, A., Jonczak, J., & Sobisz, Z. (2018). Pellia endiviifolia (Dicks.) Dumort. Liverwort with a Potential for Water Purification. *International Journal of Environmental Research*, *12*(4), 471–478. https://doi.org/10.1007/s41742-018-0105-z

Paul, D. (2017). Research on heavy metal pollution of river Ganga: A review. *Annals of Agrarian Science*, *15*(2), 278–286. https://doi.org/10.1016/j.aasci.2017.04.001

Pluskal, T., Castillo, S., Villar-Briones, A., & Orešič, M. (2010). MZmine 2: Modular framework for processing, visualizing, and analyzing mass spectrometry-based molecular profile data. *BMC Bioinformatics*, *11*. Scopus. https://doi.org/10.1186/1471-2105-11-395

Prado, C., Prado, F. E., Pagano, E., & Rosa, M. (2015). Differential Effects of Cr(VI) on the Ultrastructure of Chloroplast and Plasma Membrane of Salvinia minima Growing in Summer and Winter. Relationships With Lipid Peroxidation, Electrolyte Leakage, Photosynthetic Pigments, and Carbohydrates. *Water, Air, & Soil Pollution*, *226*(2), 8. https://doi.org/10.1007/s11270-014-2284-3

Radotić, K., Dučić, T., & Mutavdžić, D. (2000). Changes in peroxidase activity and isoenzymes in spruce needles after exposure to different concentrations of cadmium. *Environmental and Experimental Botany*, *44*(2), 105–113. https://doi.org/10.1016/S0098-8472(00)00059-9

Radulović, N. S., Filipović, S. I., Nešić, M. S., Stojanović, N. M., Mitić, K. V., Mladenović, M. Z., & Ranđelović, V. N. (2020). Immunomodulatory Constituents of Conocephalum conicum (Snake Liverwort) and the Relationship of Isolepidozenes to Germacranes and Humulanes. *Journal of Natural Products*, *83*(12), 3554–3563. https://doi.org/10.1021/acs.jnatprod.0c00585

Ramakrishna, A., & Ravishankar, G. A. (2011). Influence of abiotic stress signals on secondary metabolites in plants. *Plant Signaling and Behavior*, *6*(11), 1720–1731. Scopus. https://doi.org/10.4161/psb.6.11.17613

Rayyan, S., Fossen, T., & Andersen, Ø. M. (2010). Flavone C-Glycosides from Seeds of Fenugreek, Trigonella foenum-graecum L. *Journal of Agricultural and Food Chemistry*, *58*(12), 7211–7217. https://doi.org/10.1021/jf100848c

Roldán-Arjona, T., & Ariza, R. R. (2009). Repair and tolerance of oxidative DNA damage in plants. *Mutation Research/Reviews in Mutation Research*, *681*(2), 169–179. https://doi.org/10.1016/j.mrrev.2008.07.003

Rozentsvet, O. A., Dembitsky, V. M., & Saksonov, S. V. (2000). Occurrence of diacylglyceryltrimethylhomoserines and major phospholipids in some plants. *Phytochemistry*, *54*(4), 401–407. https://doi.org/10.1016/s0031-9422(00)00042-x

Schwartzman, R. A., & Cidlowski, J. A. (1993). Apoptosis: The Biochemistry and Molecular Biology of Programmed Cell Death*. *Endocrine Reviews*, *14*(2), 133–151. https://doi.org/10.1210/edrv-14-2-133

Shannon, P., Markiel, A., Ozier, O., Baliga, N. S., Wang, J. T., Ramage, D., Amin, N., Schwikowski, B., & Ideker, T. (2003). Cytoscape: A Software Environment for Integrated Models of Biomolecular Interaction Networks. *Genome Research*, *13*(11), 2498–2504. https://doi.org/10.1101/gr.1239303

Sharma, A., Shahzad, B., Rehman, A., Bhardwaj, R., Landi, M., & Zheng, B. (2019). Response of Phenylpropanoid Pathway and the Role of Polyphenols in Plants under Abiotic Stress. *Molecules*, *24*(13), Article 13. https://doi.org/10.3390/molecules24132452

Silva, D. B., Turatti, I. C. C., Gouveia, D. R., Ernst, M., Teixeira, S. P., & Lopes, N. P. (2014). Mass Spectrometry of flavonoid vicenin-2, based sunlight barriers in Lychnophora species. *Scientific Reports*, *4*. Scopus. https://doi.org/10.1038/srep04309

Stelmach, B. A., Müller, A., Hennig, P., Gebhardt, S., Schubert-Zsilavecz, M., & Weiler, E. W. (2001). A Novel Class of Oxylipins,sn1-O-(12-Oxophytodienoyl)-sn2-O-(hexadecatrienoyl)-monogalactosyl Diglyceride, from Arabidopsis thaliana *. *Journal of Biological Chemistry*, *276*(16), 12832–12838. https://doi.org/10.1074/jbc.M010743200

Sut-Lohmann, M., Jonczak, J., & Raab, T. (2020). Phytofiltration of chosen metals by aquarium liverwort (Monosoleum tenerum). *Ecotoxicology and Environmental Safety*, *188*, 109844. https://doi.org/10.1016/j.ecoenv.2019.109844

Tabelin, C. B., Igarashi, T., Villacorte-Tabelin, M., Park, I., Opiso, E. M., Ito, M., & Hiroyoshi, N. (2018). Arsenic, selenium, boron, lead, cadmium, copper, and zinc in naturally contaminated rocks: A review of their sources, modes of enrichment, mechanisms of release, and mitigation strategies. *Science of The Total Environment*, *645*, 1522–1553. https://doi.org/10.1016/j.scitotenv.2018.07.103

Tatituri, R. V. V., Brenner, M. B., Turk, J., & Hsu, F.-F. (2012). Structural elucidation of diglycosyl diacylglycerol and monoglycosyl diacylglycerol from Streptococcus pneumoniae by multiple-stage linear ion-trap mass spectrometry with electrospray ionization. *Journal of Mass Spectrometry: JMS*, *47*(1), 115–123. https://doi.org/10.1002/jms.2033

Tong, Y., Wang, P., Sun, J., Li, X., Wang, T., Zhou, Q., Xie, Z., Jiang, C., & Wang, J. (2021). Metabolomics and molecular networking approaches reveal differential metabolites of Radix Scrophulariae from different geographical origins: Correlations with climatic factors and biochemical

compounds in soil. *Industrial Crops and Products*, *174*, 114169. https://doi.org/10.1016/j.indcrop.2021.114169

Vitale, G. A., Sciarretta, M., Cassiano, C., Buonocore, C., Festa, C., Mazzella, V., Núñez Pons, L., D'Auria, M. V., & de Pascale, D. (2020). Molecular Network and Culture Media Variation Reveal a Complex Metabolic Profile in Pantoea cf. Eucrina D2 Associated with an Acidified Marine Sponge. *International Journal of Molecular Sciences*, *21*(17), E6307. https://doi.org/10.3390/ijms21176307

Wang, M., Carver, J. J., Phelan, V. V., Sanchez, L. M., Garg, N., Peng, Y., Nguyen, D. D., Watrous, J., Kapono, C. A., Luzzatto-Knaan, T., Porto, C., Bouslimani, A., Melnik, A. V., Meehan, M. J., Liu, W.-T., Crüsemann, M., Boudreau, P. D., Esquenazi, E., Sandoval-Calderón, M., … Bandeira, N. (2016). Sharing and community curation of mass spectrometry data with Global Natural Products Social Molecular Networking. *Nature Biotechnology*, *34*(8), Article 8. https://doi.org/10.1038/nbt.3597

Xiao, J., Capanoglu, E., Jassbi, A. R., & Miron, A. (2016). Advance on the Flavonoid C-glycosides and Health Benefits. *Critical Reviews in Food Science and Nutrition*, *56*(sup1), S29–S45. https://doi.org/10.1080/10408398.2015.1067595

Yan, A., Wang, Y., Tan, S. N., Mohd Yusof, M. L., Ghosh, S., & Chen, Z. (2020). Phytoremediation: A Promising Approach for Revegetation of Heavy Metal-Polluted Land. *Frontiers in Plant Science*, *11*. Scopus. https://doi.org/10.3389/fpls.2020.00359

Zhang, P.-C., & Xu, S.-X. (2001). Flavonoid ketohexosefuranosides from the leaves of Crataegus pinnatifida Bge. Var. Major N.E.Br. *Phytochemistry*, *57*(8), 1249–1253. https://doi.org/10.1016/S0031-9422(01)00170-4

PAPER II

Ecotoxicology and Environmental Safety 234 (2022) 113365

Contents lists available at ScienceDirect

Ecotoxicology and Environmental Safety

journal homepage: www.elsevier.com/locate/ecoenv

Antioxidant response to heavy metal pollution of Regi Lagni freshwater in *Conocephalum conicum* L. (Dum.)

Viviana Maresca [a], Giovanna Salbitani [a], Federica Moccia [b], **Piergiorgio Cianciullo** [a], Federica Carraturo[a], Sergio Sorbo[c], Marilena Insolvibile[d], Simona Carfagna[a], Lucia Panzella[b], Adriana Basile [a*]

a Department of Biology, University of Naples Federico II, Naples, Italy
b Department of Chemical Sciences, University of Naples Federico II, Naples, Italy
c CeSMA, section of Microscopy, University of Naples Federico II, Naples, Italy
d ISPRA, Italian National Institute for Environmental Protection and Research, Rome, Italy

DOI: https://doi.org/10.1016/j.ecoenv.2022.113365

Abstract

Conocephalum conicum L. is a cosmopolitan liverwort species able to respond to local environmental pollution by changing its biological features. In the present study, we assessed the different biological responses in *C. conicum* to heavy metal contamination of Regi Lagni channels, a highly polluted freshwater body. As for the in field experiment, we set up moss bags containing collected samples of the local wild growing *C. conicum*, from the upstream site (non-polluted area), and we exposed them in the three selected sites characterized by different and extreme conditions of heavy metal pollution. In addition, to better understand the contribution of heavy metals to the alterations and response of the liverwort, we performed *in vitro* tests, using the same concentration of heavy metals measured in the sites at the moment of the exposition. In both experimental settings, bioaccumulation, ultrastructural damage, reactive oxygen species production and localization, antioxidant enzymes activity (superoxide dismutase, catalase and glutathione S-transferases), glutathione (reduced and oxidized) levels, localization of compounds presenting thiol groups and phenolic content were investigated. The results showed that the samples from different sites and conditions (for *in vitro* tests) showed significant differences. In particular, the ultrastructural alterations show a trend correlated to the different exposure situations; ROS contents, glutathione, antioxidant enzyme activities, and phenolic contents were increased showing an enhancement of the antioxidant defense both by the enzymatic way and by using the synthesis of antioxidant phenolic compounds. This study confirms the ability of *C. conicum* to respond to heavy metal pollution and the responses studied are, at least partially, correlated to the presence of heavy metals. All the responses considered respond consistently with the pollution trend and they can be proposed as pollution biomarkers. Therefore, we suggest the use of *C. conicum* to identify local hot spots of pollution in further investigation.

1. Introduction

The Regi Lagni channels are a drainage and canalization work done during the Bourbon regency in the early 1600 s in the former Kingdom of Two Sicily. The channels were constructed to avoid the flooding of the ancient Clanius river that affected the nearby territories. The Regi Lagni network is constituted by mostly artificial straight channels, branching through a highly-populated area (2796,360 inhabitants) of about 1905 km2 comprising the provinces of Caserta, Avellino, Naples, and Benevento. Nowadays, Regi Lagni channels are affected by severe pollution due to the heavy urbanization and industrialization of the surrounding areas, collecting wastewaters and carrying them from the plain north of Naples to the Tyrrhenian Sea (Bove et al., 2011; di Martino, 2014; Grezzi et al., 2011). Furthermore, the network crosses areas such as "Land of Fire" and the "Triangle of Death" which are notorious for the high degree of environmental risk associated with soil and groundwaters due to illegal waste dumping and the soot fallout from uncontrolled garbage burning (Basile et al., 2009; Maresca, Sorbo, et al., 2020; Sorbo et al., 2008). Environmental pollution is the main health risk in Europe and is associated with heart disease, stroke, lung disease and lung cancer in the local population (Alberti, 2022; Senior & Mazza, 2004). The need is therefore felt to implement monitoring practices in order to obtain information on the quality of the environment. Bryophytes are frequently used for biomonitoring purposes both as bioindicators and as accumulators of pollutants, especially heavy metals. For biomonitoring purposes, we choose three sites along with the Regi Lagni Channels. The former (upstream site), representative of the unpolluted section of the channels, is located in Avella; the other two representatives of areas with the strong environmental pollution in Acerra and Castel Volturno respectively. We collected samples of the local wild growing bryophyte vegetation, being bryophytes well-knows pollution bioindicators and/or bio accumulators, and we choose *Conocephalum conicum* L. (Dum.) (Marchantiales, Bryophyta), which among the bryophytes present showed the most extensive presence, as a species to be used for our study. The *C. conicum* can grow both on humid soils and along the edges of watercourses. Along the Regi Lagni freshwater, the liverwort has been found wild-growing abundantly on the banks of the upstream site. Previous studies reported that this species was able to respond to local environmental pollution and /or heavy metal treatment by changing its ultrastructure and other biological features as Heat Shock Proteins 70 content (Basile et al., 2013).

The present study aims to investigate oxidative stress responses induced by heavy metal pollution in the Regi Lagni watercourse on *C. conicum* exposed in bags in three sites characterized by different environmental conditions. In addition, to evaluate the exact role of heavy metals in inducing the effects studied, a parallel *in vitro* study was conducted, in which the same concentrations of heavy

metals, measured in water at the time of exposure, were tested. In particular, in this study the levels of heavy metals in the surveyed sites were measured in order to determine their degree of pollution. Subsequently, various analyzes were carried out on *C. conicum* samples both exposed in field and cultivated *in vitro*. Bioaccumulation of heavy metals in the gametophyte, the activity of antioxidant enzymes (superoxide dismutase, catalase and gluathione peroxidase), quantification and localization of reactive oxygen species, ultrastructural damage, localization of compounds presenting thiol groups, reduced/ oxidized glutathione ratio, synthesis of polyphenols, compounds known to be valid antioxidants, were measured.

2. Materials and methods

2.1. Plant material

Samples of *C. conicum* were collected from upstream of the channel of the Regi Lagni (non-polluted area), identified by prof. Adriana Basile. A sample was deposited in the herbarium of the Botanical Garden of the University Federico II Napoli. The collected samples were used for both the in-field and *in vitro* experiments.

2.2. In field experiments

After collection, about 1.8 g (FW) of homogeneous samples of *C. conicum* thalli were rinsed with MilliQ Water and wrapped with > 49 mm2 - meshed nylon bags, as described in Kelly et al. (1987). For each site six samples were exposed for seven days in April 2019. In order to avoid submersion thalli were exposed at a water depth of 1 cm. The coordinates of the 3 selected sites are reported in Maresca et al. (2018) (**Fig. 1S**). Three exposure sites with different pollution degrees were chosen: (A) Avella, as pristine site, (B) Acerra, (C) Castel Volturno, as representative of the highly polluted areas: the “Triangle of Death” and “Land of Fires”, respectively. Samples from each site were merged and then splitted into three subsamples for the subsequent analyses. Water was sampled three times in each site on the day of the *C. conicum* exposure and then it was analysed for heavy metal concentration.

2.3. In vitro experiments

The samples collected from upstream of the channel of the Regi Lagni (non-polluted area), have been rinsed with MilliQ Water and cultured in Petri dishes (10 cm diameter), 20 specimens per dish, using sterile modified Mohr medium, pH 7.5 as reported in Esposito et al. (2012) and in the same medium with the addition of the metal salts. The cultures were kept for seven days in a climatic chamber and

the environmental parameters were set based on the environmental conditions recorded in the field [air temperature: at 22 ± 1.4 ◦C, and 14 ± 1.4 ◦C, mean ± SD, during day and night, respectively; relative humidity: 71 ± 3% mean ± SD, 16 h light (Photosynthetic Active Radiation 400 μmol m^2 s^{-1})/8 h dark photoperiod]. In the cultures, were added to the medium the metals as soluble salts: CdCl2, CuSO4, Pb (CH3COO)2, and ZnCl2 with the relative anions as K salts in control solutions. The concentration of heavy metals used in the *in vitro* samples was the same measured in the three surveyed sites.

The samples are indicated as follows:

– Ctrl, A, B, C, for both field and *in vitro* samples;. The *in vitro* and in field samples were performed in triplicate and repeated three times.

2.4. Analytical determination of metal in water samples and in liverwort

Heavy metals were determined in both water samples (from in-field experiments) and liverwort (in field and *in vitro* experiments). The water samples collected in the field experimental sites were analyzed by ICP-MS (Perkin-Elmer Sciex 6100) for the concentration of selected heavy metals: Cd, Cu, Pb, Zn as described in Maresca et al., 2018). After both in the field and *in vitro* experiments, concentrations of selected toxic metals (Cd, Cu, Pb, Zn) of the apical part of *C. conicum* gametophyte were determined according to Esposito et al., 2018. For both experiments, the Enrichment Factor (EF) was calculated as the ratio between the metal in the plant (mg g^{-1}) to the metal in the water (μg L^{-1}) (Ahmad et al., 2014).

2.5. Detection of ROS

A fluorescent technique using 2′ -7′ -dichlorofluorescein diacetate (DCFH-DA) has been used for quantitative measurement of ROS production according to Maresca et al. (2018). The crude protein extracts (5 uL) were mixed with a solution of DCFH-DA (uL, 100 mM).

ROS quantity was monitored by fluorescence (excitation wavelength of 350 nm and emission wavelength of 600 nm) using a multiplate reader at time 0 and after 30 min incubation at 37°C.

2.6. Response to oxidative stress

Enzyme extraction and the determination of superoxide dismutase (SOD), catalase (CAT), and glutathione S-transferases (GST) activities were performed as reported in Maresca et al. (2018).

Crude protein extracts were obtained by grinding the samples in liquid nitrogen with ceramic mortar and pestle. The pulverized samples were homogenized in cold Tris HCl Buffer pH 7.5 with EDTA 0.1 mM and DTT. The homogenates were then centrifuged at 6500 rpm for 30 min at 4°C.

Catalase (CAT, EC 1.11.1.6) activity (Units mg proteins^{-1}) was kinetically measured (for 1 min at 25 °C, 15 s each read) as a decrease in the absorbance of H2O2 at 240 nm in 2 mL quartz cuvettes with a spectrophotometer UV-Vis (Cary 300, Agilent Technologies, Inc.) using a commercial kit (Sigma–Aldrich Co., St Louis, MO, USA). and The drop in absorbance at 240 nm is linear with the consumption of H_2O_2 and was used to quantify the μmol H_2O_2 consumed (ε = 0.0436 mM−1, path length = 1 cm). By definition one unit of catalase is defined as the unit able to decompose 1.0 μmole of H2O2 per minute at pH 7.0 at 25 °C, and the CAT units in the samples were calculated accordingly.

Glutathione S-transferase (GST, EC 2.5.1.18) activity was measured using a commercial kit (CS0410, Sigma). The reactions were monitored for 6 min at 25 °C using a mul-tiplate reader (Synergy H4, Agilent Technologies, Inc.). The increase in absorbance at 340 nm that indicates the conjugation of reduced glutathione with the 1-chloro-2,4-dinitrobenzene (CDNB) was recorded and the umol of CDNB-GSH con-jugates was quantified according to their molar extinction coefficient (ε = 5.3 mM−1, path length = 0.552 cm).

The quantification of total soluble proteins was carried out with Bradford assay (Bio-rad Laboratories, Inc., Hercules, California, U.S.A.) using bovine seroalbu-min to calibrate the standard curve. Each assay was run in triplicate for each sample (N = 3)

2.7. Reduced (GSH) and total and glutathione contents

The GSH and total glutathione contents of C. conicum were determined according to Salbitani et al. (2015) with minor adjustments. Specifically, 2 g of C. conicum were crushed in mortars with liquid nitrogen, and 4 mL of 5% sulfosalicylic acid were added to the powdered tissue. The homogenates were centrifuged at 12000g for 30 min at 4 ◦C. The extract was added to the reaction buffer containing 0.1-M Na-phosphate, pH 7.00, 1-mM of EDTA, 40 μL of 0.4% DTNB, and distilled water. The GSH and total glutathione contents were determined spectrophotometrically as previously described (Salbitani et al., 2015) and were expressed in μmol g^{-1} FW.

2.8. Total Phenolic Content (TPC) assay

The different C. conicum samples, dissolved in DMSO at 10 mg/mL concentration, were added at a final dose of 0.0625 □ 0.5 mg/mL to a solution consisting of Folin-Ciocalteu reagent, 75 g/L Na2CO3, and water, in a 1:3:14 v/v/v ratio (Panzella et al., 2019). After 30 min incubation at 40 ◦C, the absorbance at 765 nm was measured. Gallic acid was used as a reference compound. Experiments were run in triplicate on each sample.

2.9. HPLC analysis

HPLC analysis was performed on the in vitro samples dissolved in methanol (5 mg/mL concentration) with an instrument equipped with a UV-Vis detector (Agilent, G1314A); a Phenomenex Sphereclone ODS column (250 × 4.60 mm, 5 μm) was used, at a flow rate of 1.0 mL/min; a 0.1% formic acid (solvent A)/methanol (solvent B) gradient elution was performed as follows: 5% B, 0–10 min; from 5% to 80% B, 10–47.5 min; the detection wavelength was 254 nm.

2.10. LC-MS analysis

LC-MS analyses were run on an Agilent LC-MS ESI-TOF 1260/ 6230DA instrument operating in positive ionization mode in the following conditions: nebulizer pressure 35 psig; drying gas (nitrogen) 5 L/min, 325 ◦C; capillary voltage 3500 V; fragmentor voltage 175 V. An Agilent Eclipse Plus C18 column, 150 × 4.6 mm, 5 μm at a flow rate of 0.4 mL/min was used, using the same eluant as above.

2.11. Confocal imaging

Samples treatment was done according to Maresca et al. (2020). ROS were localized with the fluorescent probe 2′ -7′ dichlorofluorescin diacetate (DCF-DA) solubilized in dimethyl sulphide DMSO and 10 mM Tris-HCl (pH 7.4), then dilute in MilliQ water to obtain a 25 μM staining solution. Thin thalli sections of *C.conicum* were then stained with 25 μM DCF-DA for 30 min. Stained sections were washed in Tris HCl (pH 7.4) for 10 min. Thalli sections were observed under a laser-scanning confocal microscope (Leica TCS SP5, Wetzlar, Germany) with an excitation wavelength of 476 nm and emission bandwidths 485/575 nm (green light), 610/685 nm (red light) (beginning-end). GSH and thiol-peptides were localized with monochlorobimane (MCB) solubilized in DMSO and then in MilliQ water to obtain a 100 μM staining solution. Thin thalli sections of fresh *C. conicum* were stained with 100 μM MCB (Thermo Fisher Scientific, MA, USA) for 30 min at 21 ◦C in the dark, at near neutral pH conditions. After, observations were performed under a Leica TCS SP5 confocal laser scanning microscope (CLSM) with a 40X immersion objective. Excitation of MCB and chlorophyll

was set at 405 nm wavelength, and emission detected at 460–520 nm (blue light) and 630–700 nm (red light) (beginning-end). Unstained *C.conicum* cross-sections were incubated into the same amount of DMSO solution without DCF-DA and MCB, and used as a negative control of DCF-DA and MCB. Three samples of *C.conicum* cross-sections thalli for each treatment and control condition were examined. In both ROS and GSH and thiol peptides imaging, hardware settings, particularly detector gain and amplification offset, were adjusted to optimize fluorescence intensity in samples C, and the same values were kept with all samples to allow a semiquantitative comparison between different treatments. Data collection and processing were performed with the software LAS AF (Leica). Observations were repeated 3 times for each treatment.

2.12. Transmission electron microscopy

Collected samples, after thoroughly cleaning, were cut to pick subapical central parts of the thalli, about 3 mm below the apex, cutting away the wings. Protocol preparation for transmission electron microscopy (TEM) requires the following steps: overnight fixation at 4 ◦C with glutaraldehyde 2.5% (*v/v*) buffered solution (Sorenson's sodium phosphate buffer 0.025 M, pH 7.3), postfixation with 1% (*w/v*) osmium tetroxide buffered solution, with the same buffer as before, added with KFeCN 0.8%, dehydration with alcohol up to propylene oxide, embedding in Spurr resin with subsequent polymerization at 70 ◦C in the oven. By ultramicrotomy, we obtained ultrathin 50 nm thick sections, which were collected on 300 mesh copper grids and stained with Uranyl Acetate Replacement stain (Electron Microscopy Science, Hatfield, PA, USA) and lead citrate. An EM208ES Philips TEM was employed for the observations. The observation was focused on photosynthetic parenchymata; three samples per treatment and 9 sections per sample were examined.

2.13. Statistical analysis

ROS production, SOD, CAT, GST activities, and glutathione contents were examined by one-way analysis of variance (ANOVA), followed by Tukey's multiple comparison post-hoc test. The student's t-test was performed on the results of the TPC assay. In all figures, values are presented as mean ± st. err; numbers not accompanied by the same letter are significantly different at $P < 0.05$. Data were analyzed using the software Statistica, version 7.0 (StatSoft, Tulsa, OK, USA). For the in-field and *in vitro* experiments, the relationships between bioaccumulation of heavy metals and biological responses were assessed using Pearson correlation analysis. Data from all sites (A, B, C) were analyzed together.

3. Results

3.1. Analytical determination of metal and EF in water samples and in liverwort

The concentrations of the heavy metals analyzed in the water (**Table 1S**) samples are very high and exceed the limits defined by Legislative Decree 172/2015 ("Implementation of Directive 2013/39 / EU, which amends Directives 2000/60 / EC about priority substances in the field of water policy"), especially for Cd and Pb (ref. 1 / A - Environmental quality standards in the water column and biota for substances on the priority list). Site C is affected by pressures due to the presence of ASI (Industrial Development Areas) zones, with industries subject to AIA (Integrated Environmental Authorization) (**Fig. 1S**). As regards the bioaccumulation of heavy metals in the gametophyte of *C. conicum*, the detected concentrations reflect the concentrations of heavy metals measured in the selected sites (**Table 1**). Furthermore, for all the metals measured, a greater bioaccumulation capacity is noted in the *in vitro* samples compared to those in the field, probably due to a greater bioavailability of the metals in solution (**Table 1**). **Fig. 1** shows the EF for the considered heavy metals in the two experiments. In the field experiment, the EF of Cu (**Fig. 1a**) reached the highest value in C, whereas the lower EF occurred in B. In the *in vitro* conditions, EF increased when metals concentration increased (A>B>C). Looking at the differences between in-field and *in vitro* experiments, the in field experiment had the higher EF values (A in-field>A *in vitro*; B in field>B *in vitro*; C in field>C *in vitro*). For both Zn (**Fig. 1b**) and Cd (**Fig. 1c**), EF showed the same general pattern: as the metals concentration increase, EF increased in both field and *in vitro* experiments (A> B> C in field; A> B> C *in vitro*). For each level of metals concentration, the *in vitro* EF was higher relative to the field. In the field experiment, the EF of Pb (**Fig. 1d**) decreased from A to B, whereas the C presented an intermediate EF. On the other hand, *in vitro* experiment, the EF increased as metals concentration increased (A> B> C). Looking at the differences between in-field and *in vitro*, we highlighted that in the latter conditions the EF was tendentiously lower in respect to what was found in the field experiment. It is interesting to notice that EF values between in-field and *in vitro* are approximately equivalent, except for Cu and Pb *in vitro.*

Table 1S. The concentration of heavy metals (μg L^{-1}) in waters of river measured in the three experimental sites (Avella, A; Acerra, B; Castel Volturno, C). Values are presented as mean ± st. dev; numbers not accompanied by the same letter are significantly different at $P < 0.05$, using the post-hoc Student–Newman–Keuls test. The concentrations found in the water of the three sites in field experiment were used for the *in vitro* experiments.

Heavy metal content in water (μg L^{-1})		
A	**B**	**C**

Cu	101.832 ± 2.431[a]	3621.422 ± 24.413[b]	9975.521 ± 32.831[c]
Zn	230.113 ± 9.722[a]	3151.751 ± 12.135[b]	9731.756 ± 57.212[c]
Cd	24.743 ± 1.456[a]	1003.201 ± 8.267[b]	8743.554 ± 35.234[c]
Pb	6.987 ± 0.998[a]	38.755 ± 2.601[b]	775.644 ± 11.318[c]

3.2. ROS and oxidative stress response

In vitro experiments, the production of ROS in the samples follows an increasing trend, in fact in the samples of *C. conicum* exposed to the highest concentrations (samples C) of heavy metals a higher production of ROS is observed, also samples A and B have higher ROS values than the control if there is no statistically significant difference between the two. Regarding the enzymatic activity of CAT and SOD, an increase in the enzymatic activity is observed in samples B and C compared to the control even if there are no statistically significant differences between the two, in samples A the activity of both enzymes is greater than control but lower than samples B and C. The activity of the GST enzyme is higher in samples C, in samples A and B no significant differences are observed but the enzymatic activity is still higher than in the control (**Fig. 2**). In field experiments, ROS production increases with increasing pollution of the three sites. As far as the enzymatic activity of SOD is concerned, an increase in the enzymatic activity is observed in samples B and C compared to the control even if there are no statistically significant differences between the two, in samples A the activity of SOD is greater than the control but lower than samples B and C. The activity of CAT and GST enzymes is greater in samples C, no significant differences are observed in samples A and B but the enzymatic activity is even greater than in the control (**Fig. 2**).

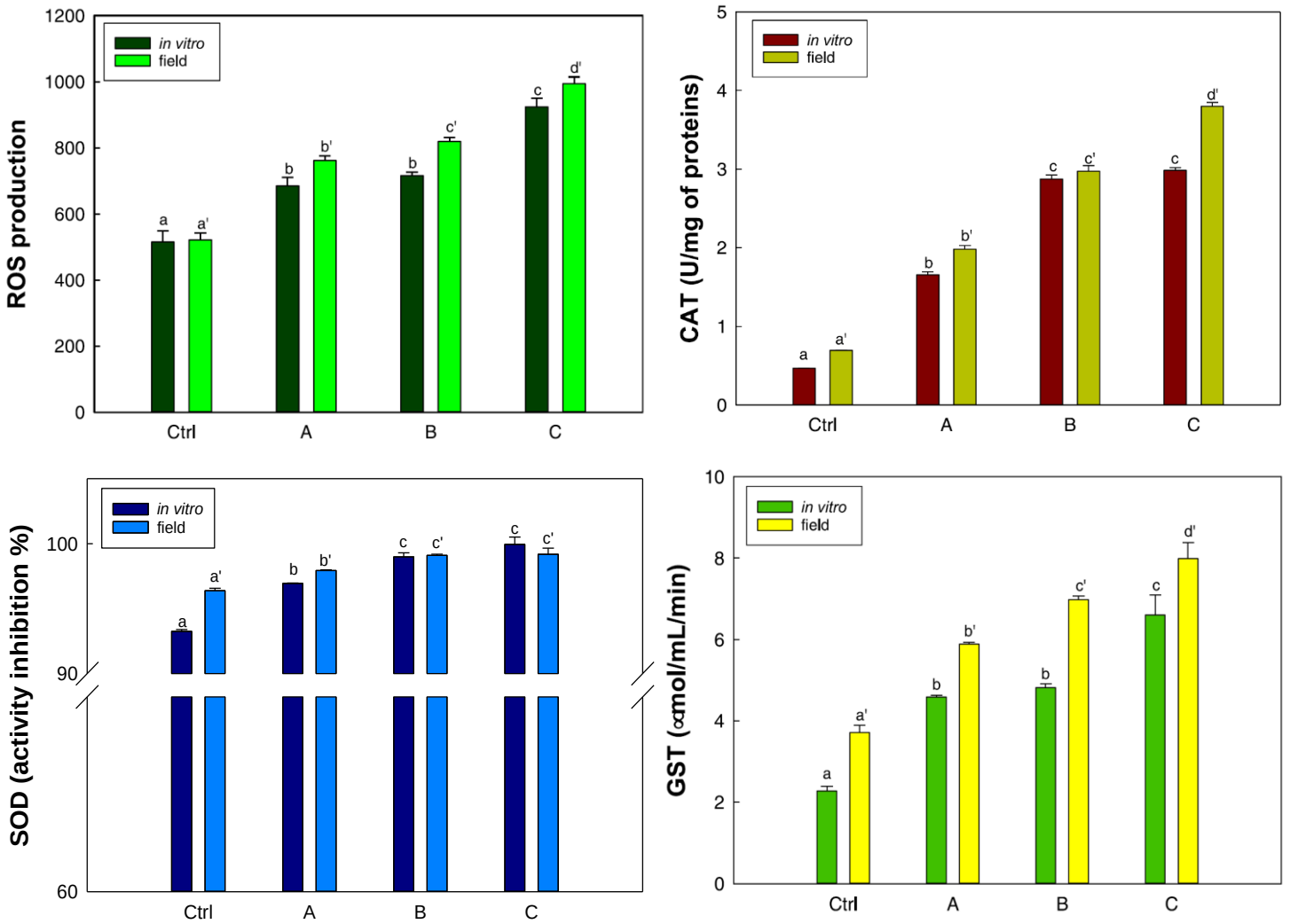

Figure 2. ROS production (fluorescence intensity, A.U.), enzymatic antioxidant responses (SOD activity inhibition %, CAT, U/mg of protein, GST, µmol/mL/min) in the samples A, B, C and control exposed in the field and *in vitro* experiments.

3.3. Glutathione contents in *C. conicum* in field and in vitro experiments

The total glutathione concentration increased in *C. conicum* exposed and collected in the three sites as previously described. Particularly, in samples B and C the values were significantly higher concerning Ctrl and Sample A. In the samples analyzed, both in the field and *in vitro* experiments, GSH contents were similar in Ctrl and A samples, while increased more significantly in C samples collected for in field experiments (**Fig. 3**). In the samples treated with a solution containing the same

heavy metals concentration found in the three field sites (*in vitro* experiments), the same trend was observed: in B and C total glutathione was higher with respect to Ctrl and A samples (**Fig. 3**).

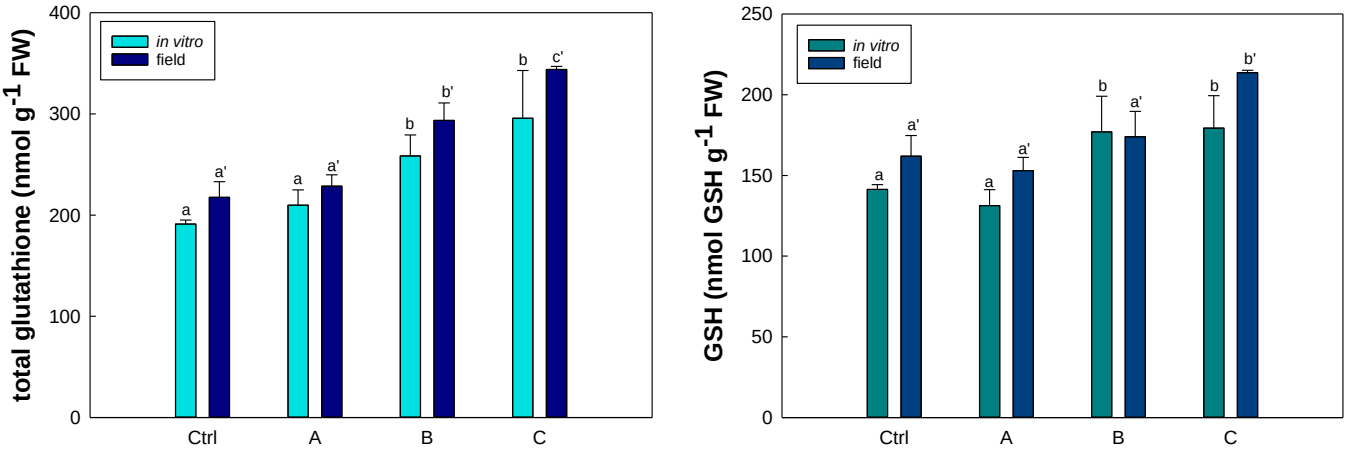

Figure 3. Reduced glutathione (GSH, nmol g^{-1} FW) and total glutathione levels (nmol g^{-1} FW) in the samples A, B, C and control exposed in the field and *in vitro* experiments.

3.4. Phenolic content

To obtain information on the effects of exposure to heavy metals on the amounts of phenolic compounds in *C. conicum*, the Folin-Ciocalteu assay was performed on both the in-field and *in vitro* samples (**Table 2**). Notably, the highest TPC values were determined for *C. conicum* samples exposed to the highest concentrations of heavy metals (samples C). Moreover, an increasing trend in TPC was observed, with samples B showing a significantly higher value compared to samples A, although for these latter no significant differences with the *in vitro* control (0.0288 ± 0.0005 mg of gallic acid/mg of the sample) were detected. As shown in **Fig. 2S**, a very good linear correlation was found between the total concentration of metals determined by ICP-MS experiments and the TPC for both the in-field and *in vitro* samples (R2 = 0.99 and 1.00, respectively), indicating that phenolic compound biosynthesis is closely related to the heavy metal exposure. To gain information on the phenolic composition, the *C. conicum* samples exposed to the different heavy metals concentrations *in vitro* were dissolved in methanol and analyzed by HPLC. The elutographic profiles (**Fig. 3**) showed for all the samples the main compound eluted at *ca.* 41 min, whose concentration was found to increase moving from sample A to sample C, *i.e.* further to exposure to increasing concentration of heavy metals. Based on LC-MS analysis, showing pseudomolecular ion peaks [M+H]+, [M+Na]+, and [M+K]+ at *m/z* 259, 281, and 297, in that order, this compound was tentatively identified as lunularic acid, which has previously been reported as one of the main phenolic components of liverworts, including *C. conicum* (Abe & Ohta, 1984; Gorham, 1977; Pryce, 1971).

Table 2 Total Phenolic content (TPC, mg gallic acid/mg sample) of *C. conicum* samples exposed to heavy metals in the field and *in vitro* experiments.

Sample	**TPC (mg gallic acid/mg sample)**	
	In-field	*In vitro*
A	0,039 ± 0,002[a]	0,0273 ± 0,0001[a]
B	0,065 ± 0,002[b]	0,0533 ± 0,0004[b]
C	0,085 ± 0,001[c]	0,0676 ± 0,0003[c]

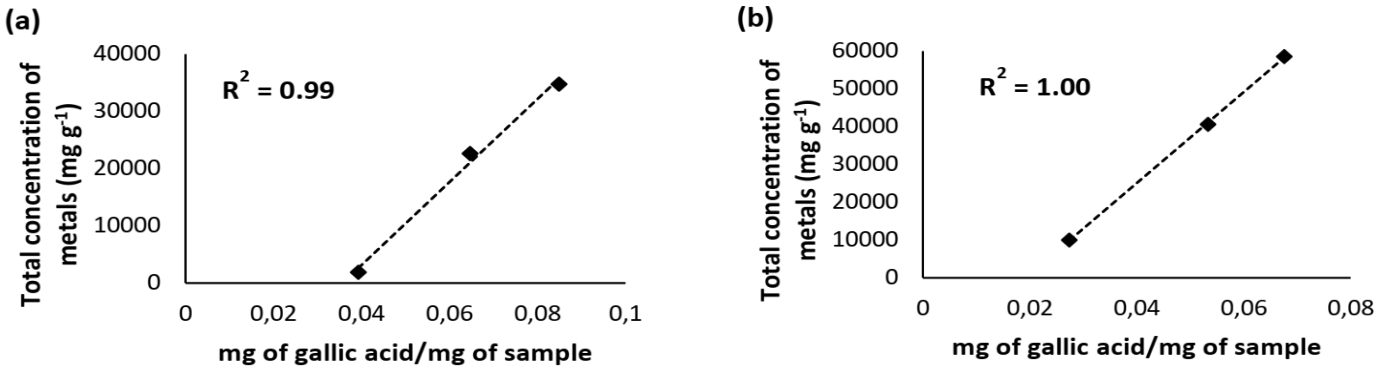

Fig. 3S. Correlation between total concentration of heavy metals (mg g^{-1}) and TPC for (a) in field and (b) *in vitro C. conicum* samples.

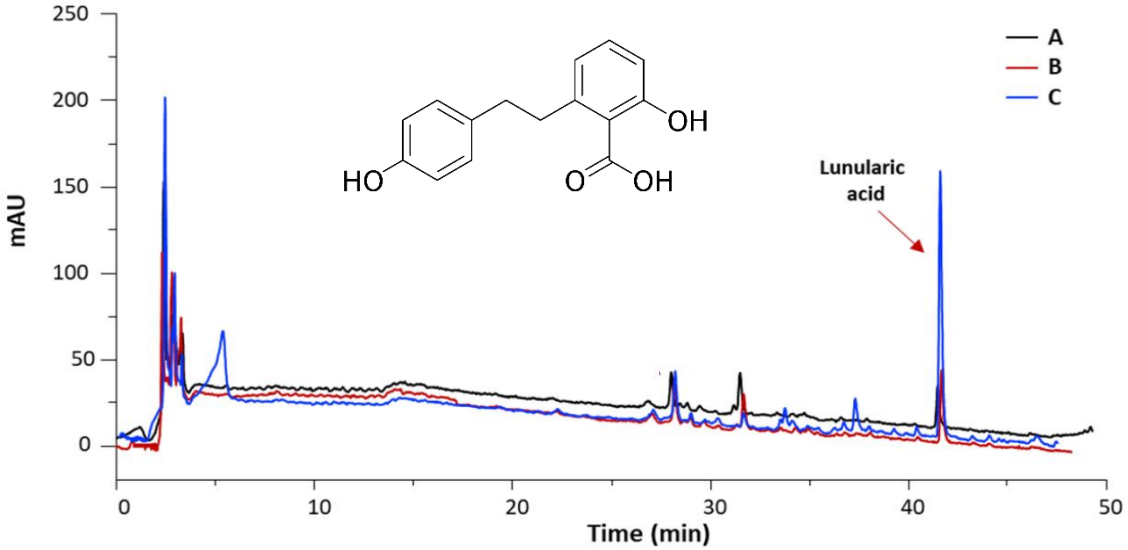

Fig. 3. HPLC profiles of *in vitro* A, B, and C *C. conicum* samples

3.5. Confocal imaging

Under the chosen settings, confocal micrographs showed no DFC signal in both the field non-exposed control and in the *in vitro*-non-treated ones, where only red autofluorescence from chloroplasts was detected (**Fig. 4**). Green fluorescence related to ROS was detectable in all the field-exposed and *in vitro*-treated samples, with an increasing signal from samples A to C (**Fig. 4**). The red signal from chloroplasts was present in all the samples. ROS signal appeared patchy, marking unevenly the cell protoplast. In samples C, the peripheral cytoplasm and plasma membrane emit strong DFC signal (**Fig. 4**). Under the steady settings, confocal micrographs showed faint MCB fluorescence from the field-non-exposed and *in vitro*-non-treated samples (controls), where red autofluorescence from chloroplasts was always detectable (**Fig. 5**). The signal from MCB increases from samples A to C, in both the field and *in vitro* experiment, and most of the blue signals seem to localize in vacuoles (**Fig. 5**).

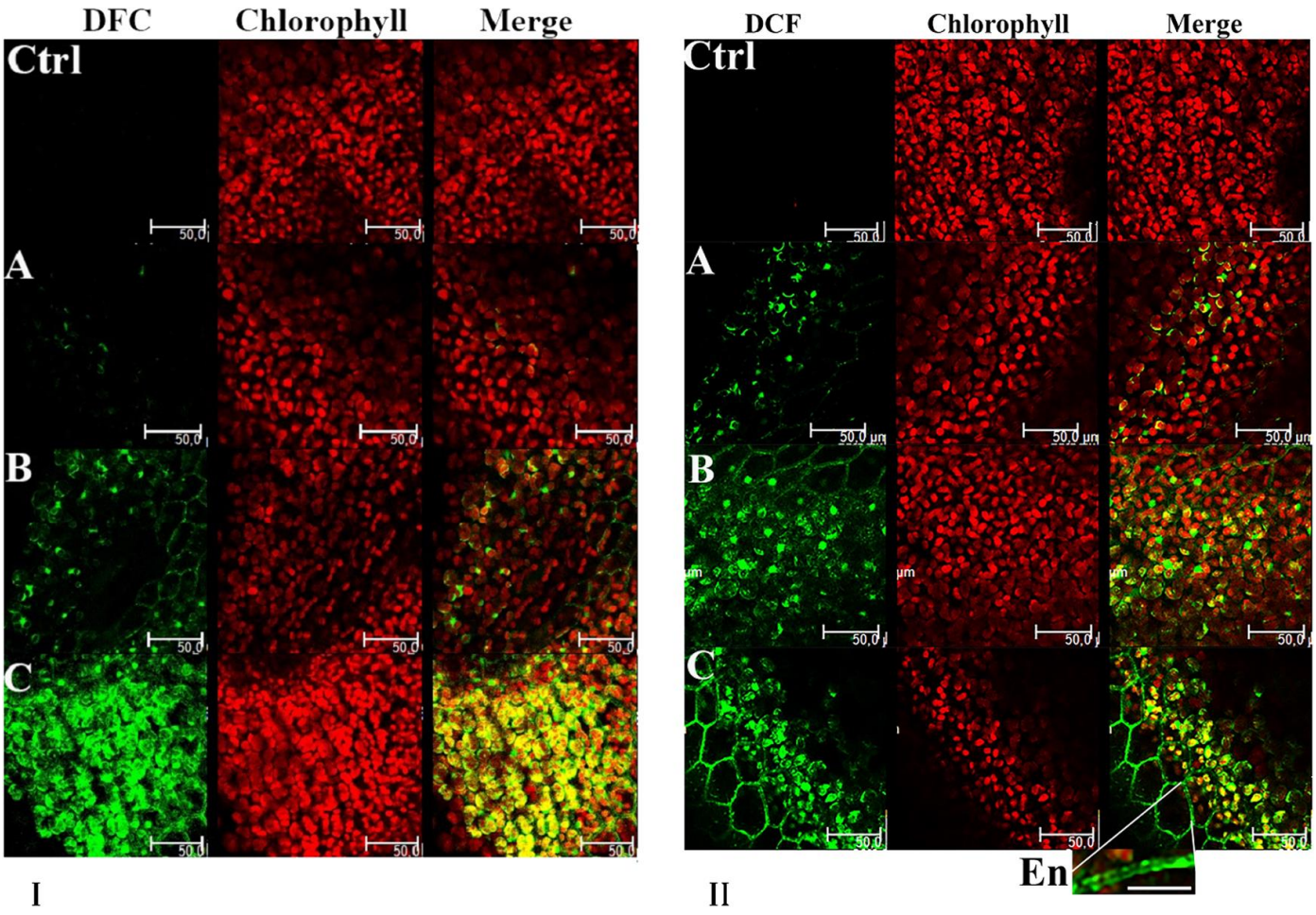

Figure 4. Confocal laser scanning microscopy (CLSM) micrographs of the photosynthetic layer from the field-exposed (I) and *in vitro*-treated (II), DCF-DA-stained *C. conicum* samples A, B, C, and the non-exposed and non-treated one (control). The first column shows DCF signal, the second displays chloroplast autofluorescence and the third is the overlay. In the non-exposed and non-treated control sample, no DFC signal was detectable, while red chloroplast autofluorescence was well evident. In samples A, B, and C (in field and *in vitro*), DCF-signal, increasing from A to C, is visible from the cytoplasm and chloroplasts of the cells along with red autofluorescence from chloroplasts. (En) The micrograph is an enlargement of a detail from the C panel where a strong ROS signal from peripheral cytoplasm and plasma membrane is shown. Scale bars: Ctrl, A, B, C: 50 μ; En: 20 μ.

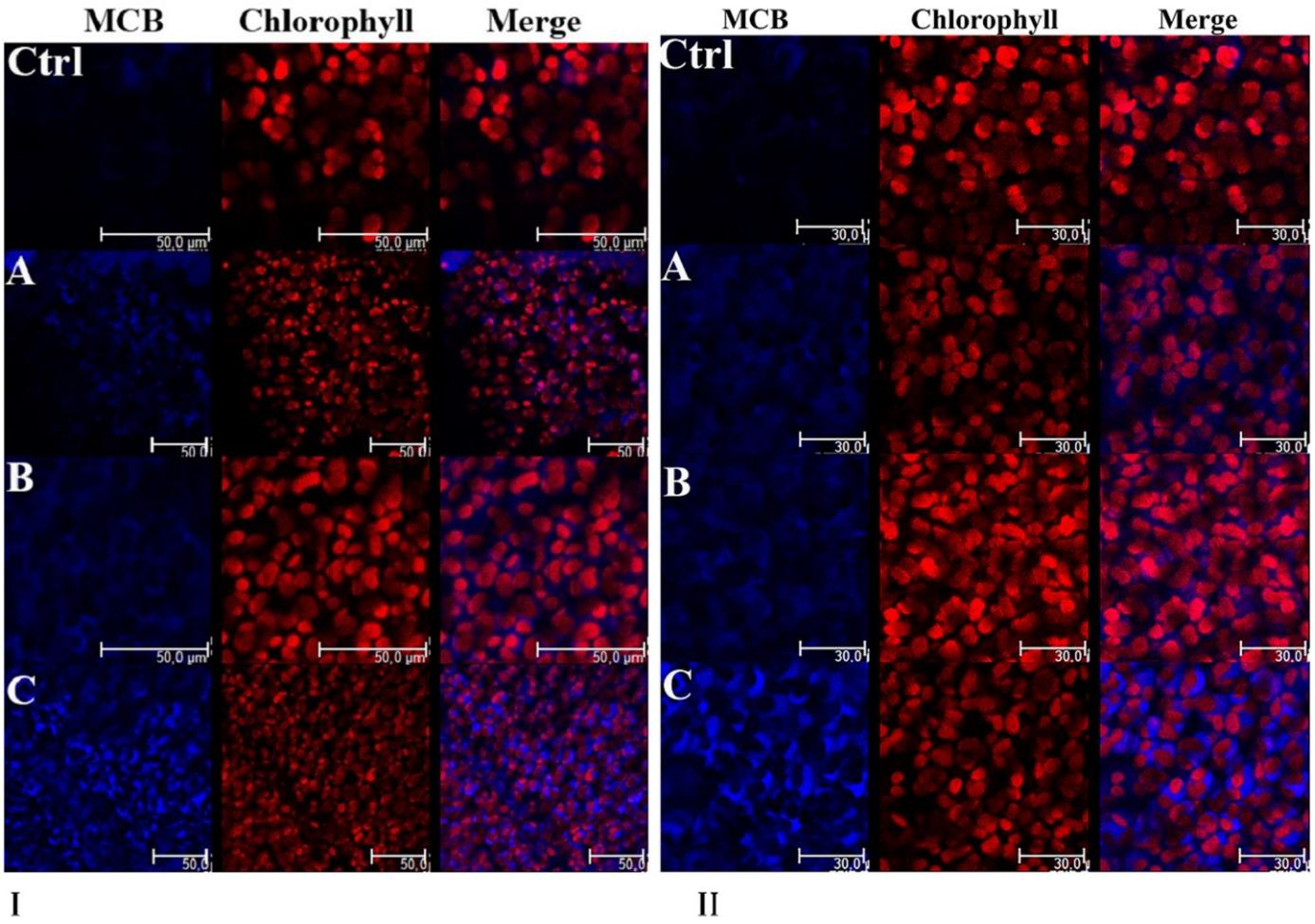

Figure 5. Confocal laser scanning microscopy (CLSM) micrographs of the photosynthetic layer of thalli from the field-exposed and the *in vitro*-treated, MCB-stained *C. conicum* samples A, B, C, and the non-exposed and non-treated one (control). The first column shows the MCB signal, the second displays chlorophyll autofluorescence and the third is the overlay. MBC signal, increasing from the non-exposed and non-treated control to samples C, is detectable in the cytoplasm of the cells along with autofluorescence from chloroplasts. Scale bars: CTRL, A, B, C: 30 μ.

3.6. Transmission electron microscopy

TEM observations showed that field-non-exposed and *in vitro*-non-treated control samples had the same ultrastructural appearance as samples A from both the field and *in vitro* experiments. Cells had a typical ultrastructure with a large central vacuole and, beneath the cell wall, typical oblong chloroplasts with well-developed thylakoids, arranged in grana and intergrana membranes, in a quite dense stroma. Inside chloroplasts starch grains and a few small dense plastoglobules are visible (**Fig. 6a, f)**. The other organelles had also a typical appearance. Mitochondria had clear cristae in a dense stroma (**Fig. 6b, g**). The samples B from both the field and *in vitro* experiments had also a comparable appearance. Chloroplasts still maintained a well-developed thylakoid system, arranged in grana and intergra, and starch grains too. Large plastoglobules and thylakoid light swellings were developed. Mitochondria still had clear cristae and a dense stroma. (**Fig. 6c, h**). Samples C from both the field and *in vitro* experiments developed comparable ultrastructural changes compared to control samples. Chloroplasts appeared swollen and bulged, thylakoids developed swellings, stroma became electron clear (**Fig. 6d, i**). At some points, the outer membrane of the chloroplasts detached from the inner one, and multilamellar bodies were developed (**Fig. 6e, j**). Mitochondria showed crista remnants in a clear stroma (**Fig. 6d**).

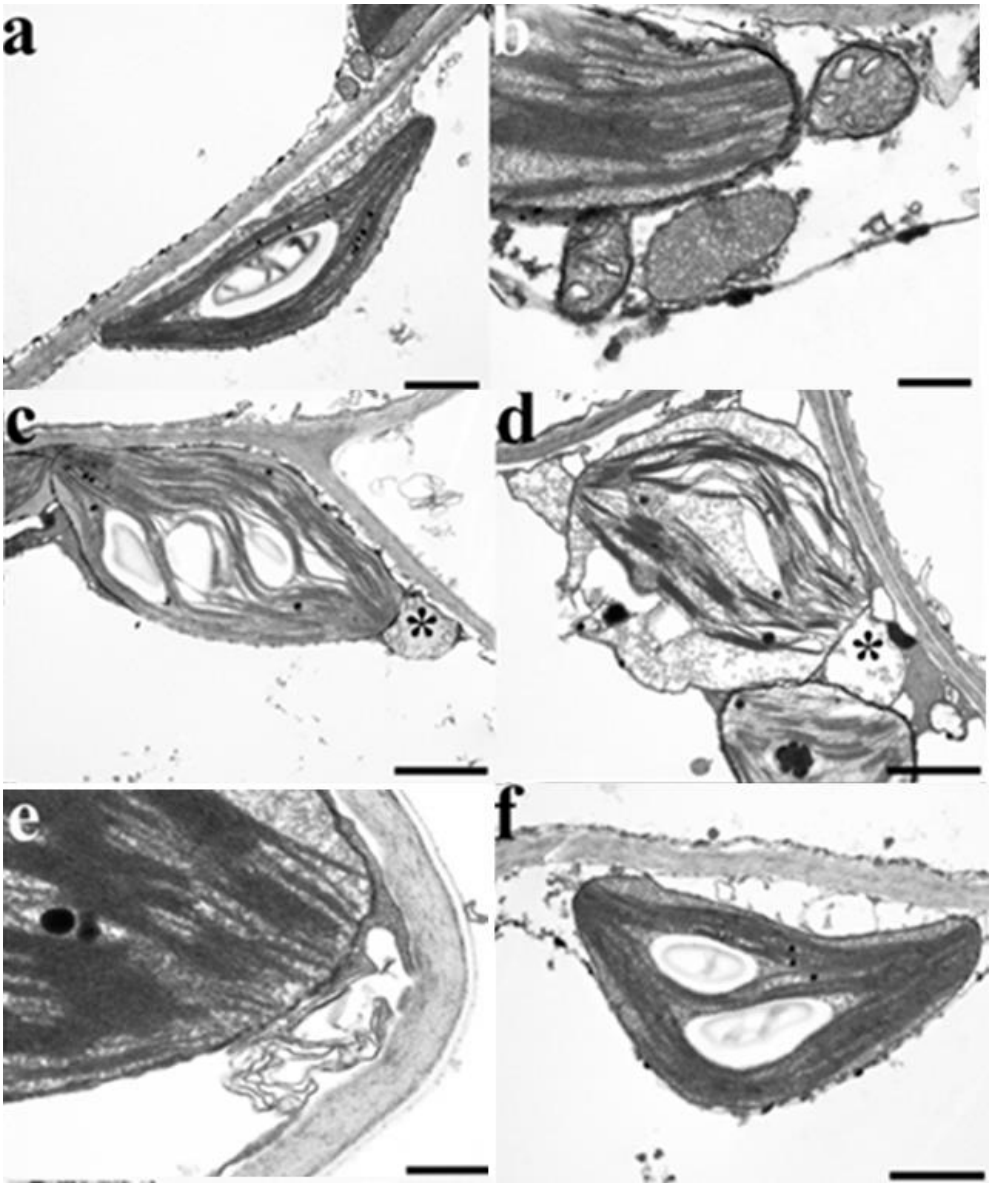

Figure 6. TEM micrographs of *C. conicum* samples after field (Figs. a-e) and *in vitro* (Figs. f-j) treatments. Figs. a-b. Field sample A. Fig a shows, beneath the cell wall, a typical lenticular chloroplast with well-developed thylakoids, arranged in grana and intergrana membranes, in a quite dense stroma, where a central starch grain and a few small dense plastoglobules are present. Fig. b. Two mitochondria with clear cristae in a dense stroma and peroxisome next to a chloroplast. Fig. c. Field sample B. An oblong chloroplast with a well-developed thylakoid system, starch grains, and a few thylakoids. Some of the thylakoids developed swellings. Next to the chloroplast is a mitochondrion with clear cristae in a quite dense stroma (asterisk). Figs. d-e. Field sample C. Fig. d. An altered swollen chloroplast where thylakoids developed large swellings and the stroma appears rather clear. A mitochondrion with crista remnants and clear stroma (asterisk). Fig. e. Beneath the cell wall, next to a chloroplast, is a multilamellar body. Fig f-g. *In vitro* sample, A. Fig. f shows an oblong chloroplast with a typical appearance, where a well-developed thylakoid system, arranged in grana and intergrana, is in a dense stroma. Two starch grains and a few plastoglobules are present (continue).

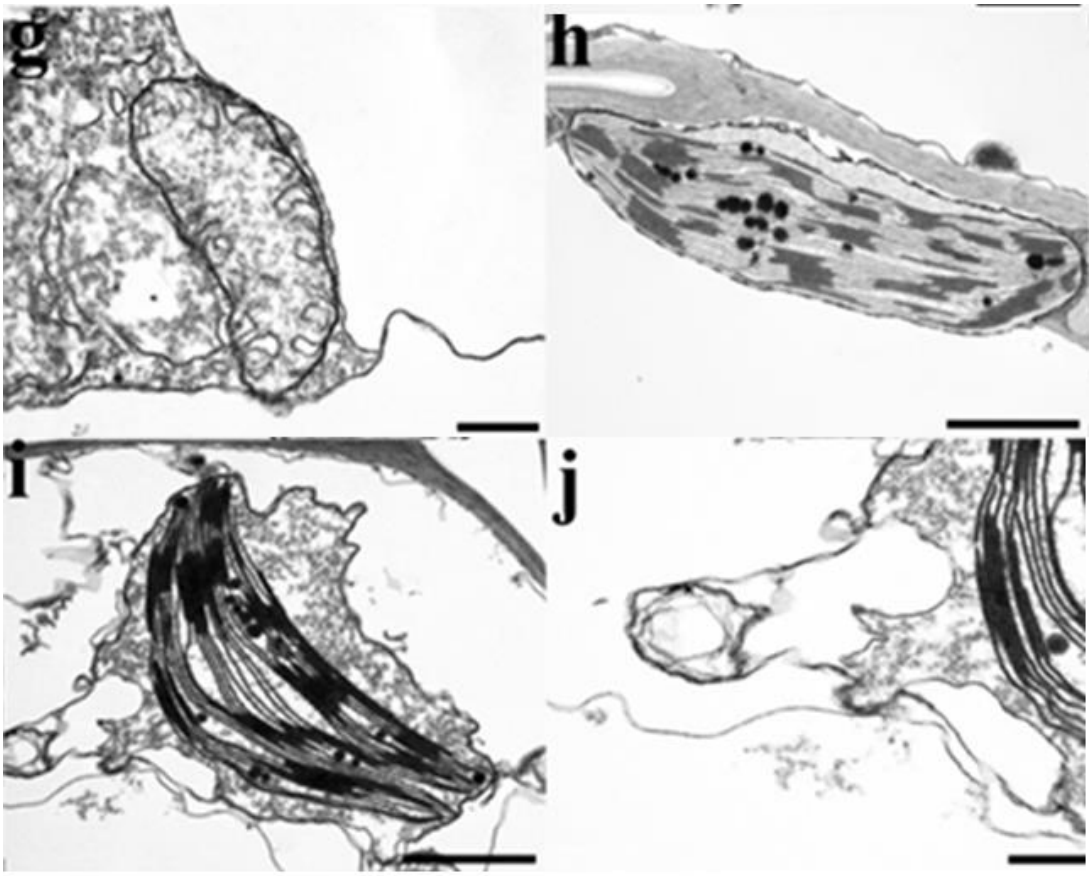

(continue) Fig. g. A mitochondrion with clear cristae in a dense stroma. Fig. h. An oblong chloroplast with grana and intergrana arrangement of thylakoids is well visible. Large dense plastoglobules are also visible. Fig. i. An altered swollen and bulged chloroplast where the well-developed thylakoids system is in a clear abundant stroma. Fig. j. Detail of fig. i. Severe swelling of the chloroplast outer membrane, which detached from the inner one at some points, leaving large spaces. Scale bars: 1 µ (a, c, d, f, h, i), 300 nm (b, e, g, j).

3.7. Pearson's correlation

Table 2S shows the Pearson correlation; data collected for in the field and *in vitro* experiment were pooled together and the correlation between the bioaccumulation of heavy metals and biological responses were derived. All biological responses resulted directly correlated with the concentration of all metals measured, and all metals were directly intercorrelated.

4. Discussion

In this work, the biological responses of the liverwort *C. conicum* to heavy metal pollution of freshwater was reported. The ability of the liverwort *C. conicum* to bioaccumulate heavy metals in both in field and *in vitro* experiments was tested. Furthermore, its tolerance was assessed through several functional and structural indicators. Heavy metal bioaccumulations in *C. conicum* varied notably among the three in field sites, linearly with the concentrations found in water samples. This results are consistent with those from Maresca et al., (2018). For the first time, a study is conducted that takes into consideration a wide range of antioxidant responses, from the activation of enzymes to the response *via* glutathione to the synthesis of molecules to counteract the increase of ROS. Furthermore, for the first time, ROS and thiol compounds cellular localization is identified. Furthermore, antioxidant responses of *C. conicum* are compared both in environmental conditions and *in vitro* in order to reduce confounding variables and to have responses that can only be compared with the concentrations of the metals detected at the 3 exposure sites in the field. As evidenced by the present results, heavy metals exposure implies ROS generation that trigger several antioxidant responses in *C. conicum*. In fact, ROS content is strongly correlated with the antioxidant activities of SOD, CAT and GST. As regards the production of ROS, they are also present at low concentrations of heavy metals, that is, both in the control and in the treated samples. These results are consistent with the idea that ROS are not only produced as a response to abiotic and biotic stresses, but they support biological processes such as cellular proliferation, physiological functions, and viability, thus being essential for plants (Mittler, 2017). Moreover, it is well known that heavy metals cause unbalances in redox homeostasis in plants, inducing the accumulations of ROS such as superoxide anion, hydroxyl radicals, and hydrogen peroxide. These results agree with those obtained on another bryophyte: in the liverwort *Lunularia cruciata* collected in different urban and country sites and *in vitro* tests, the activity of antioxidant enzymes was related to the presence of heavy metals and production and localization of reactive oxygen species (Maresca et al., 2020); The moss *L. riparium* exposed in the same Regi Lagni sites showed the biological responses to ROS activating the antioxidant enzymes (Maresca et al., 2018). All these responses were consistent with the degree of pollution of sites. It is known that the tripeptide glutathione (γ-Glu-Cys-Gly) is involved in the response of plants to environmental stress such as heavy metal exposure (Asgher et al., 2017; Carfagna et al., 2011, 2021). Furthermore, the balance between reduced and oxidized forms of glutathione (GSH and GSSG) may be implied in the regulation of stress-related marker genes at the transcriptional level. The total glutathione content increase in *C. conicum* in field and *in vitro*

experiments suggesting a major stressful environmental impact in samples from the sites of Acerra and Castel Volturno (B and C). The total and reduced form of glutathione, GSH, significantly increased in *C. conicum* samples collected in Castelvolturno (C) may have protected the liverwort from heavy metal pollution and not only, since the concentration of glutathione increased but to a minor extent in samples from *in vitro* experiments, where the only abiotic stress considered was relative to the exposition to high heavy metals concentrations. Notably, an increase in phenolic compound biosynthesis was also observed further exposure of *C. conicum* to heavy metals both in field and *in vitro* experiments, with a very good correlation between TPC values and heavy metal concentrations. This is well in line with what was previously reported in several plants in the case of heavy metal-induced toxicity (Kapoor et al., 2016; Keziah et al., 2016; Manjunath & Reddy, 2019; Rohani et al., 2019). As for the localization of ROS, under the fixed imaging settings of our confocal microscopy, both the field non-exposed samples and *in vitro* non-treated samples did not show any green DCF signal but only red autofluorescence from chloroplasts referrable to chlorophyll. That suggests that the ROS amount was under detection at least. In both the field-exposed and *in vitro*-treated samples, the green DFC signal increased from A to C, showing an increasing presence of ROS. The finding is consistent with our chemical data, demonstrating ROS amount being lowest in the field non-exposed and *in vitro* non-treated control samples and highest in C ones from both the experiments. DCF-DA enters the cells where it undergoes cleavage by cytoplasm esterases. The de-esterificated derivative stays inside the cytoplasm compartments and is not able to cross membranes due to negatively charging. The esterificated DFC-DA is not able to give significant fluorescence to effectively detect ROS; conversely, only the de-esterificated forms give fluorescence after oxidation. So, the DCF signal marks ROS inside cell compartments and allows their localization inside the cell (Kristiansen et al., 2009; Sandalio et al., 2008). In our exposed and treated samples, ROS distribution appears patchy, according to other studies on plants demonstrating a ROS localization inside specific organelles, such as nuclei, mitochondria, peroxisomes, chloroplasts, and plasma membranes rather than an even distribution inside the protoplast (Kristiansen et al., 2009). In samples C, enlargement of external protoplast and cell wall images reveals that peripheral cytoplasm and cell membrane emit a strong uneven signal, giving the appearance of emitting cell walls at low magnification. On the whole, our findings are comparable to another study on the same species exposed to Cd stress, where, in the untreated samples, no DFC signal was detected and ROS fluorescence of the treated ones was patchy in the protoplast and related to the amount of Cd supplied to the plants (Maresca et al., 2020). As for localization of SH groups, under the chosen imaging settings, confocal micrographs of MCB-labeled samples showed faint signal from the field non-exposed and *in vitro* non-treated samples, whereas the fluorescence from thiol peptides was well visible in all the exposed and treated samples,

with an increasing trend from A- to C specimens. That suggests the thiol peptide amount was lower in the control samples and their amount was related to the induced stress in the other specimens, accordingly with the chemical data. Most of the signal seems to localize in vacuoles. Those findings are in agreement with another study on *C. conicum* exposed to Cd stress, where comparable results were obtained with 2 different Cd concentrations (Maresca et al., 2020). TEM observations showed that samples A from both the field and *in vitro* experiments have a typical ultrastructure, which demonstrates that both exposures in site A and *in vitro* treatment with solution A did not impair cell ultrastructure. Samples B from both the experiments developed comparable light alterations, the ultrastructure being mostly preserved. Differently, samples C from both the experiments developed severe alterations with swelling of the whole chloroplasts and the thylakoids inside, with the outer membrane sometimes detaching from the inner one. Swelling and shrinkage of the whole cell or single organelles and membrane compartments, in general, is supposed to be caused by the loss of selective permeability control of membranes. That, in turn, depends either on direct damage to the membrane or on an energy depletion (Schwartzman & Cidlowski, 1993). If selective permeability is impaired, ions move across the membrane downstream concentration gradients, and the shifted water cause swelling or shrinkage of membrane compartments (Schwartzman & Cidlowski, 1993). In addition, ROS are a well-known cause of damage to membranes due to lipid peroxidation (Su et al., 2019). Furthermore, our finding of severe swelling phenomena in chloroplasts and thylakoids associated with mitochondria showing only crista remnants and clear stroma, evident signs of severe ultrastructure damage, suggests that energy depletion could also play a role in the development of those ultrastructure features. Samples C from both experiments developed multilamellar bodies (MLBs). Those are membrane-bound cellular structures, composed of concentric membrane layers, related to autophagic phenomena. Degradative autophagic vacuoles arise after acquiring lysosomal features from nascent, immature autophagic vacuoles, which feature multiple limiting membranes and are regarded to form by the sequestration of cytoplasm by smooth endoplasmic reticulum membranes (Hariri et al., 2000). Multilamellar bodies (MLBs) are formed by the parallel apposition of lipid membranes from the endoplasmic reticulum encircling portions of cytoplasm; the lysosomal nature of the MLB has been demonstrated by the localization of various lysosomal enzymes to this organelle (Hariri et al., 2000). Furthermore, stress stimulates autophagy, which is useful to recycle and degrade damaged cell components (Bassham, 2009; Hayward et al., 2009) and ROS have also been demonstrated to enhance autophagocytosis phenomena through lipid peroxidation (Su et al., 2019). In particular, from our data, it is clear that all the stress alterations caused by heavy metal pollution are strongly correlated with the concentrations of pollutants detected in the environment or supplied *in vitro*. This leads us to hypothesize their possible use as pollution biomarkers as all the

biological responses considered show a trend consistent with the degree of pollution of the sites. Furthermore, this study confirms the ability of the liverwort *C. conicum* to respond to heavy metal pollution in a manner consistent with the degree of pollution and therefore with the possibility of considering it a good bioindicator of environmental pollution both in urban sites (Basile et al., 2013) and aquatic environments.

5. Conclusions

The present study showed the ability of *C. conicum* as bioaccumulator of heavy metals, combining field and *in vitro* experiments, verifying its tolerance through several structural and functional indicators; the biological responses considered, ROS production and localization, antioxidant enzymes, glutathione (reduced and oxidized) levels, phenolic content, ultrastructural damage and localization of compounds presenting thiol groups responded consistently with the expected environmental stress and were related to the concentrations of the most toxic metals found in the soil and bioaccumulated in liverwort. Based on the present results, we can conclude that not only higher but also lower plants (bryophytes) can be used as an alternative first-tier assay system for the detection of environmental pollution. The combination of field and *in vitro* experiments has shown that *C. conicum* can be used as an excellent bioindicator and bioaccumulator in sites highly polluted by human activity, given its reactivity and resistance to heavy metals.

References

Abe, S., & Ohta, Y. (1984). The concentrations of lunularic acid and prelunularic acid in liverworts. *Phytochemistry*, *23*(7), 1379–1381. Scopus. https://doi.org/10.1016/S0031-9422(00)80469-0

Ahmad, S. S., Reshi, Z. A., Shah, M. A., Rashid, I., Ara, R., & Andrabi, S. M. A. (2014). Phytoremediation Potential of Phragmites australis in Hokersar Wetland—A Ramsar Site of Kashmir Himalaya. *International Journal of Phytoremediation*, *16*(12), 1183–1191. https://doi.org/10.1080/15226514.2013.821449

Alberti, P. (2022). The "land of fires": Epidemiological research and public health policy during the waste crisis in Campania, Italy. *Heliyon*, *8*(12), e12331. https://doi.org/10.1016/j.heliyon.2022.e12331

Asgher, M., Per, T. S., Anjum, S., Khan, M. I. R., Masood, A., Verma, S., & Khan, N. A. (2017). Contribution of Glutathione in Heavy Metal Stress Tolerance in Plants. In M. I. R. Khan & N. A. Khan (Eds.), *Reactive Oxygen Species and Antioxidant Systems in Plants: Role and Regulation under Abiotic Stress* (pp. 297–313). Springer. https://doi.org/10.1007/978-981-10-5254-5_12

Basile, A., Sorbo, S., Aprile, G., Conte, B., Castaldo Cobianchi, R., Pisani, T., & Loppi, S. (2009). Heavy metal deposition in the Italian "triangle of death" determined with the moss Scorpiurum

circinatum. *Environmental Pollution*, *157*(8), 2255–2260. https://doi.org/10.1016/j.envpol.2009.04.001

Basile, A., Sorbo, S., Conte, B., Cardi, M., & Esposito, S. (2013). Ultrastructural changes and Heat Shock Proteins 70 induced by atmospheric pollution are similar to the effects observed under in vitro heavy metals stress in Conocephalum conicum (Marchantiales—Bryophyta). *Environmental Pollution (Barking, Essex: 1987)*, *182*, 209–216. https://doi.org/10.1016/j.envpol.2013.07.014

Bassham, D. C. (2009). Function and regulation of macroautophagy in plants. *Biochimica et Biophysica Acta (BBA) - Molecular Cell Research*, *1793*(9), 1397–1403. https://doi.org/10.1016/j.bbamcr.2009.01.001

Bove, M. A., Ayuso, R. A., De Vivo, B., Lima, A., & Albanese, S. (2011). Geochemical and isotopic study of soils and waters from an Italian contaminated site: Agro Aversano (Campania). *Journal of Geochemical Exploration*, *109*(1), 38–50. https://doi.org/10.1016/j.gexplo.2010.09.013

Carfagna, S., Salbitani, G., Innangi, M., Menale, B., De Castro, O., Di Martino, C., & Crawford, T. W. (2021). Simultaneous Biochemical and Physiological Responses of the Roots and Leaves of Pancratium maritimum (Amaryllidaceae) to Mild Salt Stress. *Plants*, *10*(2), Article 2. https://doi.org/10.3390/plants10020345

Carfagna, S., Vona, V., Salbitani, G., Sorbo, S., Lanza, N., Conte, B., Rigano, V., Cobianchi, R., Golia, B., & Basile, A. (2011). Cysteine synthesis in Scorpiurum circinatum as a suitable biomarker in air pollution monitoring. *International Journal of Environment and Health*, *5*(1–2), 93–105. https://doi.org/10.1504/IJEnvH.2011.039859

di Martino, D. (2014, March 13). *Ecologie dell'inquinamento Progetto di territorio attraverso la bonifica* [Tesi di dottorato]. Università degli Studi di Napoli Federico II. http://www.fedoa.unina.it/10025/

Esposito, S., Sorbo, S., Conte, B., & Basile, A. (2012). Effects of Heavy Metals on Ultrastructure and HSP70S Induction in the Aquatic Moss Leptodictyum Riparium Hedw. *International Journal of Phytoremediation*, *14*(4), 443–455. https://doi.org/10.1080/15226514.2011.620904

Gorham, J. (1977). Metabolism of lunularic acid in liverworts. *Phytochemistry*, *16*(7), 915–918. Scopus. https://doi.org/10.1016/S0031-9422(00)86692-3

Grezzi, G., Ayuso, R. A., De Vivo, B., Lima, A., & Albanese, S. (2011). Lead isotopes in soils and groundwaters as tracers of the impact of human activities on the surface environment: The Domizio-Flegreo Littoral (Italy) case study. *Journal of Geochemical Exploration*, *109*(1), 51–58. https://doi.org/10.1016/j.gexplo.2010.09.012

Hariri, M., Millane, G., Guimond, M.-P., Guay, G., Dennis, J. W., & Nabi, I. R. (2000). Biogenesis of Multilamellar Bodies via Autophagy. *Molecular Biology of the Cell*, *11*(1), 255–268.

Hayward, A. P., Tsao, J., & Dinesh-Kumar, S. P. (2009). Autophagy and plant innate immunity: Defense through degradation. *Seminars in Cell & Developmental Biology*, *20*(9), 1041–1047. https://doi.org/10.1016/j.semcdb.2009.04.012

Kapoor, D., Rattan, A., Bhardwaj, R., Kaur, S., Gupta, A., & Manoj. (2016). Antioxidative defense

responses and activation of phenolic compounds in Brassica juncea plants exposed to cadmium stress. *International Journal of Green Pharmacy*, *10*(4), 228–234. Scopus.

Kelly, M. G., Girton, C., & Whitton, B. A. (1987). Use of moss-bags for monitoring heavy metals in rivers. *Water Research*, *21*(11), 1429–1435. https://doi.org/10.1016/0043-1354(87)90019-4

Keziah, J. E. J., Sharmila, S., & Rebecca, L. J. (2016). Effect of heavy metals and UV irradiation on the production of flavonoids in Indigofera tinctoria. *International Journal of Pharmaceutical Sciences Review and Research*, *39*(2), 104–107. Scopus.

Kristiansen, K. A., Jensen, P. E., Møller, I. M., & Schulz, A. (2009). Monitoring reactive oxygen species formation and localisation in living cells by use of the fluorescent probe CM-H(2)DCFDA and confocal laser microscopy. *Physiologia Plantarum*, *136*(4), 369–383. https://doi.org/10.1111/j.1399-3054.2009.01243.x

Manjunath, B., & Reddy, J. (2019). Comparative evaluation of air pollution tolerance of plants from polluted and non-polluted regions of Bengaluru. *Journal of Applied Biology and Biotechnology*, *7*(3), 63–68.

Maresca, V., Fusaro, L., Sorbo, S., Siciliano, A., Loppi, S., Paoli, L., Monaci, F., karam, E. A., Piscopo, M., Guida, M., Galdiero, E., Insolvibile, M., & Basile, A. (2018). Functional and structural biomarkers to monitor heavy metal pollution of one of the most contaminated freshwater sites in Southern Europe. *Ecotoxicology and Environmental Safety*, *163*, 665–673. https://doi.org/10.1016/j.ecoenv.2018.07.122

Maresca, V., Lettieri, G., Sorbo, S., Piscopo, M., & Basile, A. (2020). Biological Responses to Cadmium Stress in Liverwort Conocephalum conicum (Marchantiales). *International Journal of Molecular Sciences*, *21*(18), Article 18. https://doi.org/10.3390/ijms21186485

Maresca, V., Sorbo, S., Loppi, S., Funaro, F., Del Prete, D., & Basile, A. (2020). Biological effects from environmental pollution by toxic metals in the “land of fires” (Italy) assessed using the biomonitor species Lunularia cruciata L. (Dum). *Environmental Pollution (Barking, Essex*, *265*(Pt A), 115000. https://doi.org/10.1016/j.envpol.2020.115000

Mittler, R. (2017). ROS Are Good. *Trends in Plant Science*, *22*(1), 11–19. https://doi.org/10.1016/j.tplants.2016.08.002

Panzella, L., Moccia, F., Toscanesi, M., Trifuoggi, M., Giovando, S., & Napolitano, A. (2019). Exhausted woods from tannin extraction as an unexplored waste biomass: Evaluation of the antioxidant and pollutant adsorption properties and activating e ects of hydrolytic treatments. *Antioxidants*, *8*(4). Scopus. https://doi.org/10.3390/antiox8040084

Pryce, R. J. (1971). Lunularic acid, a common endogenous growth inhibitor of liverworts. *Planta*, *97*(4), 354–357. Scopus. https://doi.org/10.1007/BF00390214

Rohani, N., Daneshmand, F., Vaziri, A., Mahmoudi, M., & Saber-Mahani, F. (2019). Growth and some physiological characteristics of Pistacia vera L. cv Ahmad Aghaei in response to cadmium stress and Glomus mosseae symbiosis. *South African Journal of Botany*, *124*, 499–507. Scopus. https://doi.org/10.1016/j.sajb.2019.06.001

Salbitani, G., Vona, V., Bottone, C., Petriccione, M., & Carfagna, S. (2015). Sulfur Deprivation Results in Oxidative Perturbation in Chlorella sorokiniana (211/8k). *Plant and Cell Physiology*, *56*(5), 897–905. https://doi.org/10.1093/pcp/pcv015

Sandalio, L. M., Rodríguez-Serrano, M., Romero-Puertas, M. C., & Del Río, L. A. (2008). Imaging of reactive oxygen species and nitric oxide in vivo in plant tissues. *Methods in Enzymology*, *440*, 397–409. https://doi.org/10.1016/S0076-6879(07)00825-7

Schwartzman, R. A., & Cidlowski, J. A. (1993). Apoptosis: The Biochemistry and Molecular Biology of Programmed Cell Death*. *Endocrine Reviews*, *14*(2), 133–151. https://doi.org/10.1210/edrv-14-2-133

Senior, K., & Mazza, A. (2004). Italian "Triangle of death" linked to waste crisis. *The Lancet Oncology*, *5*(9), 525–527. https://doi.org/10.1016/S1470-2045(04)01561-X

Sorbo, S., Aprile, G., Strumia, S., Castaldo Cobianchi, R., Leone, A., & Basile, A. (2008). Trace element accumulation in Pseudevernia furfuracea (L.) Zopf exposed in Italy's so called Triangle of Death. *Science of The Total Environment*, *407*(1), 647–654. https://doi.org/10.1016/j.scitotenv.2008.07.071

Su, L.-J., Zhang, J.-H., Gomez, H., Murugan, R., Hong, X., Xu, D., Jiang, F., & Peng, Z.-Y. (2019). Reactive Oxygen Species-Induced Lipid Peroxidation in Apoptosis, Autophagy, and Ferroptosis. *Oxidative Medicine and Cellular Longevity*, *2019*, 5080843. https://doi.org/10.1155/2019/5080843

SUPPLEMENTARY MATERIALS

Table 1S. The concentration of heavy metals (μg L^{-1}) in waters of river measured in the three experimental sites (Avella, A; Acerra, B; Castel Volturno, C). Values are presented as mean ± st. dev; numbers not accompanied by the same letter are significantly different at $P < 0.05$, using the post-hoc Student–Newman–Keuls test. The concentrations found in the water of the three sites in field experiment were used for the *in vitro* experiments.

	Water		
	A	**B**	**C**
Cu	101.832 ± 2.431[a]	3621.422 ± 24.413[b]	9975.521 ± 32.831[c]
Zn	230.113 ± 9.722[a]	3151.751 ± 12.135[b]	9731.756 ± 57.212[c]
Cd	24.743 ± 1.456[a]	1003.201 ± 8.267[b]	8743.554 ± 35.234[c]
Pb	6.987 ± 0.998[a]	38.755 ± 2.601[b]	775.644 ± 11.318[c]

Table 2S. The table shows the correlation in-field and in vitro experiment, between the bioaccumulation of heavy metals and biological responses. (n=3)

	Cu/field	Zn/field	Cd/field	Pb/field	ROS/field	SOD/field	CAT/field	GST/field	GSH/field	H TOTALE/fie	TPC/field	Cu/in vitro	Zn/in vitro	Cd/in vitro	Pb/in vitro	ROS/in vitro	SOD/in vitro	CAT/in vitro	GST/in vitro	GSH/in vitro	TOTALE/in vi	TPC/in vitro
Cu/field	1																					
Zn/field	**0,84579037**	1																				
Cd/field	**0,78971308**	**0,99523079**	1																			
Pb/field	0,39299409	**0,82297987**	**0,87446924**	1																		
ROS/field	0,5552274	**0,91332997**	**0,94869776**	**0,98298203**	1																	
SOD/field	**0,8827472**	**0,99729035**	**0,98535781**	**0,77895916**	**0,88089756**	1																
CAT/field	**0,80002884**	**0,99674539**	**0,99985547**	**0,86609584**	**0,9431851**	**0,9881141**	1															
GST/field	**0,78302705**	**0,99411671**	**0,99994143**	**0,87966815**	**0,95206432**	**0,98345475**	**0,9996129**	1														
GSH/field	**0,64286402**	**0,95239047**	**0,97758895**	**0,95699207**	**0,99400047**	**0,92738093**	**0,97386849**	**0,97981022**	1													
GSH TOTALE/field	**0,81151261**	**0,9981212**	**0,99933778**	**0,85623956**	**0,93656455**	**0,99090922**	**0,99981197**	**0,99888542**	**0,9692813**	1												
TPC/field	**0,81307858**	**0,99828211**	**0,99923648**	**0,8548495**	**0,93562012**	**0,99126686**	**0,9997563**	**0,99875509**	**0,96861743**	**0,9999964**	1											
Cu/in vitro	**0,88262531**	**0,99730939**	**0,985402**	**0,77912177**	**0,88102029**	**0,99999997**	**0,98815394**	**0,9835017**	**0,92747793**	**0,99094408**	**0,99130103**	1										
Zn/in vitro	**0,84874484**	**0,99998453**	**0,9946728**	**0,81980738**	**0,91105077**	**0,99768411**	**0,99628158**	**0,99349886**	**0,95067991**	**0,99776496**	**0,99794078**	**0,99770172**	1									
Cd/in vitro	**0,79082045**	**0,99540545**	**0,99999837**	**0,87359118**	**0,94812481**	**0,98566432**	**0,99988456**	**0,99992024**	**0,9772069**	**0,9994019**	**0,99930545**	**0,98570805**	**0,99485747**	1								
Pb/in vitro	0,54145438	**0,90649935**	**0,94336167**	**0,98587419**	**0,99986437**	**0,87298292**	**0,93758487**	**0,94689719**	**0,99206428**	**0,93066502**	**0,92967932**	**0,87310939**	**0,9041369**	**0,94276057**	1							
ROS/in vitro	0,45306872	**0,85881709**	**0,9046935**	**0,99780169**	**0,99299516**	**0,8188034**	**0,89731912**	**0,90925188**	**0,97411434**	**0,88859129**	**0,88735651**	**0,81895226**	**0,85595436**	**0,90392206**	**0,99480644**	1						
SOD/in vitro	**0,97391503**	**0,94478953**	**0,9083192**	0,59139865	**0,72946753**	**0,96633544**	**0,91529918**	**0,9037389**	**0,79990582**	**0,92293751**	**0,92396775**	**0,96626868**	**0,94659754**	**0,90907362**	**0,71810315**	**0,64353784**	1					
CAT/in vitro	**0,96912665**	**0,95122337**	**0,91659284**	**0,60758623**	**0,74315213**	**0,97134124**	**0,92325785**	**0,9122118**	**0,81187939**	**0,93053412**	**0,931514**	**0,97127956**	**0,95292463**	**0,91731389**	**0,73203118**	**0,65888626**	**0,99979547**	1				
GST/in vitro	0,44193341	**0,85237184**	**0,89931825**	**0,9985495**	**0,99144697**	**0,81159185**	**0,8917537**	**0,90399851**	**0,9712241**	**0,88281091**	**0,88154654**	**0,81174335**	**0,84944995**	**0,89852652**	**0,99346195**	**0,99992248**	**0,63395741**	**0,64946865**	1			
GSH/in vitro	**0,97674934**	**0,94050262**	**0,90287156**	0,58099206	**0,72062129**	**0,96295093**	**0,9100501**	**0,89816567**	**0,79213132**	**0,91791676**	**0,91897876**	**0,96288096**	**0,94237805**	**0,90364701**	**0,70910473**	**0,63365314**	**0,9999175**	**0,99945321**	**0,62397133**	1		
GSH TOTAL/in vitro	**0,8142529**	**0,99839843**	**0,99915552**	**0,8537996**	**0,93490512**	**0,99153122**	**0,99970966**	**0,99865229**	**0,96811336**	**0,99998893**	**0,99999796**	**0,99156487**	**0,99806831**	**0,99922814**	**0,92893331**	**0,88642329**	**0,92473847**	**0,9322468**	**0,88059109**	**0,9197734**	1	
TPC/in vitro	**0,98714239**	**0,74963665**	**0,68149915**	0,24095861	0,41514702	**0,79629506**	**0,69384252**	**0,67353861**	0,51216147	**0,70767645**	**0,70957091**	**0,79613815**	**0,75330643**	**0,68282056**	0,40010745	0,3047469	**0,92512228**	**0,91725448**	0,29286407	**0,92992275**	**0,71099284**	1

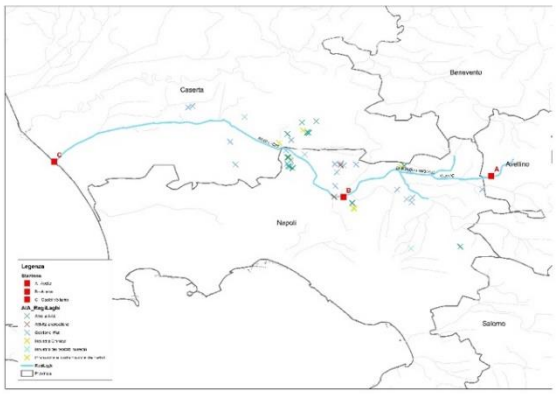

Fig. 1S. Regi Lagni monitoring stations and industries subject to IEA

PAPER III

Environmental and Experimental Botany 216 (2023) 105511

Contents lists available at ScienceDirect

Environmental and Experimental Botany

journal homepage: www.elsevier.com/locate/envexpbot

Tissue localization and the physiological effects induced by an environmentally relevant mix of heavy metals in the liverwort *Conocephalum conicum* L. Dum

Giovanna Salbitani[a], **Piergiorgio Cianciullo**[a], Viviana Maresca[a], Sergio Sorbo[b], Marilena Insolvibile[c], Francesco Loreto[a], Alessia Di Fraia[a], Adriana Basile[a], Simona Carfagna[a]

a Department of Biology, University of Naples Federico II, Naples, Italy
b CeSMA, University of Naples Federico II, Naples, Italy
c ISPRA, Italian National Institute for Environmental Protection and Research, Rome, Italy

DOI: https://doi.org/10.1016/j.envexpbot.2023.105511

Abstract

Tissue accumulation, ultrastructural alterations, oxidative stress, and effects on photosynthesis were assessed in the liverwort *Conocephalum conicum* exposed in vitro to heavy metals (HM) concentrations in three sites of the Savone River, representative of different anthropic impacts. The uptake and accumulation of HM in the thallus of the liverwort was first studied, and the biological effects in relation to the different accumulation sites of HM along thallus, ribs and wings, were then investigated, considering: bioaccumulation (by atomic absorption spectrometry), localization (by X-ray scanning electron microscopy microanalysis), ultrastructural damage of photosynthetic parenchyma (by transmission electron microscopy), oxidative stress (by ROS contents and antioxidant enzymes activities determination), photosynthesis (by chlorophyll fluorescence). The results showed the HM bioaccumulation in *C. conicum* was dependent by their concentrations in the contaminated water. As for spatial localization, HM preferentially accumulated in the nerve of gametophytes respect to the wings. With respect to tissue localization, HM were mainly found in the hyaline and in the photosynthetic parenchyma. Essential metals (Cu and Zn) were accumulated at higher concentrations with respect to non-essential metals (Pb and Cd). At the ultrastructural level, HM caused alterations of the fine structure of the cells, most evident along the nerve, inducing marked alterations of the chloroplast structure and therefore of the photosynthetic capacity. Based on the results of the presented study, *C.conicum* can be used as a marker to indicate heavy metal pollution in water natural resources.

1. Introduction

Environmental pollution is one of the global challenges in the last decades. In particular, water contamination is a major environmental problem. Industrialization, increasing population and urbanization led to worsening of water quality. The main chemical pollutants of water basins are organic matter, nutrients, pharmaceutical and personal care products, poly- and perfluoroalkyl substances, biocides, heavy metals (HM), dyes, radionuclides, plastics (Zamora-Ledezma et al., 2021). Heavy metals are among the most released anthropogenic contaminants; they are not biodegradable and tend to bioaccumulate into primary producers, affecting the entire trophic chain. At a low concentration, some HM are essentials for the optimal physiological functioning of plants (micronutrients: Cu, Zn, Fe, Mn, Mo, Ni, and Co) playing a prominent role in the synthesis of proteins, nucleic acids, photosynthetic pigments, and also taking part in the structural and functional integrity of cell membranes (Arif et al., 2016; Rengel, 1999). Other HM such as Cd, Pb, Hg have unknown physiological role but exert toxic effects also at low concentrations; therefore, their uptake and utilization are tightly controlled by the plant cells (Singh et al., 2016). Plants growing in polluted sites accumulate higher amounts of HM, and these trigger a wide range of physiological and biochemical alterations, in some cases reaching lethal levels. Nowadays, there is an active search for plant hyperaccumulators or markers of heavy metal presence in water and soil (Sytar et al., 2016). Bryophytes, in particular, are able to accumulate and tolerate high concentrations of HM. Many of them survive in contaminated areas and are considered valuable ecological bioindicators across a variety of pollution sources and environments (Maresca, et al., 2022a; Maresca, et al., 2022b). Indeed, bryophytes are pioneer plants that colonized the primitive terrestrial lands (Nickrent et al., 2000) evolving mechanisms to cope with a probably much higher HM load in the environment than today (Degola et al., 2014). The thallose liverwort *Conocephalum conicum* L. Dum (Conocephalaceae), is one of the oldest terrestrial plants (Qiu et al., 1998). It possesses no conducting bundles and no stomata, and the thallus is anchored to the soil with rhizoids (Koselski et al., 2019). The high content of uronic acid, cellulose and protein contents into cell wall, makes *C. conicum* an effective in accumulation of microelement and trace elements (Samecka-Cymerman et al., 1997), which makes this species a useful candidate as a bioindicator of HM pollution. The aim of this research was to investigate accumulation, tissue localization and possible ultrastructural alteration induced by HM exposure in *C. conicum*. Furthermore, physiological responses, such as photosynthetic performance, pigment changes and oxidative alteration of *C. conicum* were investigated.

2.Material and methods

2.1. Plant material

Samples of *C. conicum* were collected from the mountain site of Savone, identified and deposited in the herbarium of the Botanical Garden of the University of Naples Federico II. Some of these samples were used for in vitro experiments.

2.2. Location and characteristics of the sites

Three different sites of the Savone River were chosen: C1) near the river spring (41◦ 16' 13.6'' N 14◦ 02' 19.9'' E); C2) before the entrance of the watercourse in a heavily inhabited area (41◦ 9' 37.205'' N 14◦ 1' 59.033''); C3) in correspondence of the town of Mondragone (41◦ 6' 4.97'' N 13◦ 53' 33.89'' E). At each site, three water samples were collected for HM analysis as reported in Maresca et al. (2020). *C. conicum* thalli were exposed in vitro for 7 days to the concentrations of heavy metals (Cd, Pb, Zn, Cu) measured in the three different selected sites of the Savone River. The Savone (also called Savone delle ferriere) is an Italian torrent, which originates from some sources in the north-east area of the caldera of the Roccamonfina volcano, between 600 and 650 m above sea level, in the municipality of Roccamonfina. It is about 48 Km long, it has a very sinuous course, enriched by several jumps and waterfalls, and in the section of the Roccamonfina-Foce Garigliano Regional Park it crosses an area rich in woods.

2.3. Gametophyte culture

Field-grown *C. conicum* was gathered in the Savone River site C1. Plants were collected (1–3 cm wide and 5–7 cm long, obtained by cutting the dead basal part). Single gametophytes (1 g) were thoroughly washed with deionized water and then their surfaces were sterilized in 70 % ethanol (2 min) and in 2 % NaClO with a few drops of Triton X-100 (5 min). Subsequently, 20 gametophytes were washed (10 min) with distilled sterile water and put in 5-cm wide Petri dishes with 20 g of fine-granular, washed quartz (Merck). The solution wetted only the lower surface of plants and rhizoids. Gametophytes collected in the upstream site of the Savone River were immediately processed and used as controls. The specimens were cultured with 10 mL of sterile Mohr medium solution in which the same HM concentration measured in Savone River at site C1, C2 and C3 were dissolved. The solutions were replaced every two days. The cultures were kept in a climatic room with a temperature ranging from 13 to 20 ◦C (night and day temperature), 70 % constant relative humidity, and a photoperiod of 16 h light (40 μmol photons m-2 s-1) and 8 h dark. Gametophytes were monitored every two days in order to establish the effect of HM exposure on thallus growth, and browning of tissues. The specimens were maintained in the growth chamber for 7 days. Experiments on

gametophyte cultures were conducted in triplicate and repeated three times. The results are the mean ± s.e. of all the observations for each experimental set.

2.4. Analytical determination of HM in water samples and in liverworts.

The water samples collected in the field experimental sites were filtered through Whatman paper (no. 42) and analyzed by ICP-MS (Perkin-Elmer Sciex 6100) for the concentration of selected heavy metals: Cd, Cu, Pb, and Zn. Analytical quality was checked against the Standard Reference Material SRM 1463d "river water". The precision of analysis was estimated by the coefficient of variation of 3 replicates and was found to be < 10 % for all elements. As for *C. conicum* samples, the protocol reported in Maresca et al. (2018) was used. Apical parts (2 cm) were collected, dried to constant weight at 40 ◦C, and then frozen in liquid nitrogen, pulverized and homogenized with a ceramic mortar and pestle. About 300 mg of liverwort powder was mineralized with a mixture of 6 mL of 70 % HNO3, 0.2 mL of 60 % HF and 1 mL of 30 % H2O2 (ultrapure reagent grade). Digestion of samples was carried out in a microwave digestion system (Milestone Ethos 900) for a total time of 30 min. Concentrations of selected toxic metals (Cd, Cu, Pb, Zn), expressed on a dry weight basis, were determined by ICP-MS (Perkin-Elmer Sciex 6100, Elan). Analytical quality was checked by analyzing the Certified Reference Material BCR 61 "aquatic moss" (*Platyhypnidium riparioides*, Hedw.) with a recovery percentage of 84 %. The precision of analysis was estimated by the coefficient of variation of 3 replicates, and was found to be < 10 % for all elements.

2.5. Transmission electron microscopy preparation

Transmission electron microscopy (TEM) observations were performed on specimens prepared as it follows. Collected samples, after careful cleaning, were cut by a sharp blade to pick subapical parts of the thalli, about 5 mm below the apex, from the nerve and the wing areas. After fixation with 2.5 % glutaraldehyde in phosphate buffer solution (pH 7.2–7.4) overnight at 4 ◦C and post fixation with 1 % osmium tetroxide and 0.8 % KFeCN in the same buffer at room temperature for 1.5 h, specimens were dehydrated with up to 100 % alcohol and propylene oxide and then embedded in Spurr resin. Ultrathin sections, 70 nm thick, collected on 300-mesh copper grids, were stained with Uranyl Acetate Replacement UAR (Electron Microscopy Science) and lead citrate. Observations with a Philips EM 208 S TEM (Basile et al., 2001) focused on the photosynthetic parenchyma that due to the presence of chloroplast is a well-known target of pollution damage as observed in previous studies on liverworts (Basile et al., 2017; Carginale et al., 2004; Maresca et al., 2023; Maresca, Salbitani, et al., 2022b). Three specimens from each treatment were observed. For each sample, three sections were observed.

2.6. X-ray SEM microanalysis

After HM exposure, plants were thoroughly washed in distilled water for 15 min with several changes of water to eliminate unbound HM and fixed in 2 % glutaraldehyde in phosphate buffer (0.065 M, pH 7.2–7.4) for 90 min at room temperature. The tissue pieces were dehydrated with ethanol, critical-point dried, and mounted on carbon stubs, covered with a 15 nm thick carbon film and observed with a Cambridge 250 Mark 3 scanning electron microscope (SEM). The analysis was performed with an energy-dispersive detection system spectrometer and a Link AN 10,000-analyser computer system (Basile et al., 1994, 2001). Spectra were collected over 50 s live time with a 0.5 mm diameter probe current was 400 mA. The mean count rate was 1000–1500 counts per s and the take-off angle was 35◦ (Roomans and Shelburne, 1983). Spectra were processed, and quantitative information was obtained by the New ZAFPB/FLS program for deconvolution and background subtraction by least squares fitting of prefiltered spectra (Statham, 1977). This program was also used for the quantification of data by the continuum method of Hall (Hall, 1979b, 1979a) and Gupta (Gupta, 1979). The concentration of the element present is proportional to the ratio of characteristic counts (peak minus background) to the number of counts in the continuum contributed by the specimen. To make a good estimate, counts were collected at 20–40 keV. Quantification was achieved by comparison with standards of known composition. The X-Ray microscope standards, mounted in resin, were supplied by Microanalysis Consultants Ltd, Cambridge. 36 specimens (9 samples from CTRL, 9 samples from C1, 9 samples from C2 and 9 samples from C3 samples in triplicate collected from different dishes) were observed and analyzed by microanalysis.

2.7. Fluorescence parameters determination

The maximal efficiency of photochemistry of photosynthesis in control (not exposed) and HM exposed liverworts was estimated with an IMAGING-PAM M-Series Chlorophyll Fluorometer (Walz, Effeltrich, Germany). The liverworts were acclimated in the dark for 30 min before analysis. After dark adaptation, the maximal quantum efficiency of PSII in the dark (Fv/Fm, where *Fv* is the variable and *Fm* is the maximal fluorescence in dark-adapted organisms) was measured.

2.8. Determination of photosynthetic pigments

At the end of the experiment, liverworts were collected, wings and nerves separated by bistoury and immediately frozen in liquid nitrogen and stored at-80 ◦C. For extraction, frozen samples were ground in liquid nitrogen, homogenized and extracted with N,N-dimethylformamide (1:1 ratio) and transferred into glass tubes. Pigments were extracted in the dark at 4 ◦C for about 24 h. The absorbance of the samples was measured, using glass cuvettes, at 664, 647 and 470 nm. The Chl-a and Car were

calculated according to Inskeep & Bloom, (1985) and Wellburn, (1994) formula, respectively. The pigment concentrations were calculated according to Salbitani et al. (2021). Chl-b was calculated as the difference between Chl-tot and Chl-a.

2.9. Detection of reactive oxygen species (ROS) and activity of antioxidant enzymes

Wings and nerves separated as described above were collected and used for ROS and activity of antioxidant enzymes determination. One gram (fresh weight) of plant material was ground with 1 mL of chilled NaH2PO4/Na2HPO4 buffer (PBS, 50 mM, pH 7.8) containing 0.1 mM ethylenediaminetetraacetic acid (EDTA) and 1 % polyvinylpyrrolidone (PVP). The homogenate was centrifuged at 12,000g for 30 min, and the supernatant (protein extract) was collected for protein assay and the determination of ROS levels and SOD, CAT, and GST activities. For each sample, 3 replicates were measured. ROS levels were assessed using 2',7'-dichlorofluorescin diacetate (H2DCFDA). The extract was incubated with 5 µM H2DCFDA for 30 min at 37 ± 1 ◦C. ROS quantity was monitored by fluorescence (Ex:350 nm, Em: 600 nm) in 96 well microplates (Falcon™ Fischer Scientific) using a microplate reader (Bio-Rad Laboratories Inc., Hercules, CA, USA). The activity of the antioxidant enzymes catalase (CAT) (Sigma- Aldrich Co., St Louis, MO, USA), superoxide dismutase (SOD) (19160, Sigma, St Louis, MO, USA), and glutathione S-transferases (GST) (CS0410, Sigma St Louis, MO, USA) were measured following the kit instructions. CAT activity (units mg proteins-1) was measured kinetically (for 1 min at 25 ◦C, 15 s each read) as a drop in the absorbance of H2O2 at 240 nm in 2 mL quartz cuvettes. The reaction (1 mL reaction vol) was started adding 500 uL H2O2 (10 mM) to 40 µL of protein extract diluted in 460 µL PBS buffer. SOD activity was measured using the xanthine oxidase – WST1. GST activity (µmol min-1 mL-1) was assessed through the conjugation of reduced exogenous glutathione with the 1-chloro-2,4- dinitrobenzene (CDNB) The assay was performed in 96 well microplates (Falcon™ Fischer Scientific) measuring the increase in the absorbance at 340 nm of the formed CDNB-glutathione conjugates. The reaction was measured kinetically for 6 min at 25 ◦C and started adding 20 µL of protein extract buffered with PBS buffer to 180 µL of GSH (40 µM) and CDNB (20 µM). Protein concentrations were measured with Bradford method using the Bio-rad Bradford reagent (Bio-rad Laboratories, Inc.) in 96 well microplates reading the absorbance at 595 nm.

2.10. Statistical analysis

Data were examined by one-way analysis of variance (ANOVA) and Tukey's test. In all figures, values are presented as mean ± standard error or standard deviation; numbers not accompanied by the same letter are significantly different at $p < 0.05$. For the student t test significant differences were

marked with asterisks (* $p < 0.05$, ** $p < 0.01$, *** $p < 0.001$). The software used for the analysis was SigmaPlot 14, Systat Software, Inc., USA).

3. Results and discussion

3.1. Heavy metal concentrations in the river

The HM concentration detected in the three sites of the Savone river are shown in **Table 1**. The concentrations of all HM were within the legal limits at site C1 (Italian Legislative Decree 152/2006). In particular, the most toxic HM such as cadmium (Cd) and lead (Pb) were below detection value. The situation changed in the C2 site, where an increase of all metals was measured, and in C3, a dramatic increase of all HM was observed (**Table 1**). This increase can be related to the use of the land, essentially agricultural up to site C2. On C3, a widespread fraudulent use of the territory, due to the presence of toxic fires and uncontrolled waste spills towards the terminal area of the river course, around the city of Mondragone, in addition to the obvious effect of extensive urbanization and anthropization, could be the cause of the significant increase of HM. In fact, copper (Cu) can be related to the use of the territory, this time from an agricultural point of view, being copper sulfate ($CuSO_4$) still used as algaecide and fungicide in crops (Weitbrecht et al., 2021). Generally, zinc is released into the environment both naturally (e.g., volcanoes, wind-blown dust, and forest fires) and via anthropogenic activities such as electroplating industry, smelting and refining, mining, biosolids, but the majority of reported contaminations directly affecting people's health was caused by the latter (Tabelin et al., 2018). However, due to the lack of precise data in the land use in the proximity of the Savone River, certain hypotheses cannot be moved toward a punctual characterization of the emission sources.

Table 1 Concentrations of HMs found in the Savone River at the sites: site C1 (41◦ 16′ 13.6″ N 14◦ 02′ 19.9″ E), site C2 (41◦ 9′ 37.205″ N 14◦ 1' 59.033″) site C3 (41◦ 6′ 4.97'' N 13◦ 53′ 33.89'' E) expressed as μg L-1.

	Zn	**Cu**	**Cd**	**Pb**
C1	0.4 ± 0.1	1.78 ± 0.4	< 0.01	< 0.01
C2	12.87 ± 2.3	4.35 ± 1.1	0.21 ± 0.1	0.34 ± 0.2
C3	25.3 ± 4.5	7.35 ± 1.6	2.34 ± 1.1	3.41 ± 1.3

3.2. Chlorophyll fluorescence

Fluorescence parameters were measured to assess possible differences in maximal photosynthetic capacity after 7-d exposure to the different experimental conditions (CTRL, C1, C2 and C3). As shown by **Fig. 1-A** the samples exposed to the highest HM concentration (C3) showed faded colours, which are indicative of photosystem damage, as indicated by the reduced maximal quantum yield of PSII (Fv/Fm, **Fig. 1- B**). The Imaging-PAM provides us with an in vivo numerical estimate of the Fv/Fm and helps us to understand where the damage is located. The colour of Fv/Fm image was uniform blue in control samples (CTRL). Then, the colour of Fv/Fm image was blue with sporadic green and yellow for HM-treated plants. The colours shifting from blue to yellow indicate great reductions of the maximum efficiency of PSII photochemistry. After seven days of exposure to C3 concentrations, the gametophytes showed a deflection in the Fv/Fm in the nerve area, probably due to the intense transport of water and solutions in the most abundant hyaline parenchyma in this area. PSII is a large pigment-protein complex located into the thylakoid membranes, where it carries out a fundamental role in photosynthetic electron transport (Müh & Zouni, 2020). Therefore, the reduced ratio of Fv/Fm indicates HM toxicity on the photochemistry of photosynthesis.

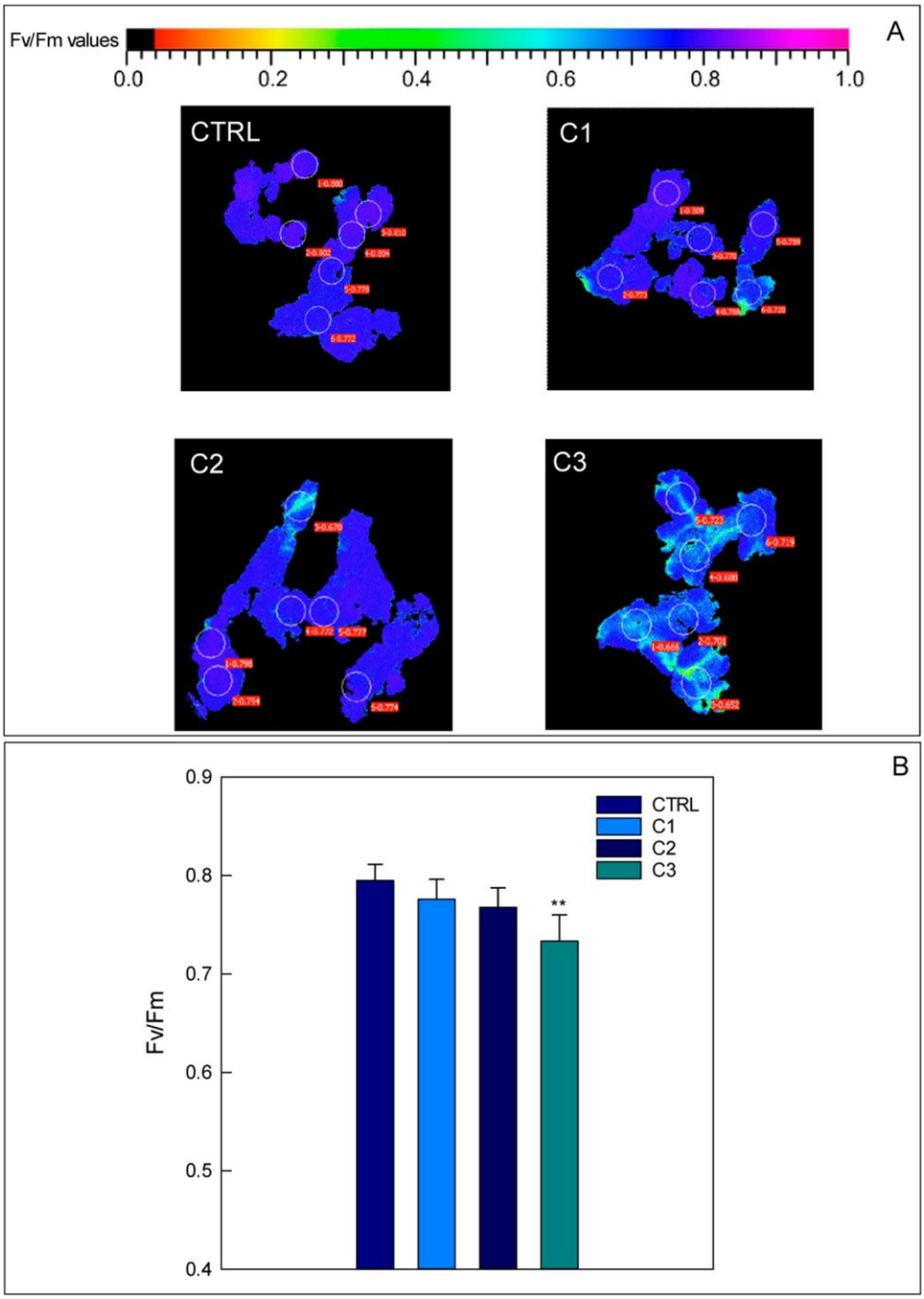

Figure 1. Maximal quantum efficiency of photosystem II (Fv/Fm). (A) Representative images of Fv/Fm of experimental conditions were obtained by Imaging-PAM. The false-colour scale indicating the Fv/Fm values and ranging from black (0.0) to purple (1.0) is shown. B) Values of Fv/Fm of C. conicum after 7 days of treatment (B). Error bars represent SD (n = 15). Significant differences respect to CTRL (not exposed sample) were determined by one-way ANOVA with post-hoc Tukey HSD Test (**$p < 0.01$).

3.3. Pigment contents

Pigments such as total chlorophylls and carotenoids were measured in the exposed (C1, C2 and C3) and not exposed (CTRL) samples of *C. conicum* (**Fig. 2**). A comparison, in pigment contents, between wings and nerves was also made, in the different conditions. A general reduction of pigments was observed in the samples exposed to HM. Already under C1 conditions, a reduction of chlorophylls was observed with respect to controls, but only in the nerves and not in the wings; probably due to lower HM concentration in the surrounding water, the pollutants affected at first nerves and then spread to the wings. The change in photosynthetic pigments content give information on the state of health of the plant. The level of chlorophylls in the cell directly reflects the photosynthetic capacity of plants. In *C. conicum*, the HM exposure reduces the content of both chlorophyll a and b and this reduction (of chlorophylls) could correlate with a damage of photosystems. In particular, the decrease in the content of chlorophylls could be attributed to a reduction of their synthesis due to the inhibition of the reductive steps in the biosynthetic pathways of these photosynthetic pigments (Chandra & Kang, 2016). In fact, the protochlorophyllide reductase, the key enzyme involved in the reduction of protochlorophyll to chlorophyll, is well known to be inhibited by HM. In addition, the photosynthetic membranes are very sensitive to HM and in particular to Cd, which was suggested to firstly affect chlorophyll content, then the photochemical activity of PSII and oxygen-evolving complex, and later the PSI activity (Dobrikova et al., 2021; Wang et al., 2022). In photosynthesis, carotenoids act as antenna pigments, transmitting the captured light energy to chlorophylls, but they also have the function to scavenge free radicals (Polívka et al., 2004). In fact, carotenoids are known to quench the oxidizing species and triplet state of the chlorophylls, which are involved in the oxidative damage of cellular components (Candan & Tarhan, 2003). Carotenoids in *C. conicum* seem to be less vulnerable to the negative impact of HM as compared to chlorophylls, in fact no important changes were observed in HM exposed plants.

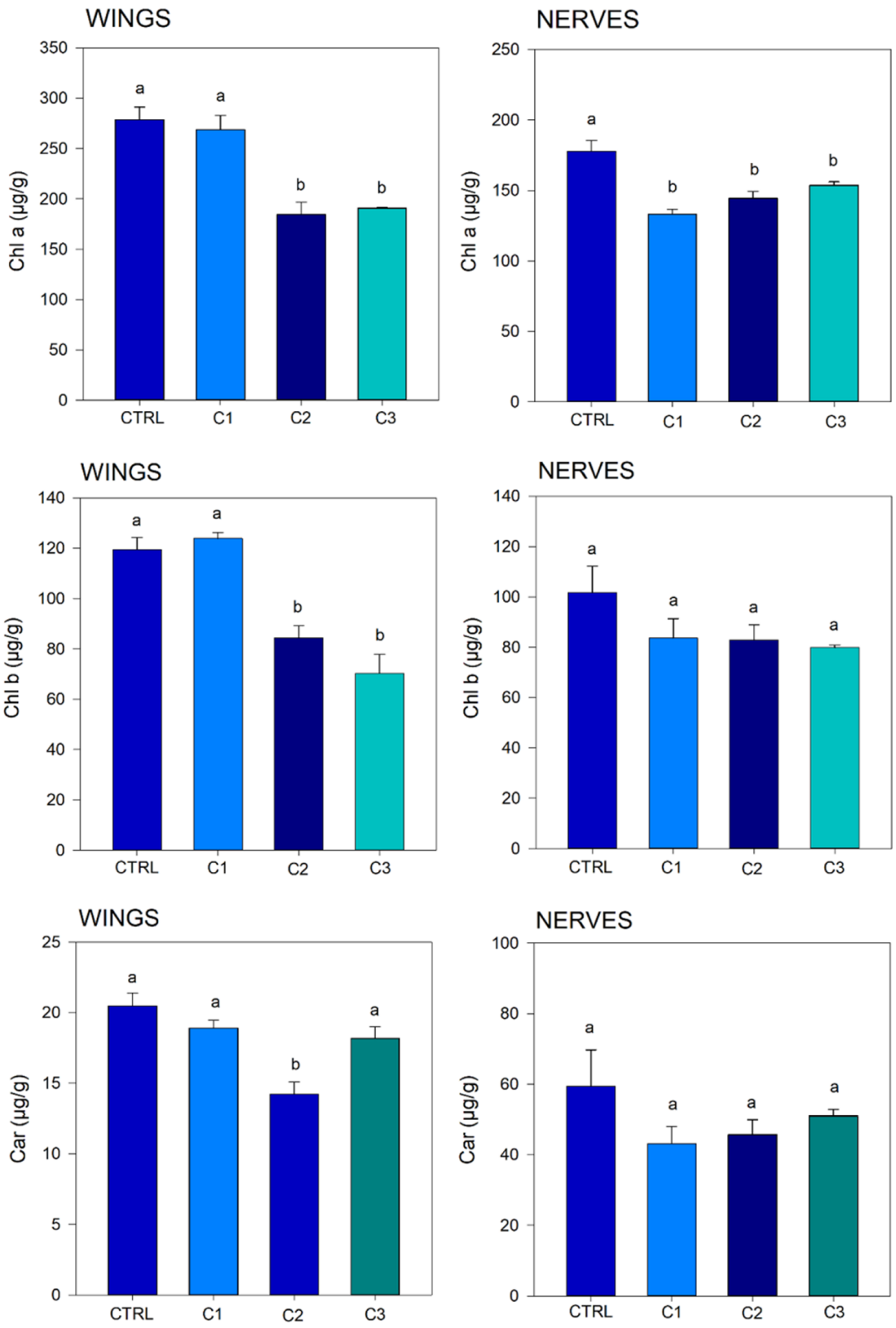

Figure 2. Pigment contents in control and treated *C. conicum*. The liverworts were exposed for 7 d at different concentrations of heavy metals found in three different sites of Savone river (other details in material and methods). Error bars represent SD ($n = 3$). Significant differences between treated and control samples were determined by one-way ANOVA with post-hoc Tukey's ($p < 0.05$).

3.4. Detection of ROS and activity of antioxidant enzymes

Antioxidant activity was assessed by measuring ROS levels and antioxidant enzyme activity in different parts of *C. conicum* thalli nerve and wings. As can be seen from **Fig. 3**, the C1 samples have ROS levels comparable to the control. In C2 and C3, however, ROS levels increased compared to the control, and in both cases the levels were higher in the nerve than in the wings. Exposure to HM can cause damage to plant cells directly or indirectly through its increased production of ROS. Plant cells are able to respond to elevated levels of ROS by activating their enzymatic and non-enzymatic antioxidant defence systems. The main enzymes involved in these defence mechanisms are ROS quenching enzymes such as catalase, superoxide dismutase and glutathione S-transferases. There is growing evidence suggesting stress mechanisms caused by non-Fenton metals (e.g., Pb, Ni, Cd, Cr, etc.) in plant cells may indirectly lead to the production of superoxide radicals, induce lipid peroxidation, increase the activity of some of the key enzymes of antioxidant metabolism and cause severe damages to different cellular organelles and biomolecules (Radotić et al., 2000). This would therefore explain the increased activity of the antioxidant enzymes SOD, CAT and GST in samples C2 and C3 compared to both C1 and the control. The C1 samples showed no significant differences from the controls. As was the case with ROS levels, enzymes activities were also higher in nerves than in wings. A higher concentration of HM in the nerve than in the wings could explain these differences both in the levels of ROS and of the enzymatic activities in the different parts of *C. conicum* thalli.

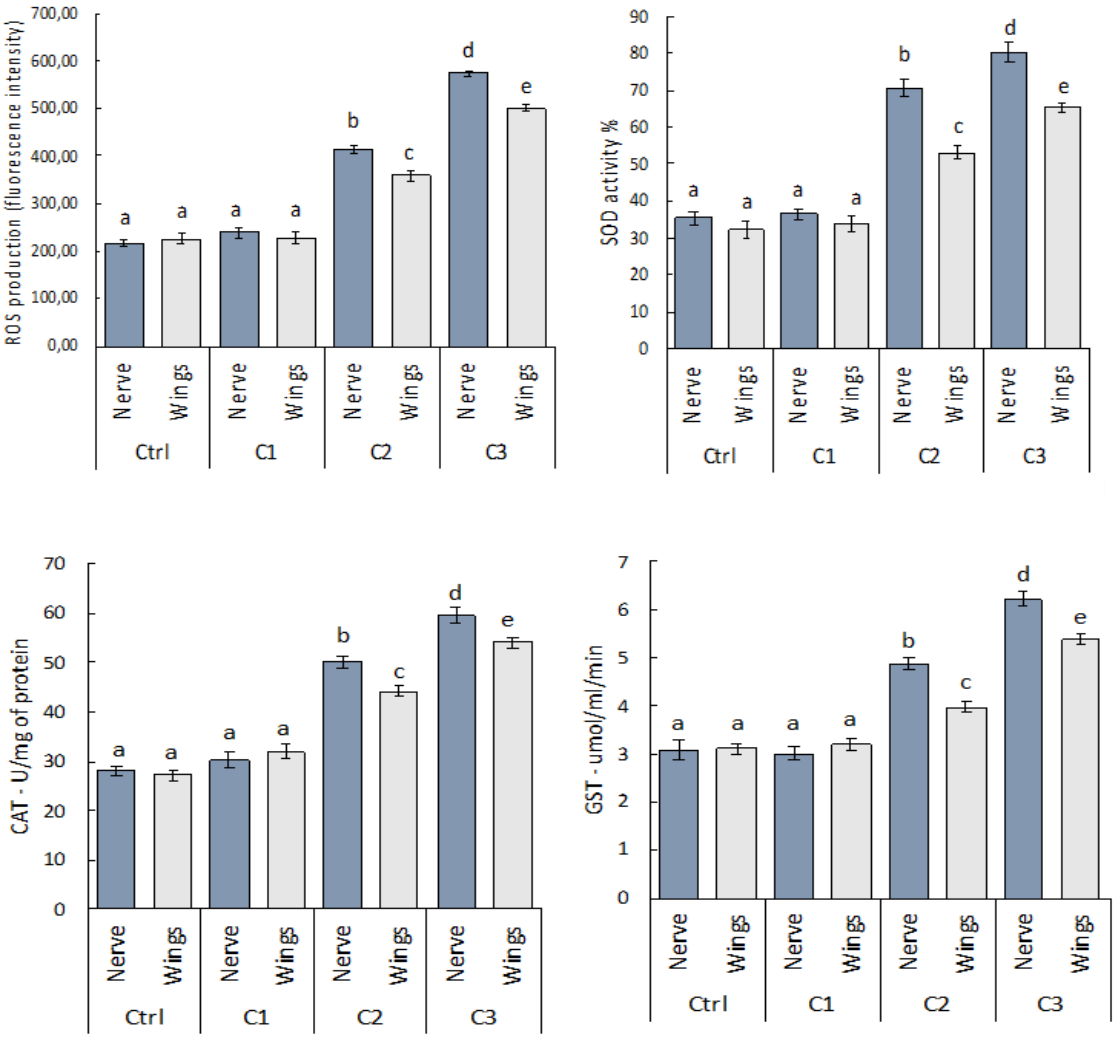

Figure 3. ROS production and antioxidant/detoxifying enzyme activities SOD, CAT, and GST in the control and in *C. conicum* samples from nerve and wing areas after culturing with C1, C2, and C3 heavy metal mixtures. Bars not accompanied by the same letter (a–e) were significantly different at $p < 0.05$. Data are the mean of three independent experiments ± SE (n = 5).

3.5. Heavy metal concentrations in C. conicum gametophyte

Zn, Cu, Pb and Cd contents (µg g^{-1}) were measured in the whole thalli of *C. conicum* after a 7-day from HM exposure. As shown in **Table 2**, the concentrations of the tested HM in the thalli increased with those of the exposure solutions. The absence of HM at C1 (both in water and in *C. conicum* thalli) indicated the excellent preservation of the sampling area. In C2 and C3, *C. conicum* thalli accumulated the highest amounts of HM, with Zn and Cu 32- and 7.6-fold higher than in C1, respectively. Toxic HM (Cd and Pb) were significantly higher in C3 (12 and 6.1 µg g^{-1}) than the controls (<LOD), C1 (<LOD), and C2 samples (0.8 and 1.3 µg g1). The data are in line with previous

studies that tested *C. conicum* for HM accumulation (Maresca et al., 2020, 2023). However, *C. conicum* thallus is composed by layers of differentiated cells along the dorso-ventral axis (**Fig. 4**). Thus, to investigate the accumulation of the tested HM in the different cell layers, an X-ray SEM microanalysis was conducted.

Table 2. Zn, Cu, Cd, and Pb contents and EC ratios in *C. conicum* gametophytes cultured in vitro (7 days) with C1, C2, and C3 heavy metal concentrations. Concentrations are expressed as mean (µg g-1) ± s.e. EC for Cd and Pb are not determined (n.d.) since their contents in CTRLs are < LOD. Means marked with different letters are statistically significant for one-way ANOVA ($p < 0.05$). The control (CTRL) is the not exposed sample. Comparison between control (not exposed) and exposed samples was expressed as Exposed-to-control ratio (EC) calculated as: [Concentration HM]exposed/[Concentration HM]control.

	Zn	Cu	Cd	Pb
CTRL	1.1 ± 0.1^{a}	4.6 ± 0.1^{a}	< 0.01	< 0.01
C1	1.5 ± 0.1^{a}	5.1 ± 0.9^{a}	< 0.01	< 0.01
EC1	1.36	1.10	n.d.	n.d.
C2	3.2 ± 0.6^{b}	18.4 ± 1.8^{b}	0.8 ± 0.1^{a}	1.3 ± 0.3^{a}
EC2	2.90	4.0	n.d.	n.d.
C3	35.3 ± 2.6^{c}	35.2 ± 3.2^{c}	12 ± 2.1^{b}	6.1 ± 0.7^{b}
EC3	32.10	7.65	n.d.	n.d.

3.6. Tissue and cellular localization of HM

HM localization and quantification was carried out by X-ray SEM microanalysis of different thallus tissues in gametophytes of *C. conicum* (**Fig. 5**). HM concentrations (%) were measured along the axis horizontal (wing to nerve to wing) of the thallus. Cd and Pb start being detected in the C2 and C3 with higher concentrations (% metals) in the nerve in respect to the wings (Cd 0.6–2.1 % vs. 1.2–3.3 % and Pb 0.3–2.1 % vs. 0.9–4.6 %). Whereas, the transverse HM localization showed that the highest % of HM occur in both wings and nerve hyaline parenchyma (2.1 % and 3.3 % respectively). Generally, the HM concentration progressively increased from the upper and lower epidermis to the hyaline parenchyma. The thallus of *C conicum* consists of a cutinized upper epidermis, a thin layer of photosynthetic parenchyma, a layer of hyaline parenchyma, and a lower epidermis provided with rhizoids and ventral scales arranged in opposite rows (**Fig. 4**). The present data suggest that toxic

metals Cd and Pb accumulate mostly in the hyaline parenchyma, where they could be translocated into the vacuoles as a defensive strategy against HM (Basile et al., 2001; Bellini et al., 2020; Degola et al., 2014). The hyaline parenchyma consists of highly vacuolated cells with wall thickening perpendicular to the main axis of cells ("reticulate" cells) and, between walls, a thickening of primary pit fields (Castaldo-Cobianchi & Giordano, 1985). The presence of cell wall thickening could increase the hyaline parenchyma HM adsorption capacity. It has been suggested that the hyaline parenchyma play a role in the symplastic and apoplastic water and solute transport that pass through the rhizoids and the nerve (Castaldo-Cobianchi & Giordano, 1985). In a previous study (Degola et al., 2014), the X-ray TEM microanalysis of the liverworts *Lunularia cruciata* exposed to Cd indicated that this metal, apart from the cell wall, was mostly accumulated into the vacuoles together with increased sulphur content probably due to thiol chelating agents. Present results showed that essential (not toxic) metals (Cu and Zn) were more equally distributed among the tissues than toxic HM (Cd and Pb). These results corroborate the idea of a specific mechanism devoted to the immobilization of toxic HM. Data from imaging PAM (**Fig. 1**) suggest that after 7 days of exposure the decrease in Fv/Fm is mostly localized in the nerve sector of the C3 exposed thalli. This demonstrates that the concentrations detected through X-ray microanalysis in the nerve area of C3 exposed samples are able to exert a localized alteration of the photosynthetic process.

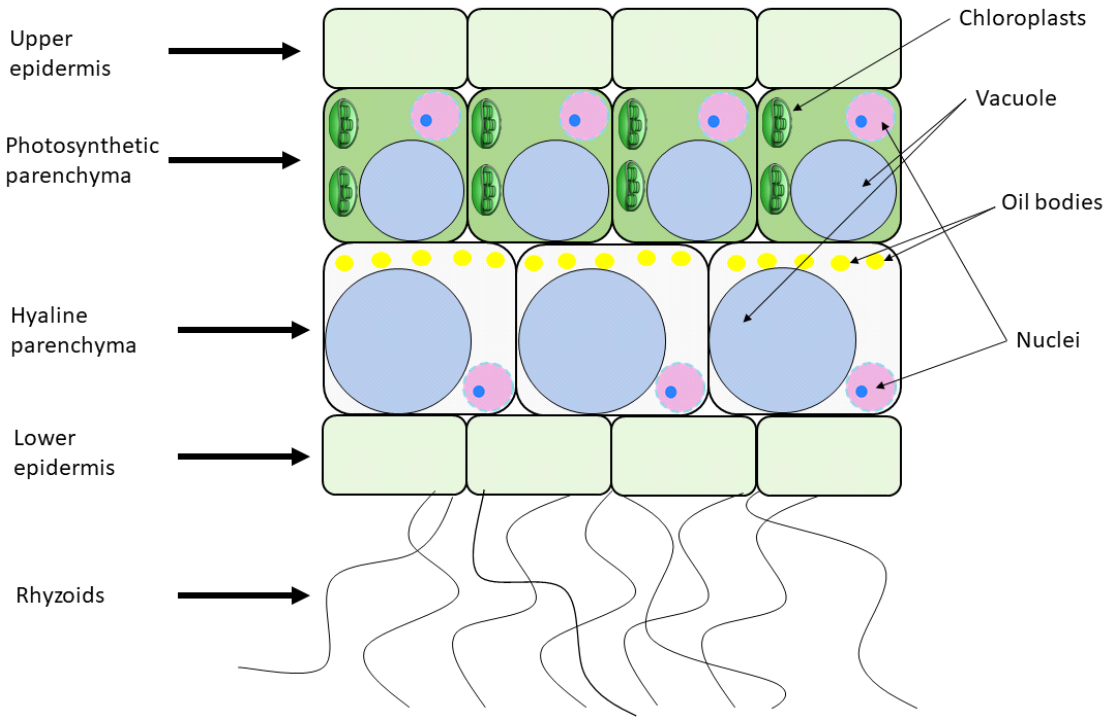

Figure 4. Scheme illustrating the transversal section of the gametophyte of *C. conicum* as described in detail in the text.

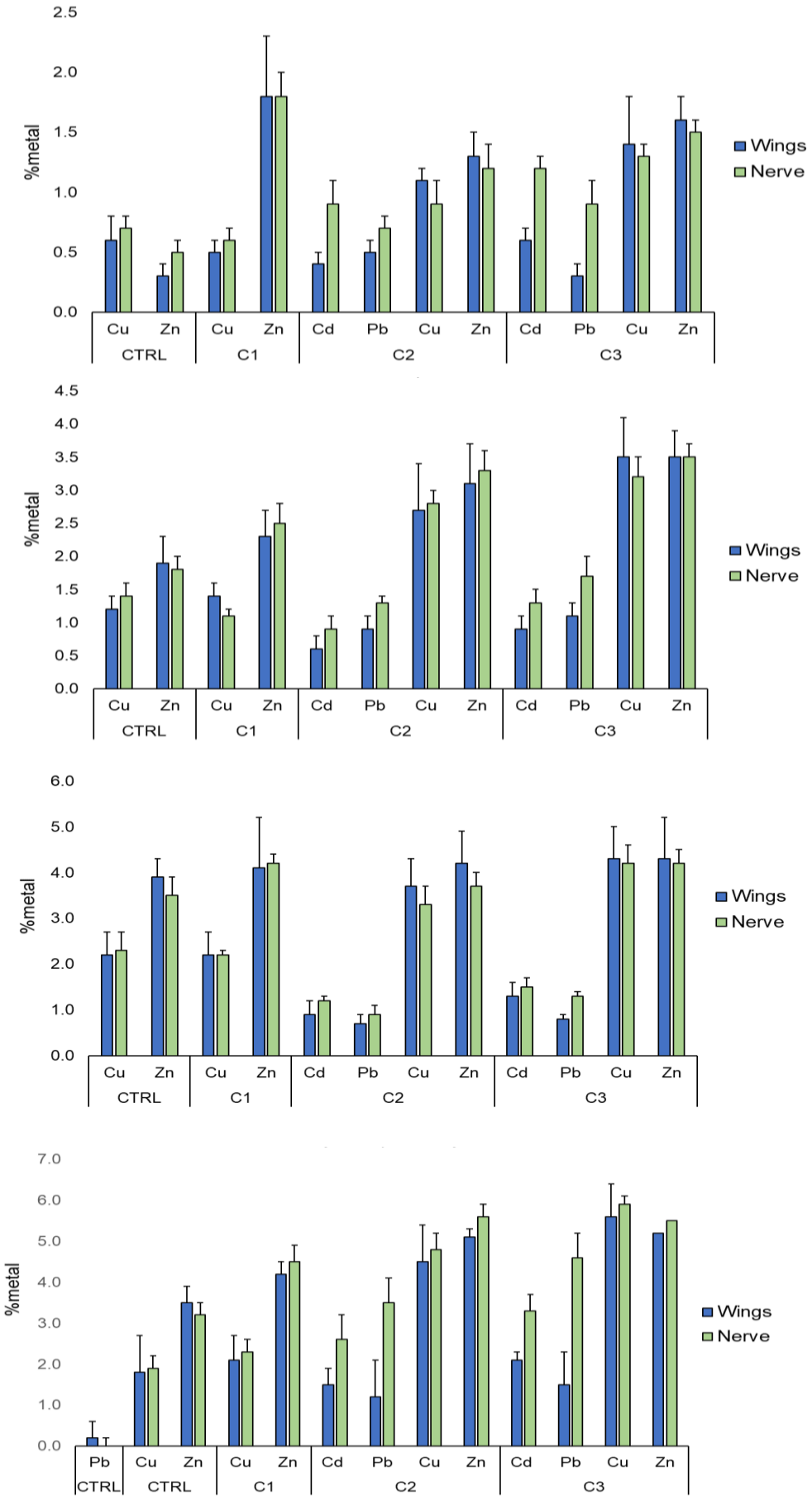

Figure 5. Mean metals concentrations (%metal) ± st.err. measured through X-ray microanalysis in a) upper epidermis, b) lower epidermis, c) photosynthetic parenchyma, d) hyaline parenchyma of the nerve and the wings of *C. conicum* thalli. Data marked with asterisks are significant for the Student t test (* $p < 0.05$, ** $p < 0.01$, *** $p < 0.001$).

3.7. TEM observations

TEM observations showed a typical appearance of chloroplasts from both the nerve and wing areas of *C. conicum* thalli cultured with C1 mixture. Under these conditions of exposure to low HM, a well-developed thylakoid system with grana and intergrana thylakoids, starch grains and a few plastoglobules was visible (**Fig. 6a, b**). Exposure to C2 rendered similar TEM images, with normal chloroplasts on both the nerve and wing areas (**Fig. 6c, d**). C3 condition was harmful to the nerve area where severe damage was evident, being chloroplasts dramatically swollen, but still showing grana and intergrana thylakoids (**Fig. 6e**). However, C3 was not so harmful to the chloroplasts from the wing areas, which showed a preserved ultrastructure but an increase of plastoglobules (**Fig. 6, f**). TEM observations of *C. conicum* thalli exposed in vitro to freshwater pollution of Savone river confirmed the findings of Maresca et al., (2022)a and (2022b), as they also reported severe damage of the ultrastructure, most of all in chloroplasts, only in samples exposed to the most polluted site in Regi Lagni channels (Italy). Our present experiments indicate that the nerve areas are mostly affected, whereas it is remarkable that the wing areas still maintain most of the typical ultrastructure. A recent in vitro experiment tested *C. conicum* thalli exposed to freshwater pollution at two sites of Sarno river. These TEM observations showed severe alterations of chloroplasts after in vitro culturing with HM concentrations such as those of the downstream site (C3) (Maresca et al., 2023). Previous experiments already demonstrated the sensitivity of plant ultrastructure to freshwater pollution, as shown with the liverwort *Pellia neesiana* (Basile, et al., 2017), the moss *Leptodyctyum riparium* (Esposito et al., 2018) and the angiospermophyte *Lemna minor* (Basile et al., 2015). In all cases, local freshwater pollution induced evident ultrastructure changes, downstream conditions being always the most harmful. In our present experiment ultrastructural alterations can also be related to the found increase of HM, most of all the highly toxic Pb and Cd, in the freshwater of the exposition sites. In the different experiments, including the present one, chloroplasts undergo swelling and show an increase of plastoglobules as observed in the other ultrastructural (Basile et al., 2015; Hakmaoui et al., 2007; Maresca et al., 2023; Maresca et al., 2022b). Swelling and shrinkage of the whole cell or

its compartments may indicate loss of selective permeability of membranes, which can be caused by a damage to the membrane or may be the effect of an energy depletion (Schwartzman & Cidlowski, 1993). When selective permeability is damaged, ions moving across the membrane according to concentration gradients may change water uptake and distribution, thus causing swelling or shrinkage of membrane compartments (Schwartzman & Cidlowski, 1993). As already shown in a previous work, exposure of *C. conicum* to HM induces ROS (Maresca, et al., 2022b), which are harmful to membranes due to lipid peroxidation and to the consequent changes of membrane permeability (Su et al., 2019). Plastoglobules are a lipoprotein subcompartment in chloroplasts, whose increase is often related to stress and senescence (Bréhélin et al., 2007; Tkalec et al., 2008). Exposure to high concentrations of HM was shown to induce an increase of plastoglobules in different plant species (Minkina et al., 2018). Plastoglobule increases can be related to membrane alterations in plastids, as plastoglobules accumulate lipids, proteins, and pigments released during the reorganization of grana under the effect of stress factors (Titov et al., 2007). However, plastoglobules also actively stock tocopherols (Vidi et al., 2006) that can mitigate photo-oxidation of membrane lipids and photo-inactivation of photosystem II (Havaux et al., 2005). Under oxidative stress, the tocopherols that are stored in plastoglobules can move to thylakoid membranes to scavenge ROS species (Bréhélin et al., 2007). Therefore, we may regard the increase of plastoglobules as an active protective response of plant cells against the stress induced by pollution. Consequently, our data suggest that the nerve area is affected by such a severe damage to metabolism that this active protective response is prevented.

That could explain the lacking of that ultrastructure change in the wing area.

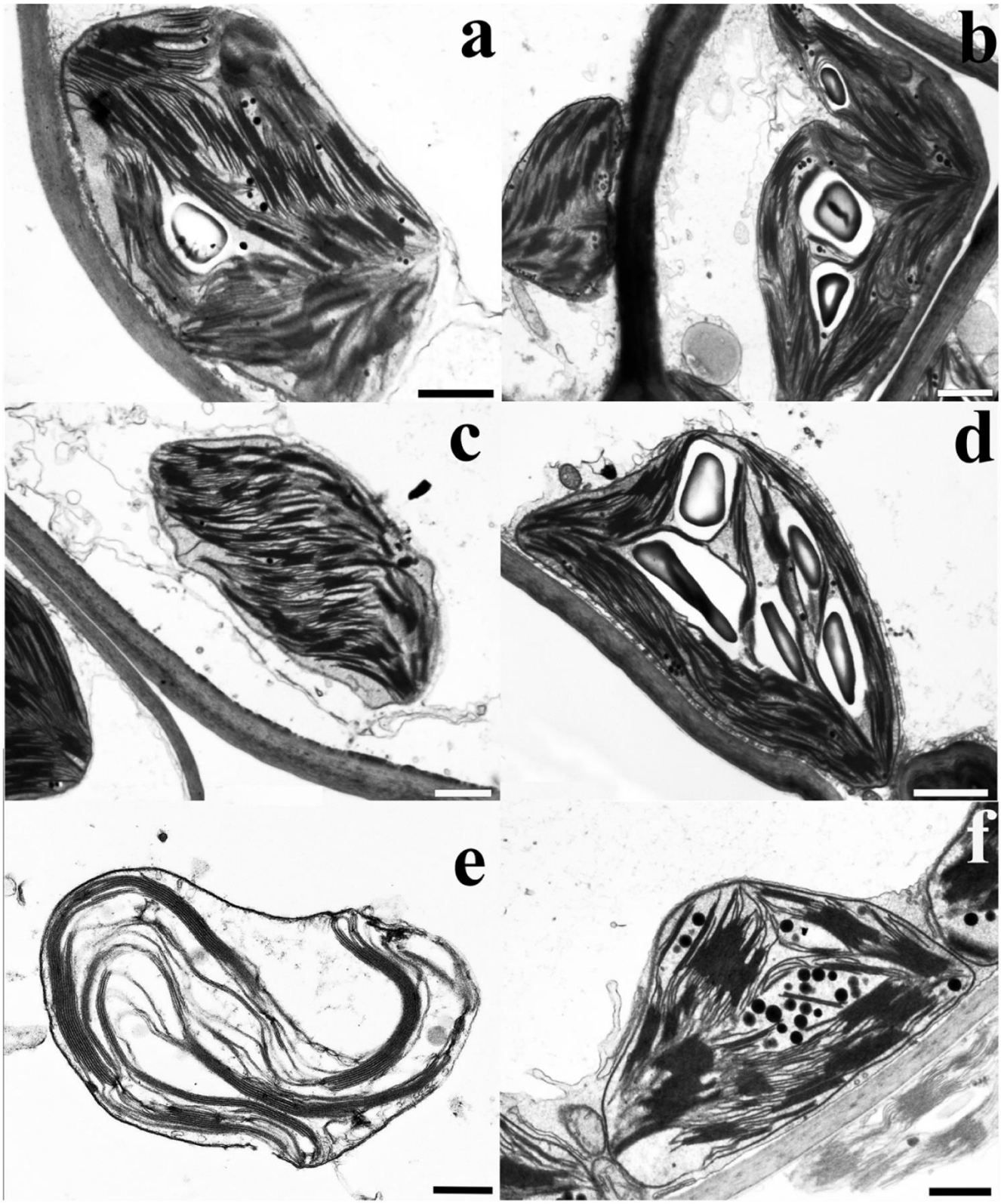

Figure 6. The figure shows TEM micrographs of photosynthetic parenchyma of *C. conicum* thallus from nerve (first column) and wing (second column) areas after culturing with C1 (a, b), C2 (c, d), and C3 (e, f) heavy metal mixtures. (a) An oblong chloroplast with well-developed grana and intergrana thylakoids, a few small electron dense plastoglobules and a starch grain. (b) Normal

chloroplasts with grana and intergrana thylakoids and starch grains. (c, d) The chloroplasts from both nerve and wing areas save a typical appearance: grana and intergrana thylakoids are abundant and starch grains can be visible. (e) A severely swollen chloroplast; grana and intergrana thylakoids are still visible. (f) A chloroplast with an abundant thylakoid system and numerous plastoglobules is taken.

4. Conclusion

In this paper the liverworts *C. conicum* was exposed to environmentally relevant concentrations of HM derived from a real case scenario (Savone River). The bioaccumulation and the damage were dependent by HM concentrations in the water. For the first time has been evaluated the tissue localization of HM. *C. conicum* preferentially accumulated HM in the nerve of gametophytes with respect to the wings. HM were mainly found in the hyaline and in the photosynthetic parenchyma. The exposure to HM induces alterations of the fine structure of the cells, most evident along the nerve, inducing marked alterations of the chloroplast structure and therefore of the photosynthetic capacity.

References

Arif, N., Yadav, V., Singh, S., Singh, S., Ahmad, P., Mishra, R. K., Sharma, S., Tripathi, D. K., Dubey, N. K., & Chauhan, D. K. (2016). Influence of High and Low Levels of Plant-Beneficial Heavy Metal Ions on Plant Growth and Development. *Frontiers in Environmental Science*, *4*. https://www.frontiersin.org/articles/10.3389/fenvs.2016.00069

Basile, A., Cogoni, A. E., Bassi, P., Fabrizi, E., Sorbo, S., Giordano, S., & Cobianchi, R. C. (2001). Accumulation of Pb and Zn in gametophytes and sporophytes of the moss Funaria hygrometrica (Funariales). *Annals of Botany*, *87*(4), 537–543. Scopus. https://doi.org/10.1006/anbo.2001.1368

Basile, A., Giordano, S., Cafiero, G., Spagnuolo, V., & Castaldo-Cobianchi, R. (1994). Tissue and cell localization of experimentally-supplied lead in Funaria hygrometrica Hedw. Using X-ray SEM and TEM microanalysis. *Journal of Bryology*, *18*(1), 69–81. https://doi.org/10.1179/jbr.1994.18.1.69

Basile, A., Loppi, S., Piscopo, M., Paoli, L., Vannini, A., Monaci, F., Sorbo, S., Lentini, M., & Esposito, S. (2017). The biological response chain to pollution: A case study from the "Italian Triangle of Death" assessed with the liverwort Lunularia cruciata. *Environmental Science and Pollution Research*, *24*(34), 26185–26193. https://doi.org/10.1007/s11356-017-9304-y

Basile, A., Sorbo, S., Cardi, M., Lentini, M., Castiglia, D., Cianciullo, P., Conte, B., Loppi, S., & Esposito, S. (2015). Effects of heavy metals on ultrastructure and Hsp70 induction in Lemna minor L. exposed to water along the Sarno River, Italy. *Ecotoxicology and Environmental Safety*, *114*, 93–101. https://doi.org/10.1016/j.ecoenv.2015.01.009

Basile, A., Sorbo, S., Lentini, M., Conte, B., & Esposito, S. (2017). Water pollution causes ultrastructural and functional damages in Pellia neesiana (Gottsche) Limpr. *Journal of Trace Elements in Medicine and Biology*, *43*, 80–86. https://doi.org/10.1016/j.jtemb.2016.11.014

Bellini, E., Maresca, V., Betti, C., Castiglione, M. R., Fontanini, D., Capocchi, A., Sorce, C., Borsò, M., Bruno, L., Sorbo, S., Basile, A., & Sanità di Toppi, L. (2020). The Moss Leptodictyum riparium Counteracts Severe Cadmium Stress by Activation of Glutathione Transferase and Phytochelatin Synthase, but Slightly by Phytochelatins. *International Journal of Molecular Sciences*, *21*(5), Article 5. https://doi.org/10.3390/ijms21051583

Bréhélin, C., Kessler, F., & van Wijk, K. J. (2007). Plastoglobules: Versatile lipoprotein particles in plastids. *Trends in Plant Science*, *12*(6), 260–266. https://doi.org/10.1016/j.tplants.2007.04.003

Candan, N., & Tarhan, L. (2003). Relationship among chlorophyll-carotenoid content, antioxidant enzyme activities and lipid peroxidation levels by Mg2+ deficiency in the Mentha pulegium leaves. *Plant Physiology and Biochemistry*, *41*(1), 35–40. https://doi.org/10.1016/S0981-9428(02)00006-2

Carginale, V., Sorbo, S., Capasso, C., Trinchella, F., Cafiero, G., & Basile, A. (2004). Accumulation, localisation, and toxic effects of cadmium in the liverwort Lunularia cruciata. *Protoplasma*, *223*(1), 53–61. https://doi.org/10.1007/s00709-003-0028-0

Castaldo-Cobianchi, R., & Giordano, S. (1985). The wall structure of the 'reticulate' cells of Conocephalum conicum (L.) Dum., observed by SEM. *Journal of Bryology*, *13*(3), 407–410. https://doi.org/10.1179/jbr.1985.13.3.407

Chandra, R., & Kang, H. (2016). Mixed heavy metal stress on photosynthesis, transpiration rate, and chlorophyll content in poplar hybrids. *Forest Science and Technology*, *12*(2), 55–61. https://doi.org/10.1080/21580103.2015.1044024

Degola, F., De Benedictis, M., Petraglia, A., Massimi, A., Fattorini, L., Sorbo, S., Basile, A., & Sanità di Toppi, L. (2014). A Cd/Fe/Zn-Responsive Phytochelatin Synthase is Constitutively Present in the Ancient Liverwort Lunularia cruciata (L.) Dumort. *Plant and Cell Physiology*, *55*(11), 1884–1891. https://doi.org/10.1093/pcp/pcu117

Dobrikova, A. G., Apostolova, E. L., Hanć, A., Yotsova, E., Borisova, P., Sperdouli, I., Adamakis, I.-D. S., & Moustakas, M. (2021). Cadmium toxicity in Salvia sclarea L.: An integrative response of element uptake, oxidative stress markers, leaf structure and photosynthesis. *Ecotoxicology and Environmental Safety*, *209*, 111851. https://doi.org/10.1016/j.ecoenv.2020.111851

Esposito, S., Loppi, S., Monaci, F., Paoli, L., Vannini, A., Sorbo, S., Maresca, V., Fusaro, L., Karam, E. A., Lentini, M., Lillo, A. D., Conte, B., Cianciullo, P., & Basile, A. (2018). In-field and in-vitro study of the moss Leptodictyum riparium as bioindicator of toxic metal pollution in the aquatic environment: Ultrastructural damage, oxidative stress and HSP70 induction. *PLOS ONE*, *13*(4), e0195717. https://doi.org/10.1371/journal.pone.0195717

Gupta, B. L. (1979). The Electron Microprobe X-Ray Analysis Of Frozen-Hydrated Sections With New Information On Fluid Transporting Epithelia. In C. P. Lechene & R. R. Warner (Eds.), *Microbeam Analysis in Biology* (pp. 375–408). Academic Press. https://doi.org/10.1016/B978-0-12-440340-6.50029-7

Hakmaoui, A., Ater, M., Bóka, K., & Barón, M. (2007). Copper and cadmium tolerance, uptake and effect on chloroplast ultrastructure. Studies on Salix purpurea and Phragmites australis. *Zeitschrift Fur Naturforschung. C, Journal of Biosciences*, *62*(5–6), 417–426. https://doi.org/10.1515/znc-2007-5-616

Hall, T. A. (1979a). Biological X-Ray Microanalysis. *Journal of Microscopy*, *117*(1), 145–163. https://doi.org/10.1111/j.1365-2818.1979.tb00236.x
Hall, T. A. (1979b). Problems Of The Continuum-Normalization Method For The Quantitative Analysis Of Sections Of Soft Tissue. In C. P. Lechene & R. R. Warner (Eds.), *Microbeam Analysis in Biology* (pp. 185–208). Academic Press. https://doi.org/10.1016/B978-0-12-440340-6.50019-4

Havaux, M., Eymery, F., Porfirova, S., Rey, P., & Dörmann, P. (2005). Vitamin E Protects against Photoinhibition and Photooxidative Stress in Arabidopsis thaliana. *The Plant Cell*, *17*(12), 3451–3469. https://doi.org/10.1105/tpc.105.037036

Inskeep, W. P., & Bloom, P. R. (1985). Extinction Coefficients of Chlorophyll a and b in N,N-Dimethylformamide and 80% Acetone. *Plant Physiology*, *77*(2), 483–485.

Koselski, M., Trebacz, K., & Dziubinska, H. (2019). The role of vacuolar ion channels in salt stress tolerance in the liverwort Conocephalum conicum. *Acta Physiologiae Plantarum*, *41*(7), 110. https://doi.org/10.1007/s11738-019-2889-7

Maresca, V., Bellini, E., Landi, S., Capasso, G., Cianciullo, P., Carraturo, F., Pirintsos, S., Sorbo, S., Sanità di Toppi, L., Esposito, S., & Basile, A. (2022). Biological responses to heavy metal stress in the moss Leptodictyum riparium (Hedw.) Warnst. *Ecotoxicology and Environmental Safety*, *229*, 113078. https://doi.org/10.1016/j.ecoenv.2021.113078

Maresca, V., Fusaro, L., Sorbo, S., Siciliano, A., Loppi, S., Paoli, L., Monaci, F., karam, E. A., Piscopo, M., Guida, M., Galdiero, E., Insolvibile, M., & Basile, A. (2018). Functional and structural biomarkers to monitor heavy metal pollution of one of the most contaminated freshwater sites in Southern Europe. *Ecotoxicology and Environmental Safety*, *163*, 665–673. https://doi.org/10.1016/j.ecoenv.2018.07.122

Maresca, V., Lettieri, G., Sorbo, S., Piscopo, M., & Basile, A. (2020). Biological Responses to Cadmium Stress in Liverwort Conocephalum conicum (Marchantiales). *International Journal of Molecular Sciences*, *21*(18), Article 18. https://doi.org/10.3390/ijms21186485

Maresca, V., Salbitani, G., Moccia, F., Cianciullo, P., Carraturo, F., Sorbo, S., Insolvibile, M., Carfagna, S., Panzella, L., & Basile, A. (2022). Antioxidant response to heavy metal pollution of Regi Lagni freshwater in Conocephalum conicum L. (Dum.). *Ecotoxicology and Environmental Safety*, *234*, 113365. https://doi.org/10.1016/j.ecoenv.2022.113365

Maresca, V., Teta, R., Finamore, C., Cianciullo, P., Sorbo, S., D'Auria, M. V., & Basile, A. (2023). Heavy metal stress induces adaptative responses in the liverwort Conocephalum conicum L. (Dum.): An integrated biologic and metabolomic study. *Environmental and Experimental Botany*, *209*, 105292. https://doi.org/10.1016/j.envexpbot.2023.105292

Minkina, T., Fedorenko, G., Nevidomskaya, D., Fedorenko, A., Chaplygin, V., & Mandzhieva, S. (2018). Morphological and anatomical changes of Phragmites australis Cav. Due to the uptake and accumulation of heavy metals from polluted soils. *Science of The Total Environment*, *636*, 392–401. https://doi.org/10.1016/j.scitotenv.2018.04.306

Müh, F., & Zouni, A. (2020). Structural basis of light-harvesting in the photosystem II core complex. *Protein Science*, *29*(5), 1090–1119. https://doi.org/10.1002/pro.3841

Nickrent, D. L., Parkinson, C. L., Palmer, J. D., & Duff, R. J. (2000). Multigene Phylogeny of Land Plants with Special Reference to Bryophytes and the Earliest Land Plants. *Molecular Biology and Evolution*, *17*(12), 1885–1895. https://doi.org/10.1093/oxfordjournals.molbev.a026290
Polívka, T., Pullerits, T., Frank, H. A., Cogdell, R. J., & Sundström, V. (2004). Ultrafast Formation of a Carotenoid Radical in LH2 Antenna Complexes of Purple Bacteria. *The Journal of Physical Chemistry B*, *108*(39), 15398–15407. https://doi.org/10.1021/jp0483019

Qiu, Y.-L., Cho, Y., Cox, J. C., & Palmer, J. D. (1998). The gain of three mitochondrial introns identifies liverworts as the earliest land plants. *Nature*, *394*(6694), 671–674. https://doi.org/10.1038/29286

Radotić, K., Dučić, T., & Mutavdžić, D. (2000). Changes in peroxidase activity and isoenzymes in spruce needles after exposure to different concentrations of cadmium. *Environmental and Experimental Botany*, *44*(2), 105–113. https://doi.org/10.1016/S0098-8472(00)00059-9

Rengel, Z. (1999). Heavy Metals as Essential Nutrients. In M. N. V. Prasad & J. Hagemeyer (Eds.), *Heavy Metal Stress in Plants: From Molecules to Ecosystems* (pp. 231–251). Springer. https://doi.org/10.1007/978-3-662-07745-0_11

Roomans, G. M. (n.d.). Basic methods in biological X-ray microanalysis. *(No Title)*. Retrieved November 28, 2023, from https://cir.nii.ac.jp/crid/1130000794149059328

Salbitani, G., Del Prete, F., Carfagna, S., Sansone, G., & Barone, C. M. A. (2021). Enhancement of Pigments Production by Nannochloropsis oculata Cells in Response to Bicarbonate Supply. *Sustainability*, *13*(21), 11904. https://doi.org/10.3390/su132111904

Samecka-Cymerman, A., Marczonek, A., & Kempers, A. J. (1997). Bioindication of Heavy Metals in Soil by Liverworts. *Archives of Environmental Contamination and Toxicology*, *33*(2), 162–171. https://doi.org/10.1007/s002449900238

Schwartzman, R. A., & Cidlowski, J. A. (1993). Apoptosis: The Biochemistry and Molecular Biology of Programmed Cell Death*. *Endocrine Reviews*, *14*(2), 133–151. https://doi.org/10.1210/edrv-14-2-133

Singh, S., Parihar, P., Singh, R., Singh, V. P., & Prasad, S. M. (2016). Heavy Metal Tolerance in Plants: Role of Transcriptomics, Proteomics, Metabolomics, and Ionomics. *Frontiers in Plant Science*, *6*. https://doi.org/10.3389/fpls.2015.01143

Statham, P. J. (1977). Deconvolution and background subtraction by least-squares fitting with prefiltering of spectra. *Analytical Chemistry*, *49*(14), 2149–2154. https://doi.org/10.1021/ac50022a014

Su, L.-J., Zhang, J.-H., Gomez, H., Murugan, R., Hong, X., Xu, D., Jiang, F., & Peng, Z.-Y. (2019). Reactive Oxygen Species-Induced Lipid Peroxidation in Apoptosis, Autophagy, and Ferroptosis. *Oxidative Medicine and Cellular Longevity*, *2019*, 5080843. https://doi.org/10.1155/2019/5080843

Sytar, O., Brestic, M., Taran, N., & Zivcak, M. (2016). Chapter 14—Plants Used for Biomonitoring and Phytoremediation of Trace Elements in Soil and Water. In P. Ahmad (Ed.), *Plant Metal Interaction* (pp. 361–384). Elsevier. https://doi.org/10.1016/B978-0-12-803158-2.00014-X

Tabelin, C. B., Igarashi, T., Villacorte-Tabelin, M., Park, I., Opiso, E. M., Ito, M., & Hiroyoshi, N. (2018). Arsenic, selenium, boron, lead, cadmium, copper, and zinc in naturally contaminated rocks: A review of their sources, modes of enrichment, mechanisms of release, and mitigation strategies. *Science of The Total Environment*, *645*, 1522–1553. https://doi.org/10.1016/j.scitotenv.2018.07.103

Titov, A. F., Akimova, T. V., & Venzhik, Yu. V. (2007). Effect of root heating on the tolerance of barley leaf cells and ultrastructure of chloroplasts and mitochondria. *Doklady Biological Sciences*, *415*(1), 324–327. https://doi.org/10.1134/S0012496607040229

Tkalec, M., Prebeg, T., Roje, V., Pevalek-Kozlina, B., & Ljubešić, N. (2008). Cadmium-induced responses in duckweed Lemna minor L. *Acta Physiologiae Plantarum*, *30*(6), 881–890. https://doi.org/10.1007/s11738-008-0194-y

Vidi, P.-A., Kanwischer, M., Baginsky, S., Austin, J. R., Csucs, G., Dörmann, P., Kessler, F., & Bréhélin, C. (2006). Tocopherol cyclase (VTE1) localization and vitamin E accumulation in chloroplast plastoglobule lipoprotein particles. *The Journal of Biological Chemistry*, *281*(16), 11225–11234. https://doi.org/10.1074/jbc.M511939200

Wang, S., Wufuer, R., Duo, J., Li, W., & Pan, X. (2022). Cadmium Caused Different Toxicity to Photosystem I and Photosystem II of Freshwater Unicellular Algae Chlorella pyrenoidosa (Chlorophyta). *Toxics*, *10*(7), Article 7. https://doi.org/10.3390/toxics10070352

Weitbrecht, K., Schwab, S., Rupp, C., Bieler, E., Dürrenberger, M., Bleyer, G., Schumacher, S., Kassemeyer, H.-H., Fuchs, R., & Schlücker, E. (2021). Microencapsulation – An innovative technique to improve the fungicide efficacy of copper against grapevine downy mildew. *Crop Protection*, *139*, 105382. https://doi.org/10.1016/j.cropro.2020.105382

Wellburn, A. R. (1994). The Spectral Determination of Chlorophylls a and b, as well as Total Carotenoids, Using Various Solvents with Spectrophotometers of Different Resolution. *Journal of Plant Physiology*, *144*(3), 307–313. https://doi.org/10.1016/S0176-1617(11)81192-2

Zamora-Ledezma, C., Negrete-Bolagay, D., Figueroa, F., Zamora-Ledezma, E., Ni, M., Alexis, F., & Guerrero, V. H. (2021). Heavy metal water pollution: A fresh look about hazards, novel and conventional remediation methods. *Environmental Technology & Innovation*, *22*, 101504. https://doi.org/10.1016/j.eti.2021.101504

PAPER IV

Ecotoxicology and Environmental Safety 229 (2022) 113078

Contents lists available at ScienceDirect

Ecotoxicology and Environmental Safety

journal homepage: www.elsevier.com/locate/ecoenv

Biological responses to heavy metal stress in the moss *Leptodictyum riparium* (Hedw.) Warnst

Viviana Maresca [a,1] , Erika Bellini [b,1] , Simone Landi [a,1] , Giorgia Capasso [a] , **Piergiorgio Cianciullo** [a] , Federica Carraturo [a] , Stergios Pirintsos [c,d] , Sergio Sorbo [e] , Luigi Sanità di Toppi [b] , Sergio Esposito [a,*] , Adriana Basile [a,*]

a Department of Biology, University of Naples "Federico II", 80126 Naples, Italy
b Department of Biology, University of Pisa, 56126 Pisa, Italy
c Department of Biology, University of Crete, 71409 Heraklion, Greece
d Botanical Garden, University of Crete, 741 00 Rethymnon, Greece
e CeSMA, Microscopy Section, University of Naples "Federico II", 80126 Naples, Italy

DOI: https://doi.org/10.1016/j.ecoenv.2021.113078

Abstract

Leptodictyum riparium, a widely distributed aquatic moss, can both tolerate and accumulate very high concentrations of toxic heavy metals, with only slight apparent damage. Here we report the effects on photosynthetic yield, glutathione (GSH), phytochelatin (PCn) synthesis, nitrogen metabolism and cellular localization of molecules rich in SH groups in *L. riparium* exposed in vitro to heavy metals. We simulated the concentrations of Cu, Zn, Cd, Pb detected in Regi Lagni, Italy, one of the most contaminated freshwater sites in Southern Europe, in the laboratory to test how the moss responds to heavy metal contamination. There was a steady decrease of photosynthetic efficiency correlated with the heavy metal concentrations and ultrastructural organization. All PCn levels increased significantly as the concentration of heavy metals increased, while the GSH levels did not appear to be particularly affected. A significant increase of GDH and NADH-GOGAT activities increased with increasing heavy metal concentration. Immunoblotting analysis revealed an increase of the chl-GS2 while no significant increase was detected in the cyt-GS1. These results give insight into the molecular events underlying the metal-tolerance of the aquatic moss *L. riparium* exposed to environmental heavy metal concentrations.

1. Introduction

The aquatic moss *Leptodictyum riparium* (Hedw.) Warnst (*Bryophyta*) can tolerate and accumulate very high concentration of heavy metals (metals that have a specific density of more than 5 g/cm^3), including Cadmium (Cd) (Basile et al., 2012a; Esposito et al., 2012, 2018; Maresca et al., 2018), with bioconcentration levels higher than other plants, including some angiosperms, suffering minimal apparent damage. Due to its tolerance and accumulation capability, *L. riparium* has been chosen as candidate organism for biomonitoring heavy metals in natural environmentals as well as for phytoremediation projects. (Basile et al., 2012b; Esposito et al., 2018; Maresca et al., 2018). Indeed, *Leptodictyum riparium* was among the ten macrophytes that have been proposed for the biomonitoring of toxic metals in European rivers and streams bym Say et al. (1981)

Recently, *L. riparium* was used to monitor the state of environmental pollution in two of the most polluted waterways in Campania, Italy; the Sarno river and a system of artificial canals known as Regi Lagni (Esposito et al., 2018; Maresca et al., 2018). The Regi Lagni is a channel system that catches meteoric and waste waters, routing them from the zones sited north of Naples to the Tyrrhenian Sea. The heavy industrialization (i.e., chemical industry, intensive farming) as well as urbanization of the areas near the Regi Lagni resulted in a severe contamination of these water bodies (Bove et al., 2011; Grezzi et al., 2011). Furthermore, the Regi Lagni catchment comprises two zones, the "Land of Fires" and the "Triangle of Death" that have been exploited for illegal waste disposal and contaminated by the ash fallout from uncontrolled garbage incineration which caused dangerous pollution of groundwater and soil (Senior & Mazza, 2004). This severe contamination had a long-term health effect on the local human population, causing an alarming increase in cerebrum-vascular diseases and cancers (Senior & Mazza, 2004). In an earlier study, *L. riparium* was used to monitor heavy metals pollution in Regi Lagni channels (Maresca et al., 2018). The investigation was carried out installing moss bags in three sites according to a pollution gradient from the less polluted to the more polluted zone. Biological responses such as bioaccumulation of heavy metals, ROS production, antioxidant enzyme activity, DNA damage and HSP70 induction were measured. Heavy metals accumulated in the moss tissues causing severe ultra-structural damages and biochemical responses at higher concentration.

Nevertheless, in natural field conditions the effect of other environmental variables on heavy metal accumulation and potential damage to *L. riparium* , should be investigated. For example, when the chlorophyll fluorescence of moss is used to biomonitor heavy metal contamination in aquatic environments, where both heat stress and high light are present at the same time, the fluorescence

parameters are seriously reduced, resulting in inaccurate measures (Chen et al., 2018). Consequently, controlled experiments focused only on the variables of interest, can strengthen the correspondence between the biological responses and the impact of the variables.

To better evaluate the responses of the moss *L. riparium* to heavy metal contamination, and specifically its photosynthetic yield, the presence of glutathione, phytochelatins, nitrogen metabolism, and the cellular localization of molecules rich in SH groups, a controlled experiment was performed. Hence, this study aims to investigate the molecular and biochemical responses of *L. riparium* under controlled conditions, after exposure to external heavy metal sources, comparable to those detected in the three sites of the Regi Lagni (Maresca et al., 2018), in order to improve the knowledge about the tolerance of *L. riparium* to heavy metal stress, and strengthen the idea that this moss could be suitable for biomonitoring in natural field conditions.

2. Materials and methods

2.1. Plant material and growth conditions

Leptodictyum riparium gametophytes were gathered from a water spring in the central zone of the Botanical Garden of the University of Naples "Federico II" (Italy). The gametophytes were carefully washed with deionized water and sterilized with a solution of 7% (v/v) NaClO and a few drops of Triton X-100, then rewashed with deionized water.

Samples were individually put into Petri dishes filled with 25 mL of sterile tap water (control) or heavy metals mix (Cu, Zn, Cd and Pb - concentrations are reported in **Table 1S**) for total exposure of 7 days. Then gametophytes were exposed in vitro to the same heavy metal concentrations detected in the three stations along the Regi Lagni reported by Maresca et al. (2018) and shown in **Table 1S.** The samples were cultured in a growth chamber with a temperature in the range of 15 °C ± 1.3 °C / 20 ± 1.3 °C night/day, 70% ± 4% relative humidity RH, 16 h/8 h light/dark cycle and a 40 μmol m^{-2} s^{-1} photosynthetic photon flux density.

To confirm the absence of damage due to the sterilization process, *L. riparium* gametophytes were observed every two days with a Leitz Aristoplan microscope (Leitz,Wetzlar, Germany) and a Wild Heerbrugg M3Z binocular microscope (Leica, Nussloch, Germany) (Bellini et al., 2020). The plant material was grown in triplicate and all the experiments were repeated at least three times.

2.2. Extraction of thiol peptides from *L. riparium* gametophytes and analysis by HPLC-ESI-MS-MS

Samples of *L. riparium* gametophytes were extracted according to a previously published method (Bellini et al., 2019) with some modifications. Briefly, the extracts instead of being filtered by a Minisart RC4 0.45–μm filter (Sartorius, Goettingen, Germany) were ultrafiltered through Amicon® Ultra (10 K device) centrifugal filters (Merk, Germany) at 14000 g, 4 °C for 30 min and samples were stored at − 80 °C until analysis. The HPLC-ESI-MS-MS analyses were all performed by the instrument layout and the procedure described in Bellini et al. (2019)

2.3. Confocal laser imaging

Samples treatment was according to Maresca et al. (2020a). In short, phylloids were stained with 100 μM MCB (Thermo Fisher Scientific, MA, USA) for 30 min at 21 °C in the dark, at near neutral pH conditions. After, observation was performed under a Leica TCS SP5 confocal laser scanning microscope (CLSM) with a 40X immersion objective. Excitation of MCB and chlorophyll was set at 405 nm wavelength, and emission detected at 460–520 nm (begin-end) and 630–700 nm (begin-end), respectively. Detector gain and offset values were kept fixed to compare the different results.
MCB stock was made as a 50 mM solution in dimethyl sulfoxide (DMSO). A 100 μM solution was prepared adding sterile water to dilute the stock solution. Unstained *L. riparium* gametophytes were incubated into the same amount of DMSO used for the 100 μM MCB solution and used as a negative control of MCB. Three samples of *L. riparium* gametophytes for each treatment and control condition were examined.

2.4. Photochemical efficiency

Photosynthetic efficiency was assessed using the widely used and classical indicator F_V/F_m, which indicates for the Photosystem II (PSII) the potential quantum yield of primary photochemistry (Maxwell & Johnson, 2000), and the performance index (PI_{ABS}), a global indicator that resumes the contribution of all parameters on PS I and PSII functionality which was also used to express the overall vitality of the samples. The energy cascade from light absorption by PSII to electron transport involves the absorption of photon flux by antenna pigments (ABS), creating excited chlorophyll. The excitation energy in part is dissipated (DI) as heating and fluorescence emission, and in part is profitably addressed to the reaction centre (RC) as trapping flux (TR); in the RC the excitation is converted into redox energy by reducing the electron acceptor Q_A to Q_A- which

is then reoxidised to Q_A leading to the electron transport (ET) and later to CO_2 fixation (Strasser et al., 2004).

PI_{ABS} is given by the equation:

$$PI_{ABS}=RC/ABS\times\varphi P_0/(1-\varphi P_0)\times\psi_0/(1-\psi_0)$$

where φP_0 expresses the probability that an absorbed photon will be trapped by the reaction centre of PSII, it represents the maximum quantum yield of primary photochemistry and roughly corresponds to F_V/F_m, and ψ_0 expresses the probability that a trapped exciton, a quantum of electronic excitation, enters the transport chain and moves an electron further than Q_A.

Measurements were carried out with a Plant Efficiency Analyser (Handy PEA, Hansatech Instruments Ltd, UK) at the temperature of 20 ± 1.3 °C. After dark-adaptation for 30 min, gametophytes were lightened for 1 s with a saturating excitation pulse (3500 μmol s^{-1} m^{-2}) of red light (650 nm) from a LED into the sensor and the fluorescence emission were recorded. Nine measurements were taken for each treatment and the fluorescence data were processed by PEA plus software (Hansatech Instruments, Pentney, King's Lynn, UK).

2.5. Transmission electron microscopy

Gametophyte fixation was carried out with a 3% (v/v) glutaraldehyde solution in a phosphate buffer (pH 7.2–7.4) for 2 h at room temperature. Post-fixation was performed with buffered 1% (w/v) OsO_4 for 1.5 h at room temperature. Dehydration employed ethanol up to propylene oxide and was followed by embedding into Spurr's epoxy medium. Ultrathin (50 nm) sections were collected onto 300 mesh Cu grids and stained with Uranyl Replacement Stain (Electron Microscopy Science, Hatfield, PA, USA) and lead citrate. A Philips EM 208 S TEM was employed for observation and nine samples for each treatment were examined.

2.6. NADH-GOGAT and NADH-GDH activities determination

NADH-GOGAT and NADH-GDH were extracted by grounding 150 mg of *L. riparium* in a buffer containing 100 mM KH_2PO_4 buffer (pH 7.5), 2 mM EDTA, 2 mM dithiothreitol (DTT) and plant-specific proteases inhibitor cocktail (Sigma P9599, Merck-Sigma-Aldrich, USA). GOGAT and GDH activities were measured by following the oxidation of NADH at 340 nm using a Cary 60 spectrophotometer (Agilent Technologies, Santa Clara, USA) at 25 °C. as described previously (Jallouli et al., 2019).

2.7. Western blotting

Proteins were extracted by grinding samples in liquid nitrogen 300 mg of tissue, then powder was suspended in 600 µl of solution containing 50 mM Tris-HCl (pH 8.0), 5 mM $MgCl_2$, 4 mM EDTA, 10% glycerol, 15 µM $NADP^+$, 1 µl/30 µg plant-specific proteases inhibitor cocktail (Sigma P9599, Merck-Sigma-Aldrich, USA). Then, proteins were separated by SDS-PAGE and transferred on a nitrocellulose membrane (Ge Healthcare) using the Transblot-turbo (Biorad, CA, Usa) as previously described (Ayadi et al., 2020). Membranes were incubated with primary antibodies for Glutamine synthetase 1 and 2 (GS) and for nitrate reductase (NR) (Agrisera, Vannas, Sweden). After incubating the membrane with horseradish peroxidase (HRP)-linked secondary antibody, cross-reacting polypeptides were identified by enhanced chemioluminescence (ECL) reaction (Ayadi et al., 2020).

2.8. Statistical analysis

Statistical significance of PCn, GSH and photochemical efficiency data was inferred through two-way ANOVA, followed by Tukey's post-hoc test. Data were reported as the mean ± SE. The threshold of statistical significance was set at $p < 0.05$, unless otherwise specified.

3. Results

3.1. Production of thiol-peptides

The production of thiol peptides in response to heavy metals was evaluate by HPLC-ESI-MS-MS analyses to understand whether they were one of the main detoxification mechanisms involved (**Figure 1**). The amount of GSH detected was almost constant even in the presence of high concentrations of heavy metals. Differently, the PCn were produced, although at trace levels, in response to heavy metals. Indeed, the PCn levels progressively increased with the increase of heavy metal concentrations. Furthermore, PCn with higher degrees of polymerization were only produced in samples exposed to S2 and S3 with the highest concentrations of heavy metals.

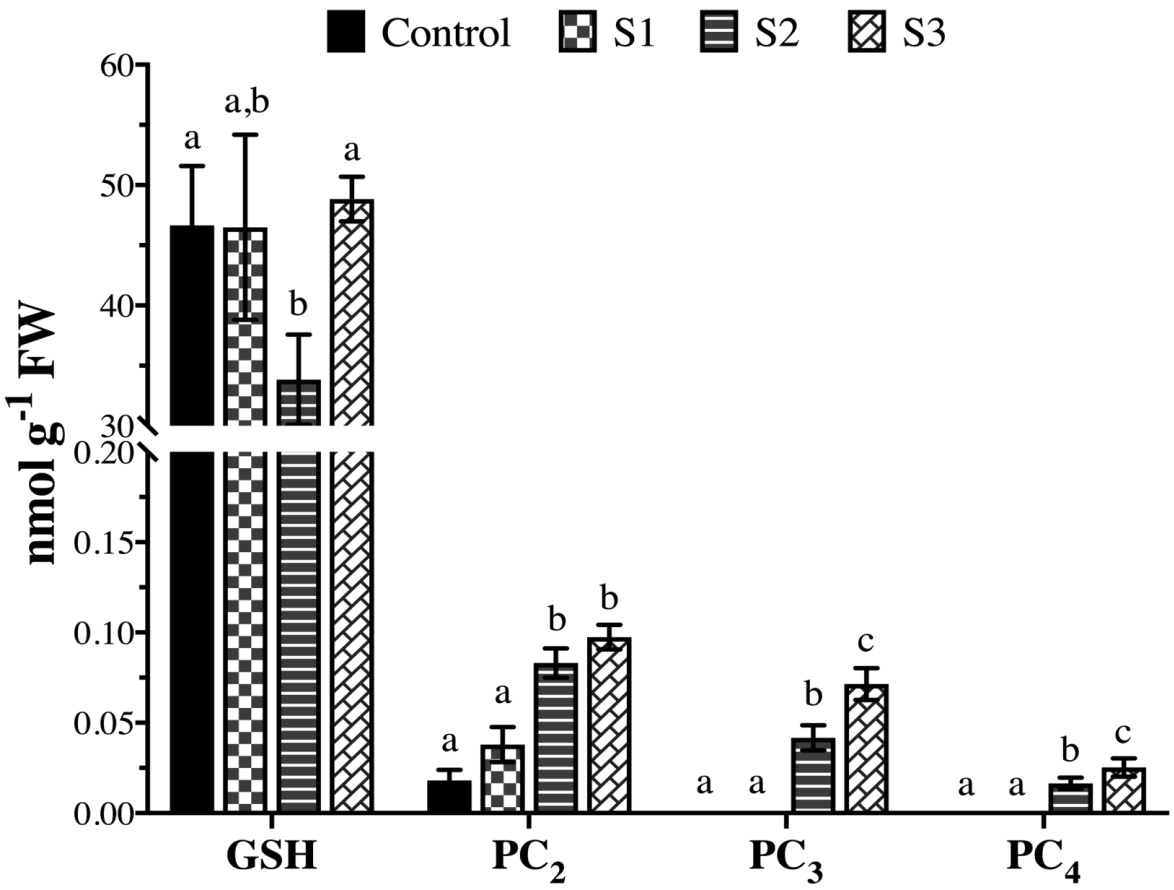

Figure 1. Content of GSH and PCn in L. riparium gametophytes, exposed to Control Solution, S1, S2 and S3 for 7 days. Values are mean ± SE; within each group of thiol peptides, bars not accompanied by the same letter are significantly different at $p < 0.05$ (one-way ANOVA followed by Tukey's multiple comparison post-hoc test).

3.2. Confocal laser imaging

In S-unexposed and MCB-unstained samples (**Figure 2.a**), autofluorescence from the cell wall (blue) and chloroplasts (red) was visible. After staining with MCB, all the samples showed both MCB signals from both the cytoplasm underneath the cell wall and the vacuoles and chloroplast autofluorescence (**Figure 2. b-e**). The S3-treated samples gave a slightly higher blue signal.

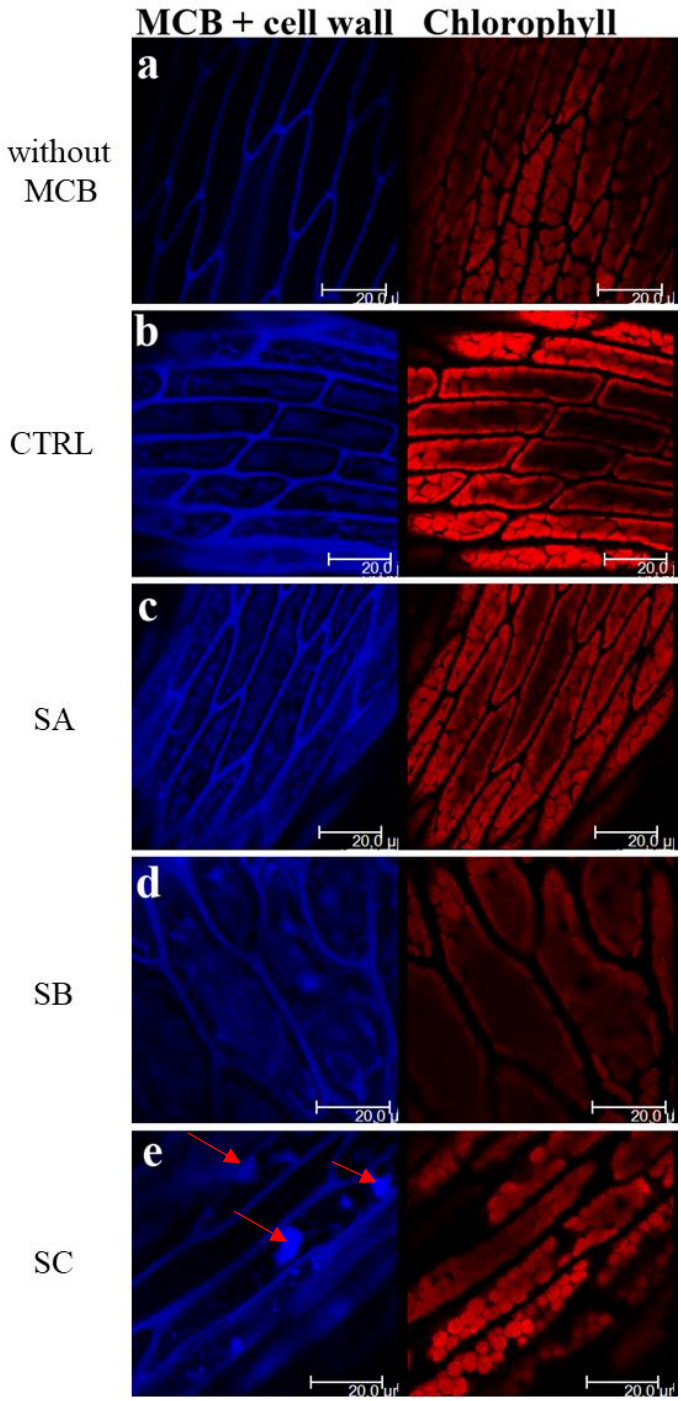

Figure 2. Confocal laser scanning microscopy (CLSM) micrographs of *L. riparium* phylloids treated without (a, b) and with S1 (c), S2 (d), and S3 (e) solutions for 7 days, unstained (a) and stained with MCB (b-e). The I column shows MCB signal and cell wall autofluorescence, the II reports the chlorophyll autofluorescence and the III is the merge. (a) In the S-unexposed, only DMSO-treated samples, autofluorescence is visible from the cell wall (blue) and chloroplasts (red). (b) In the S-untreated, MCB-stained samples, MCB signal is already visible from the cytoplasm beneath the cell wall and the vacuoles (blue). (c-e) In the S1-S3 treated, MCB-stained samples MCB signal still localises in the cytoplasm underneath the cell wall and the vacuoles, with a slightly higher emission in the S3-treated specimens (e). (For interpretation of the references to colour in this figure legend, the reader is referred to the web version of this article.)

3.3. Photochemical efficiency

Chlorophyll fluorescence was used to further evaluate the effects of heavy metal stress on photosynthesis. Control samples (not reported) of *L. riparium* showed no changes in chlorophyll fluorescence over a period of 7 days. While on the contrary (**Table 1**) both F_V/F_m and PI_{ABS} decreased gradually after exposure to heavy metal stresses in *L. riparium* indicating that the potential quantum yield of primary photochemistry and the overall vitality of the samples are degraded.

Table 1. F_V/F_m: indicator of photosynthetic efficiency; PI: performance index; Different letters in each column indicate statistically significant ($p < 0.05$) differences between treatments.

	F_V/F_m	PI_{ABS}
S1	0.811 ± 0.052	0.792 ± 0.024
S2	0.731 ± 0.020	0.286 ± 0.012
S3	0.612 ± 0.014	0.148 ± 0.017

3.4. Transmission electron microscopy

TEM observations were already shown in Maresca et al. (2018). Chloroplasts from the S2- and S3-treated samples developed ultrastructural changes. S1-treated samples have chloroplasts with a regular appearance (**Figure 3**). In the S2-treated specimens, some thylakoids were swollen, whereas in the S3-treated samples chloroplasts were misshaped, thylakoids appeared ill-defined and ill-distinguishable and large lipid droplets developed in the stroma (**Figure 3**).

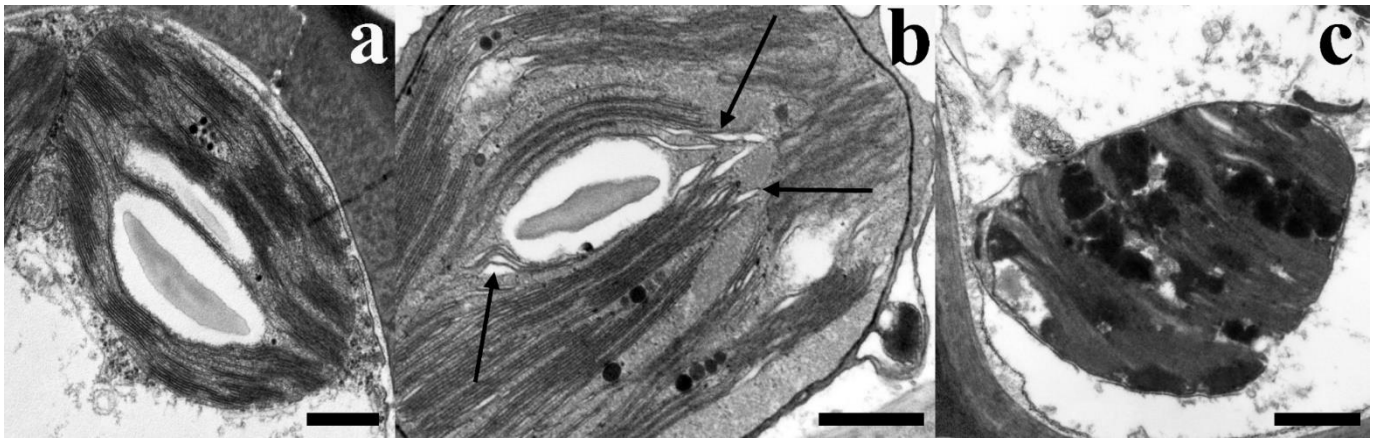

Figure 3. TEM micrographs of chloroplasts from samples exposed to S1 (a), S2 (b), and S3 (c). **a.** A typical chloroplast with grana and intergrana thylakoids and starch grains. A few plastoglobules are visible in the stroma. **b.** In the chloroplast swollen thylakoids are well evident (arrows). **c.** A misshaped chloroplast where thylakoid membranes are ill-defined, grana and intergrana thylakoids are not well distinguishable and large lipid droplets are present. **Scale bars 500 nm**.

3.5. Nitrogen uptake and metabolism

The effects of heavy metals on nitrate reduction and nitrogen metabolism in different sites were analysed by monitoring the enzymatic activities of GDH and NADH-GOGAT; and protein occurrences of GS1, GS2 and NR. As shown in **Figures 4** and **5**, both nitrate reduction and nitrogen metabolism were significantly influenced by different concentrations of heavy metals observed in sites 1, 2 and 3.

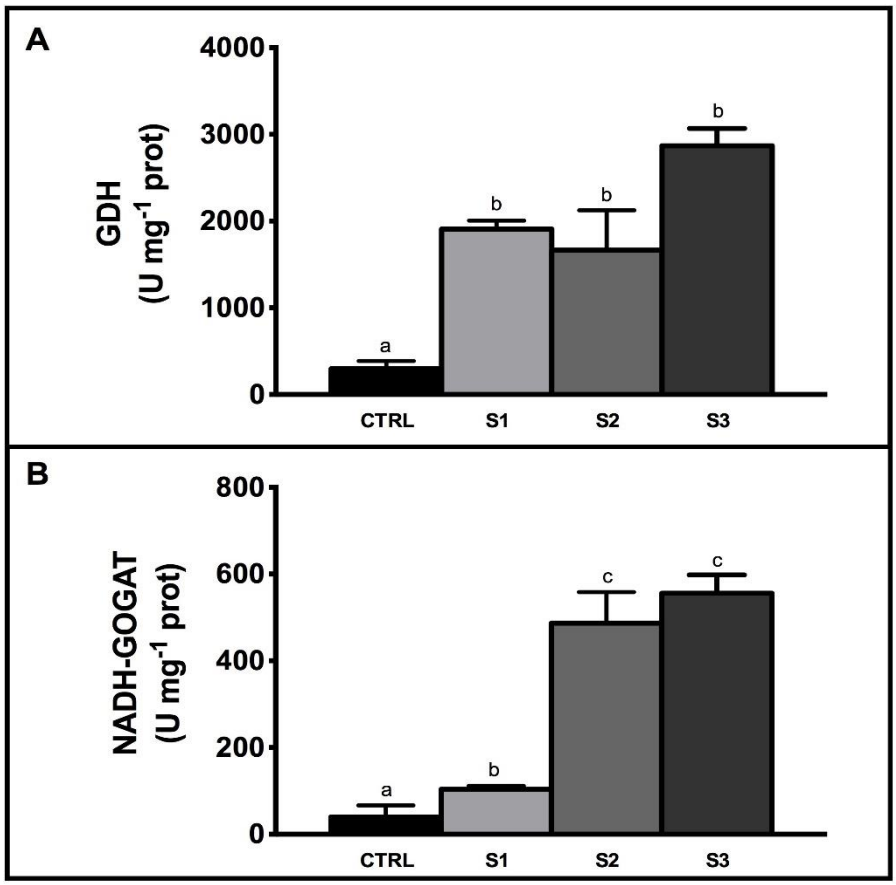

Figure 4. GDH (A) and NADH-GOGAT (B) activities in leaf of *L. riparium* exposed for 7 days to control (black bars), S1 (light grey bars), S2 (medium grey bars) and S3 solutions (dark grey bars). Letters indicate significant differences between control, S1, S2 and S3.

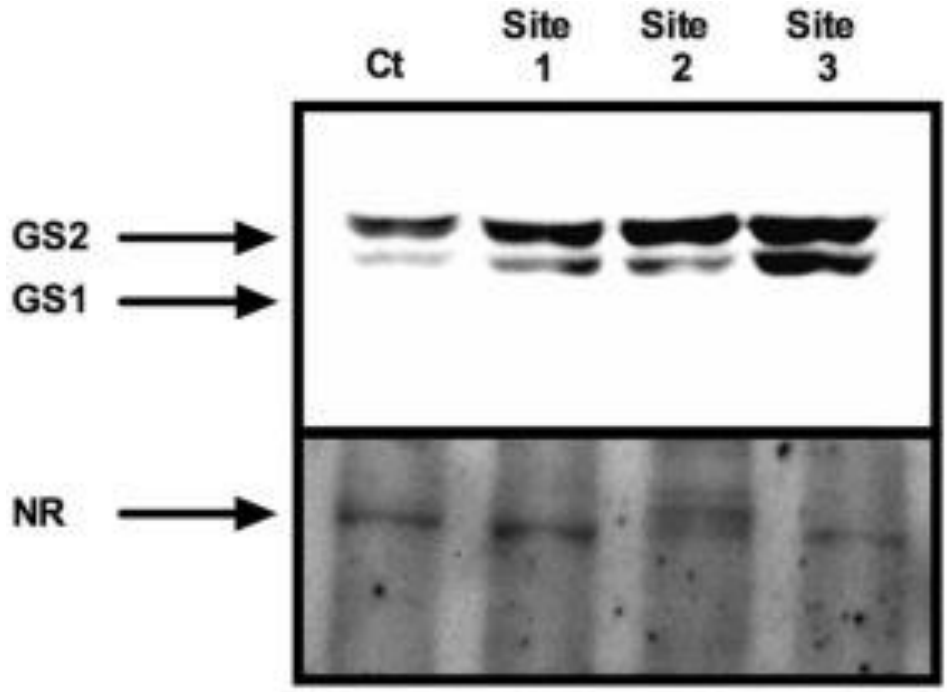

Figure 5. Immunoblotting of leaf extract of *L. riparium* exposed for 7 days to control, site 1, site 2 and site 3 solutions using antibodies raised against Glutamine synthetase 1 and 2 (GS1 and GS2 – 50 – 40 kDa) and against nitrate reductase (NR – 104 kDa).

GDH represents an abiotic stress responsive gene, playing major roles both by an alternative nitrogen assimilation enzyme both for the re-assimilation of the excess of ammonia released during stress (Jallouli et al., 2019; Zhou et al., 2015). As shown in **Figure 4A**, the activity of GDH significantly increased in site 1, 2 and 3 compared with controls. Particularly, the heavy metals induced an increase of GDH of about 4.48, 6.67 and 9.61-fold change by comparing S1, S2 and S3 vs control, respectively.

NADH-GOGAT showed marked and significant increased activities at higher concentrations of heavy metals of site 2 and 3, while a reduced increase was reported at higher heavy metals levels observed in site 1 (**Figure 4B**). In details, heavy metals induced an increase of NADH-GOGAT of 2.62, 12 and 14-fold change comparing S1, S2 and S3 vs control, respectively. Immunoblotting analysis showed an increased occurrence of the chloroplastic GS2 (44–45 kDa) in site 2 and 3, while the GS1 (39–40 kDa) showed difference only in S3 (**Figure 5**).

NR showed a slight increase in occurrence at lower heavy metals concentrations, while reduced changes were reported among controls and site 2 and 3, respectively.

4. Discussion

The present study gives new insights into the molecular events underlying the metal-tolerance of the aquatic moss *L. riparium* exposed to environmental heavy metal concentrations. Heavy metals play a central role in the physiology of plants, providing essential in some cases, micronutrients for plant growth, as well as being toxic in other cases. An excess of heavy metals may induce toxic effects on plant growth, development, and reproduction (Basile, et al., 2012a; Esposito et al., 2018; Lentini et al., 2018). In this study we simulated environmental pollution conditions commonly found in natural conditions (Regi Lagni, Maresca et al., 2018) to further investigate about the effects of naturally occurred conditions induced by anthropogenic influence. Different parameters were evaluated to give a comprehensive overview of heavy metals effects on moss physiology. We found that exposure to heavy metals induced severe effects in *L. riparium* plants causing reduced photosynthesis, phytochelatin and GSH content and on nitrogen metabolism. It is well known that nitrogen and the metabolism of heavy metals are strictly related (Landi & Esposito, 2017; Lentini et al., 2018; Singh & Prasad, 2017; Yang et al., 2020). The heavy metal mix (S1, S2 and S3 conditions) induced significant activation of nitrogen metabolism in L. *riparium*. Our results clearly demonstrated an activation of GS2, GOGAT and GDH upon all stress conditions tested. Generally, N is connected to abiotic stress response, by competing for reductants necessary for the antioxidant response, particularly in the presence of metals and metalloids (Ben Azaiez et al., 2020; Giansoldati et al., 2012; Lentini et al., 2018). At the same time, N and divalent cations shared similar transporters (Mao et al., 2014). An excess of N could increase the uptake of Fe, Zn, Cu, Ca, Hg and other cations, depending on plant species (Yang et al., 2020). In contrast, several higher crops (e.g. maize, pea, bean, and rice) showed lower activity of GS upon uptake of heavy metals (Lee et al., 2013; Saini et al., 2021). The overexpression of GS in rice has been reported as an effective strategy to counteract the effects of Cd exposure (Lee et al., 2013). Our results showed a natural predisposition of L. *riparium* to increase the GS2 protein occurrence. Similarly, *Pisum sativum* and *Populus* plants subjected to chromium (Cr) or Cd exposure reported an increased GDH and GS enzymatic activity, respectively (Gangwar et al., 2011; F. Zhang et al., 2014). Particularly, GDH plays critical roles upon abiotic stresses functioning both as an alternative N assimilation path and detoxifying the excess NH_4 released during perturbing conditions (Ben Azaiez et al., 2020; Jallouli et al., 2019; Zhou et al., 2015). Upon heavy metal exposure, metals were chelated in roots and moved to the shoots using GSH and PCn (Yang et al., 2020). An adequate N uptake is necessary to maintain this chelation process regulating the GSH and non-protein thiols content and regulating the expression of PC synthase and GSH synthase genes expression (Finkemeier et al., 2003; Innocenti et al., 2007; Yang et al., 2020).

The synthesis of GSH and PCn were observed also via biochemical approach confirming that *L. riparium* counteracts heavy metal stress with a detoxification system employing thiol peptide compounds (Bellini et al., 2020). Specifically, PCn synthesis was promptly induced by the exposure of heavy metals, but PCn with higher polymerization degree (PC_3 and PC_4) were synthesized only at higher concentrations. Moreover, relatively high GSH levels were detected both in the controls and in treated samples. In fact, GSH levels do not seem to be influenced by heavy metal treatment, probably due to an efficient and prompt synthesis of GSH that compensates for its use for PCn synthesis. The confocal imaging results show that MCB signal is emitted from the cytoplasm underneath the cell walls and the vacuoles of control and exposed samples (S1, S2 and S3), with a slight increase only in the S3-treated specimens. That is consistent with our chemical data, showing presence of GSH and PCn in all the examined samples, with a higher amount of PCn in the S3-treated specimens. The localization of labelled thiols in both the cytoplasm and vacuoles also agrees with a previous study on *L. riparium* with two different Cd concentrations: staining was reported from the same cell compartments with differential distributions related to the Cd concentrations and staining times (Bellini et al., 2020).

The ultrastructural appearance of the samples reflects the cellular stress induced by the increase in the concentration of heavy metals (Maresca et al., 2018). Heavy metal-induced damage to membranes or depletion of energy inside the cell can lead to swelling and/or shrinkage of cell compartments because of loss of selective permeability, a well-known function typical of biological membranes (Bellini et al., 2021). The ultrastructure alteration of chloroplasts was related to heavy metal concentrations in field and in vitro experiments on bryophytes (Basile et al., 2009, 2013; Basile et al., 2012a; Basile et al., 2012b; Esposito et al., 2018; Maresca et al., 2020b). In addition, chloroplasts appeared regular in S1-treated samples, while in S2- and S3-treated samples they developed changes. The ultrastructural damages of chloroplasts can also be explained with the overproduction of ROS, which eventually leads to lipid peroxidation of cell membranes (Farmer & Mueller, 2013), injury to thylakoids (Blokhina et al., 2003) and development of a senescent appearance (Prochazkova et al., 2001). S3-treated chloroplasts showed worse damage to cell membranes with ill-defined thylakoids and accumulation of lipid droplets probably from damaged membranes (Dalla Vecchia et al., 2005; F.-Q. Zhang et al., 2007). The severe alterations observed in S3-treated agree with our data on photosynthetic efficiency, which progressively decreases from S1- to S3-treated specimens. Our results support both the potential quantum yield of primary photochemistry and the overall vitality of *L. riparium* samples exposed to Cu, Zn, Cd and Pb concentrations, in a simulation lab experiment of polluted conditions, are degraded. These results strengthen the suggestion that this moss responding to heavy metal pollution could be suitable for biomonitoring activities in field conditions.

Nevertheless, considering that our results concern conditions where two or more metal contaminants co-exist in the natural environment, it is still difficult to judge the contribution of each metal to the biological response.

Despite these findings, several obstacles exist; for example, in the study of Basile et al., (2012b) on different mosses, intracellular concentrations of heavy metals that act as micronutrients, such as Cu and Zn, remained rather constant regardless of their extracellular concentrations, while the accumulation of the elements with no metabolic function, such as Pb and Cd increased, with increasing metal supply in the environment. Moreover, in the study of Rau et al., (2007), comparing equimolar metal concentrations, Zn and Pb treatment in the range of 25–100 μM caused in not measurable influence of the metals on chlorophyll fluorescence in *F. antipyretica* moss, while Cu and Cd concentration of 100 μM, significantly decreased fluorescence. Thus, the relationship between extracellular and intracellular metal concentrations is metal dependent and the chlorophyll fluorescence measurements show a metal-specific influence of the potential quantum yield of primary photochemistry. Nevertheless, considering that a) most of the previous research focuses on stress of certain, separate heavy metals (Rau et al., 2007), b) two or more metal contaminants usually co-exist in a natural environment, c) mosses often suffer many heavy metals at the same time in the real natural conditions, and d) other environmental variables may influence the biological response, we provide a promising methodology, which needs further calibration and standardization to show the relationship between pollution and the biological responses of potential plant bioremediators, and to assess the contribution of each metal to different biological responses.

In this paper, the moss *L. riparium* is confirmed as an excellent bioindicator of heavy metal pollution as it responds with metabolic variations consistent with the extent of stress. While all the biological responses considered can be used as indicators of a general stress situation, the study of variations in the presence of phytochelatins is particularly interesting as it can be considered a specific indicator of heavy metal stress. Finally, it should be emphasized that presently the induction of phytochelatins in response to metals in the Bryophyta has been reported only in *L. cruciata*, exposed both in vitro (Degola et al., 2014) and to environmental pollution (Maresca et al., 2020b) but data were lacking on how mosses respond. Therefore, this represents the first work to our knowledge that demonstrates the induction of phytochelatins in relation to environmentally relevant concentrations of heavy metals in mosses.

References

Ayadi, S., Jallouli, S., Landi, S., Capasso, G., Chamekh, Z., Cardi, M., Paradisone, V., Lentini, M., Karmous, C., Trifa, Y., & Esposito, S. (2020). Nitrogen assimilation under different nitrate nutrition in Tunisian durum wheat landraces and improved genotypes. *Plant Biosystems - An International Journal Dealing with All Aspects of Plant Biology*, *154*(6), 924–934. https://doi.org/10.1080/11263504.2020.1722274

Basile, A., Sorbo, S., Aprile, G., Conte, B., Castaldo Cobianchi, R., Pisani, T., & Loppi, S. (2009). Heavy metal deposition in the Italian "triangle of death" determined with the moss Scorpiurum circinatum. *Environmental Pollution*, *157*(8), 2255–2260. https://doi.org/10.1016/j.envpol.2009.04.001

Basile, A., Sorbo, S., Conte, B., Cardi, M., & Esposito, S. (2013). Ultrastructural changes and Heat Shock Proteins 70 induced by atmospheric pollution are similar to the effects observed under in vitro heavy metals stress in Conocephalum conicum (Marchantiales – Bryophyta). *Environmental Pollution*, *182*, 209–216. https://doi.org/10.1016/j.envpol.2013.07.014

Basile, A., Sorbo, S., Conte, B., Cobianchi, R. C., Trinchella, F., Capasso, C., & Carginale, V. (2012). Toxicity, Accumulation, and Removal of Heavy Metals by Three Aquatic Macrophytes. *International Journal of Phytoremediation*, *14*(4), 374–387. https://doi.org/10.1080/15226514.2011.620653

Basile, A., Sorbo, S., Pisani, T., Paoli, L., Munzi, S., & Loppi, S. (2012). Bioacumulation and ultrastructural effects of Cd, Cu, Pb and Zn in the moss Scorpiurum circinatum (Brid.) Fleisch. & Loeske. *Environmental Pollution*, *166*, 208–211. https://doi.org/10.1016/j.envpol.2012.03.018

Bellini, E., Betti, C., & Sanità di Toppi, L. (2021). Responses to Cadmium in Early-Diverging Streptophytes (Charophytes and Bryophytes): Current Views and Potential Applications. *Plants*, *10*(4), Article 4. https://doi.org/10.3390/plants10040770

Bellini, E., Borsò, M., Betti, C., Bruno, L., Andreucci, A., Ruffini Castiglione, M., Saba, A., & Sanità di Toppi, L. (2019). Characterization and quantification of thiol-peptides in Arabidopsis thaliana using combined dilution and high sensitivity HPLC-ESI-MS-MS. *Phytochemistry*, *164*, 215–222. https://doi.org/10.1016/j.phytochem.2019.05.007

Bellini, E., Maresca, V., Betti, C., Castiglione, M. R., Fontanini, D., Capocchi, A., Sorce, C., Borsò, M., Bruno, L., Sorbo, S., Basile, A., & Sanità di Toppi, L. (2020). The Moss Leptodictyum riparium Counteracts Severe Cadmium Stress by Activation of Glutathione Transferase and Phytochelatin Synthase, but Slightly by Phytochelatins. *International Journal of Molecular Sciences*, *21*(5), Article 5. https://doi.org/10.3390/ijms21051583

Ben Azaiez, F. E., Ayadi, S., Capasso, G., Landi, S., Paradisone, V., Jallouli, S., Hammami, Z., Chamekh, Z., Zouari, I., Trifa, Y., & Esposito, S. (2020). Salt Stress Induces Differentiated Nitrogen Uptake and Antioxidant Responses in Two Contrasting Barley Landraces from MENA Region. *Agronomy*, *10*(9), Article 9. https://doi.org/10.3390/agronomy10091426

Blokhina, O., Virolainen, E., & Fagerstedt, K. V. (2003). Antioxidants, oxidative damage and oxygen deprivation stress: A review. *Annals of Botany*, *91 Spec No*, 179–194. https://doi.org/10.1093/aob/mcf118

Bove, M. A., Ayuso, R. A., De Vivo, B., Lima, A., & Albanese, S. (2011). Geochemical and isotopic study of soils and waters from an Italian contaminated site: Agro Aversano (Campania). *Journal of Geochemical Exploration*, *109*(1), 38–50. https://doi.org/10.1016/j.gexplo.2010.09.013

Chen, Y.-E., Mao, H.-T., Ma, J., Wu, N., Zhang, C.-M., Su, Y.-Q., Zhang, Z.-W., Yuan, M., Zhang, H.-Y., Zeng, X.-Y., & Yuan, S. (2018). Biomonitoring chromium III or VI soluble pollution by moss chlorophyll fluorescence. *Chemosphere*, *194*, 220–228. https://doi.org/10.1016/j.chemosphere.2017.11.177

Dalla Vecchia, F., Rocca, N. L., Moro, I., De Faveri, S., Andreoli, C., & Rascio, N. (2005). Morphogenetic, ultrastructural and physiological damages suffered by submerged leaves of Elodea canadensis exposed to cadmium. *Plant Science*, *168*(2), 329–338. https://doi.org/10.1016/j.plantsci.2004.07.025

Degola, F., De Benedictis, M., Petraglia, A., Massimi, A., Fattorini, L., Sorbo, S., Basile, A., & Sanità di Toppi, L. (2014). A Cd/Fe/Zn-Responsive Phytochelatin Synthase is Constitutively Present in the Ancient Liverwort Lunularia cruciata (L.) Dumort. *Plant and Cell Physiology*, *55*(11), 1884–1891. https://doi.org/10.1093/pcp/pcu117

Esposito, S., Loppi, S., Monaci, F., Paoli, L., Vannini, A., Sorbo, S., Maresca, V., Fusaro, L., Karam, E. A., Lentini, M., Lillo, A. D., Conte, B., Cianciullo, P., & Basile, A. (2018). In-field and in-vitro study of the moss Leptodictyum riparium as bioindicator of toxic metal pollution in the aquatic environment: Ultrastructural damage, oxidative stress and HSP70 induction. *PLOS ONE*, *13*(4), e0195717. https://doi.org/10.1371/journal.pone.0195717

Esposito, S., Sorbo, S., Conte, B., & Basile, A. (2012). Effects of Heavy Metals on Ultrastructure and HSP70S Induction in the Aquatic Moss Leptodictyum Riparium Hedw. *International Journal of Phytoremediation*, *14*(4), 443–455. https://doi.org/10.1080/15226514.2011.620904

Farmer, E. E., & Mueller, M. J. (2013). ROS-mediated lipid peroxidation and RES-activated signaling. *Annual Review of Plant Biology*, *64*, 429–450. https://doi.org/10.1146/annurev-arplant-050312-120132

Finkemeier, I., Kluge, C., Metwally, A., Georgi, M., Grotjohann, N., & Dietz, K.-J. (2003). Alterations in Cd-induced gene expression under nitrogen deficiency in Hordeum vulgare. *Plant, Cell & Environment*, *26*(6), 821–833. https://doi.org/10.1046/j.1365-3040.2003.01014.x

Gangwar, S., Singh, V. P., Srivastava, P. K., & Maurya, J. N. (2011). Modification of chromium (VI) phytotoxicity by exogenous gibberellic acid application in Pisum sativum (L.) seedlings. *Acta Physiologiae Plantarum*, *33*(4), 1385–1397. https://doi.org/10.1007/s11738-010-0672-x

Giansoldati, V., Tassi, E., Morelli, E., Gabellieri, E., Pedron, F., & Barbafieri, M. (2012). Nitrogen fertilizer improves boron phytoextraction by Brassica juncea grown in contaminated sediments and alleviates plant stress. *Chemosphere*, *87*(10), 1119–1125. https://doi.org/10.1016/j.chemosphere.2012.02.005

Grezzi, G., Ayuso, R. A., De Vivo, B., Lima, A., & Albanese, S. (2011). Lead isotopes in soils and groundwaters as tracers of the impact of human activities on the surface environment: The Domizio-Flegreo Littoral (Italy) case study. *Journal of Geochemical Exploration*, *109*(1), 51–58. https://doi.org/10.1016/j.gexplo.2010.09.012

Innocenti, G., Pucciariello, C., Le Gleuher, M., Hopkins, J., de Stefano, M., Delledonne, M., Puppo, A., Baudouin, E., & Frendo, P. (2007). Glutathione synthesis is regulated by nitric oxide in Medicago truncatula roots. *Planta*, *225*(6), 1597–1602. https://doi.org/10.1007/s00425-006-0461-3

Jallouli, S., Ayadi, S., Landi, S., Capasso, G., Santini, G., Chamekh, Z., Zouari, I., Ben Azaiez, F. E., Trifa, Y., & Esposito, S. (2019). Physiological and Molecular Osmotic Stress Responses in Three Durum Wheat (Triticum Turgidum ssp Durum) Genotypes. *Agronomy*, *9*(9), Article 9. https://doi.org/10.3390/agronomy9090550

Landi, S., & Esposito, S. (2017). Nitrate Uptake Affects Cell Wall Synthesis and Modeling. *Frontiers in Plant Science*, *0*. https://doi.org/10.3389/fpls.2017.01376

Lee, H. J., Abdula, S. E., Jang, D. W., Park, S.-H., Yoon, U.-H., Jung, Y. J., Kang, K. K., Nou, I. S., & Cho, Y.-G. (2013). Overexpression of the glutamine synthetase gene modulates oxidative stress response in rice after exposure to cadmium stress. *Plant Cell Reports*, *32*(10), 1521–1529. https://doi.org/10.1007/s00299-013-1464-8

Lentini, M., De Lillo, A., Paradisone, V., Liberti, D., Landi, S., & Esposito, S. (2018). Early responses to cadmium exposure in barley plants: Effects on biometric and physiological parameters. *Acta Physiologiae Plantarum*, *40*(10), 178. https://doi.org/10.1007/s11738-018-2752-2

Mao, Q. Q., Guan, M. Y., Lu, K. X., Du, S. T., Fan, S. K., Ye, Y.-Q., Lin, X. Y., & Jin, C. W. (2014). Inhibition of nitrate transporter 1.1-controlled nitrate uptake reduces cadmium uptake in Arabidopsis. *Plant Physiology*, *166*(2), 934–944. https://doi.org/10.1104/pp.114.243766

Maresca, V., Fusaro, L., Sorbo, S., Siciliano, A., Loppi, S., Paoli, L., Monaci, F., karam, E. A., Piscopo, M., Guida, M., Galdiero, E., Insolvibile, M., & Basile, A. (2018). Functional and structural biomarkers to monitor heavy metal pollution of one of the most contaminated freshwater sites in Southern Europe. *Ecotoxicology and Environmental Safety*, *163*, 665–673. https://doi.org/10.1016/j.ecoenv.2018.07.122

Maresca, V., Lettieri, G., Sorbo, S., Piscopo, M., & Basile, A. (2020). Biological Responses to Cadmium Stress in Liverwort Conocephalum conicum (Marchantiales). *International Journal of Molecular Sciences*, *21*(18), Article 18. https://doi.org/10.3390/ijms21186485

Maresca, V., Sorbo, S., Loppi, S., Funaro, F., Del Prete, D., & Basile, A. (2020). Biological effects from environmental pollution by toxic metals in the “land of fires” (Italy) assessed using the biomonitor species Lunularia cruciata L. (Dum). *Environmental Pollution*, *265*, 115000. https://doi.org/10.1016/j.envpol.2020.115000

Maxwell, K., & Johnson, G. N. (2000). Chlorophyll fluorescence—A practical guide. *Journal of Experimental Botany*, *51*(345), 659–668. https://doi.org/10.1093/jxb/51.345.659

Prochazkova, D., Sairam, R. K., Srivastava, G. C., & Singh, D. V. (2001). Oxidative stress and antioxidant activity as the basis of senescence in maize leaves. *Plant Science*, *161*(4), 765–771. https://doi.org/10.1016/S0168-9452(01)00462-9

Rau, S., Miersch, J., Neumann, D., Weber, E., & Krauss, G.-J. (2007). Biochemical responses of the aquatic moss Fontinalis antipyretica to Cd, Cu, Pb and Zn determined by chlorophyll fluorescence and protein levels. *Environmental and Experimental Botany*, *59*, 299–306. https://doi.org/10.1016/j.envexpbot.2006.03.001

Saini, S., Kaur, N., & Pati, P. K. (2021). Phytohormones: Key players in the modulation of heavy metal stress tolerance in plants. *Ecotoxicology and Environmental Safety*, *223*, 112578. https://doi.org/10.1016/j.ecoenv.2021.112578

Say, P. J., Harding, J. P. C., & Whitton, B. A. (1981). Aquatic mosses as monitors of heavy metal contamination in the river etherow, great britain. *Environmental Pollution Series B, Chemical and Physical*, *2*(4), 295–307. https://doi.org/10.1016/0143-148X(81)90026-4

Senior, K., & Mazza, A. (2004). Italian "Triangle of death" linked to waste crisis. *The Lancet Oncology*, *5*(9), 525–527. https://doi.org/10.1016/S1470-2045(04)01561-X

Singh, S., & Prasad, S. M. (2017). Effects of 28-homobrassinoloid on key physiological attributes of Solanum lycopersicum seedlings under cadmium stress: Photosynthesis and nitrogen metabolism. *Plant Growth Regulation*, *82*(1), 161–173. https://doi.org/10.1007/s10725-017-0248-5

Strasser, R. J., Tsimilli-Michael, M., & Srivastava, A. (2004). Analysis of the Chlorophyll a Fluorescence Transient. In G. C. Papageorgiou & Govindjee (Eds.), *Chlorophyll a Fluorescence: A Signature of Photosynthesis* (pp. 321–362). Springer Netherlands. https://doi.org/10.1007/978-1-4020-3218-9_12

Yang, Y., Xiong, J., Tao, L., Cao, Z., Tang, W., Zhang, J., Yu, X., Fu, G., Zhang, X., & Lu, Y. (2020). Regulatory mechanisms of nitrogen (N) on cadmium (Cd) uptake and accumulation in plants: A review. *The Science of the Total Environment*, *708*, 135186. https://doi.org/10.1016/j.scitotenv.2019.135186

Zhang, F., Wan, X., & Zhong, Y. (2014). Nitrogen as an important detoxification factor to cadmium stress in poplar plants. *Journal of Plant Interactions*, *9*(1), 249–258. https://doi.org/10.1080/17429145.2013.819944

Zhang, F.-Q., Wang, Y.-S., Lou, Z.-P., & Dong, J.-D. (2007). Effect of heavy metal stress on antioxidative enzymes and lipid peroxidation in leaves and roots of two mangrove plant seedlings (Kandelia candel and Bruguiera gymnorrhiza). *Chemosphere*, *67*(1), 44–50. https://doi.org/10.1016/j.chemosphere.2006.10.007

Zhou, Y., Zhang, C., Lin, J., Yang, Y., Peng, Y., Tang, D., Zhao, X., Zhu, Y., & Liu, X. (2015). Over-expression of a glutamate dehydrogenase gene, MgGDH, from Magnaporthe grisea confers tolerance to dehydration stress in transgenic rice. *Planta*, *241*(3), 727–740. https://doi.org/10.1007/s00425-014-2214-z

Supplementary data

Table 1S. The concentration of heavy metals (μg l^{-1}) in waters of Regi Lagni measured in the three experimental sites (Avella, S_1; Acerra, S_2; Castel Volturno, S_3). Values are presented as mean ± st. dev; numbers not accompanied by the same letter are significantly different at $P < 0.05$, using the post-hoc Student–Newman–Keuls test. The concentrations found in the water of the three sites in field experiment were used for the *in vitro* experiments.

	Regi Lagni		
	S_1	S_2	S_3
Cu	113.83 ± 3.71[a]	4743.46 ± 24.41[b]	10812.52 ± 43.94[c]
Zn	262.40 ± 11.51[a]	4260.64 ± 11.02[b]	396728.84 ± 1633.1[c]
Cd	27.94 ± 2.60[a]	1804.90 ± 9.38[b]	278743.55 ± 685.84[c]
Pb	7.54 ± 1.18[a]	35.94 ± 4.50[b]	943.77 ± 22.53[c]

FINAL REMARKS AND HIGHLIGHTS

Heavy metals are well-known environmental pollutants owing to their toxicity, longevity in the atmosphere, and ability to accumulate in the human body via bioaccumulation. The pollution of terrestrial and aquatic ecosystems with toxic heavy metals is a major environmental concern that has consequences for the human and ecosystems health.

I employed two species of bryophytes, the thallose semiaquatic liverwort *Conocephalum conicum* and the aquatic moss *Leptodictyum riparium*, to assess how they react to environmentally relevant concentrations of heavy metals. *Conocephalum conicum* is a semiaquatic thallose liverworts with a widespread circumpolar distribution in Europe. Similarly, *Leptodictyum riparium* is an aquatic pleurocarpous moss with a cosmopolitan distribution. Due to their wide distribution together with the ease of recognition and in vitro cultivation both species are excellent candidates of being employed in biomonitoring investigations, both in transplant field experiments or by direct collection from the areas under investigation. The present work expands the knowledge about the employability of these two species in a biomonitoring network, through the application of a wide set of biomarkers such as the activation of the enzymatic and non-enzymatic antioxidant systems, phytochelatins synthesis, glutathione synthesis, nitrogen metabolism, genotoxicity, as well as several metabolic targets, chloroplast ultrastructure to assess the impact on the selected bryophytes. The responses have been measured both in vitro to test environmentally relevant concentrations of HMs measured in different freshwaters bodies from Campania region (Sarno river, Savone river and Regi Lagni Channels). Data on tissue concentrations of heavy metals alone does not provide information about the actual levels of exposure of the organisms in the ecosystems. The chemical analysis has the flaw of considering the bulk concentrations without knowing the real exposure doses. Thus, heavy metals concentrations data can be integrated with the measurement of biological responses (i.e., environmental biomakers) which can inform scientists and regulators about the real pressure on key organisms.

The present PhD work gives highlights into the employability of these two widespread bryophytes to assess freshwater bodies quality with a multiple biomarkers approach for both scientific and regulatory purposes.

The main highlights can be resumed as follow:

- The sets of biomarkers measured in *C. conicum* and *L. riparium* showed a good degree of correlation with the tested HMs at environmentally relevant concentrations both *in vitro* and field transplant experiments.

- The studies showed that several biomarkers can be taken into account to spot differences in exposures: from enzymatic activities to secondary metabolites analysis.

- The selected bryophytes, *C. conicum* and *L. riparium,* can be useful tool to assess the impact of HMs pollution in freshwaters bodies using a multiple biomarkers approach.

- The present works put the basis for the employments of the environmental biomarkers in transplants experiments for the assessment of the quality of freshwater bodies for both scientific and regulatory purposes.